Fair Sharing of Channel Resources in the Coexistence of Heterogeneous Wireless Networks

A Dissertation
presented in partial fulfillment of requirements
for the degree of Ph.D. Degree in Engineering Science
in the Electrical Engineering
at The University of Mississippi

by

Sudat Tuladhar

May 2022

ABSTRACT

Increasing spectrum resources in cellular networks are always needed to carry the exponential data traffic growth in wireless cellular networks. Limited spectrum resources in the licensed band have necessitated Long-Term Evolution (LTE) to explore available unlicensed spectrum where an incumbent WiFi system already exists. With the deployment of Licensed Assisted Access (LAA) that utilizes Listen Before Talk (LBT) for channel access in the unlicensed spectrum along with an incumbent WiFi, the coexistence of LAA and WiFi with acceptable fairness is a major challenge. In this work, we address the issues of licensed assisted access coexisting with incumbent WiFi in an unlicensed spectrum and provide solutions to dynamically tune system parameters of LAA stations to achieve maximum total throughput from the overall system taking into account fair allocation of throughput and airtime across different networks and stations. One major system parameter we study is the contention window size for back-off. Using the method of coupled Markov Chain, we show how an inherent trade-off between throughput and airtime fairness can be managed by adjusting the CW size of LAA. For single-channel, we show how coexistence with WiFi can be managed better with LAA-Cat3 than LAA-Cat4 when total throughput and fairness are to be taken into account. For multi-carrier sensing, we establish better coexistence by optimizing contention window sizes of each LAA station separately using an assignment technique based on a genetic algorithm. We extend our work into dual-carrier aggregation where some stations have the ability to combine two independent channels into a single aggregated channel to achieve higher performance. We show that in such a dual-carrier aggregation scenario, the distribution of stations (partition) over an individual and aggregated channel, and the system parameters (contention window size and load intensity) could be optimized to ensure fair allocation of resources without affecting the secondary channel too much.

LIST OF ABBREVIATIONS

5G-NR 5th Generation New Radio

AP Access Point

CA Carrier Aggregation

CC Component Carrier

CCA Clear Channel Assessment

COT Channel Occupancy Time

CSMA-CA Carrier Sense Multiple Access-Collision Avoidance

CTS Clear To Send

CW Contention Window

DCF Distributed Coordination Function

DIFS Distributed Inter-Frame Space

DTX Discontinuous Transmission

eNB evolved Node Base station

FR Frequency Range

GA Genetic Algorithm

ISM Industrial, Scientific and Medical

LAA Licensed Assisted Access

LBT Listen Before Talk

LSTM Long Short Term Memory

LTE Long Term Evolution

LTE-U LTE-Unlicensed

MC Markov Chain

MCS Modulation and Coding Scheme

MIMO Multiple Input Multiple Output

NFC Near Field Communication

NR New Radio

OFDM Orthogonal Frequency Division Multiplexing

QAM Quadrature Amplitude Modulation

QAM Quadrature Amplitude Modulation

QPSK Quadrature Phase Shift Keying

RB Resource Block

RTS Request To Send

SIFS Short Inter-Frame Space

SINR Signal to Interference Ratio

TPC Transmit Power Control

TXOP Transmit Opportunity

WiGig Gigabit WiFi

ACKNOWLEDGEMENTS

I would like to express my sincere gratitude to my advisor Dr. Lei Cao for the continuous support, guidance and encouragement during the course of my Ph.D. studies. I am very grateful for his inspirations, encouragement, insightful suggestions and numerous discussions needed for my research.

I am grateful to my thesis committee members: Dr. Ramanarayanan "Vish" Viswanathan, Dr. John N. Daigle and Dr. Feng Wang for their valuable discussion and insightful comments which helped me widen my research from various perspectives.

Special thanks to fellow students and supporting staff members for listening, offering me advice and supporting me through this entire process.

Lastly, I would like to thank my family members and friends who have continuously encouraged me in all of my pursuits and inspired me to follow my dreams.

TABLE OF CONTENTS

LIST OF TABLES

LIST OF FIGURES

CHAPTER 1

INTRODUCTION

Third Generation Partnership Project (3GPP) has recently introduced a feature in release 13 as a part of Long Term Evolution (LTE) Advanced Pro that leverages the unlicensed 5 GHz band in combination with licensed spectrum to provide better data rates and a better user experience. The exploration of unlicensed band by LAA has caused degradation of performance of incumbent systems such as WiFi operating in the same unlicensed band. It is desirable for LAA to utilize the unlicensed band without significant impact on WiFi's performance, without modifying WiFi's system parameters and basically treating it as a legacy system. Even with the introduction of Listen Before Talk (LBT) channel access mechanism that is much similar to WiFi's Distritributed Coordination Function (DCF), a fair and harmonious coexistence between LAA and WiFi still remains a major challenge. Most of the previous works that address this coexistence issue have mainly concentrated on the throughput performance of LAA and WiFi networks, and the throughput fairness achieved between two networks. This has rather put the importance of airtime fairness under the shadows.

Our study on the coexistence of LAA and WiFi shines some light on the importance and benefit of considering airtime fairness in addition to throughput fairness to achieve better coexistence. We model the contention between LAA and WiFi using a Markov Chain (MC) model and define a fitness metric that achieves maximum throughput performance from the coexistence system ensuring both throughput and airtime fairness. We show that by leveraging the adjustable contention window (CW) size of LAA to control its access to the channel, it is possible to control both the throughput and airtime of different networks, but there exists an inherent trade-off in achieving both throughput fairness and airtime fairness.

We show that by optimizing our defined fitness metric, we can make a compromise between both fairness. We also show that LBT-Cat3 coexists better than LBT-Cat4 with WiFi when total throughput and combined throughput-airtime fairness are taken into account. Previous studies have studied the coexistence of LAA and WiFi under the assumption that the data-rate of LAA remains constant which is not the case in practice. Every LAA evolved Node B (eNB) has a different data-rate on different channels depending on the channel conditions, Multiple In Multiple Out (MIMO) antennae technology available and the Modulation and Coding Scheme (MCS) used for communication. Our work proposes adjusting the CW size of each LAA on each channel in a multi-carrier coexistence with WiFi to achieve the best fitness we described earlier. We solve the coexistence problem using Genetic Algorithm (GA) based assignment technique. We show that GA based assignment achieves higher total throughput, higher airtime fairness and thus higher fitness at the expense of some throughput fairness in comparison to the equal CW assignment technique. Such technique provides means to achieve better coexistence in real scenarios where the data-rates of LAA are always changing depending on channel conditions.

Further, there is no clear theoretical understanding how the fairness can be achieved in the case of the carrier aggregation where multiple frequency blocks (called component carriers) are assigned to the same user to increase the data rate of the user. This will clearly impact users that do not have such carrier aggregation capability. In our study, we categorize users into three separate groups: a) that can only sense primary channel, b) that can only sense secondary channel and c) that sense primary channel first and then can aggregate the secondary channel if it is also available. We model the problem using a coupled Markov Chain between different groups of users. We consider the users on the secondary channels as incumbents which need to be protected in the process of aggregating primary and the secondary channel. We explore the effects of partition (dividing available stations into primary channel sensing or dual-channel sensing) and system parameters of LAA: load intensity and CW size. We measure the effects on the total throughput of the system, fairness

achieved between groups and the impact this has on the secondary users based on maximizing different objectives: a) total throughput, b) airtime fairness, c) throughput fairness and d) combined fairness. We show that the combined fairness that takes into account both airtime and throughput fairness is still the best criteria, even for dual-carrier aggregation scenario, that ensures protection of the secondary users at the expense of some total throughput. We show that the partition plays a dominating role than adjusting system parameters: CW size and load intensity. Hence, throughout this study we highlight the importance of airtime fairness along with throughput fairness in managing the fair coexistence of heterogeneous networks between LAA and WiFi in single-carrier, multi-carrier and dual-carrier aggregation scenarios.

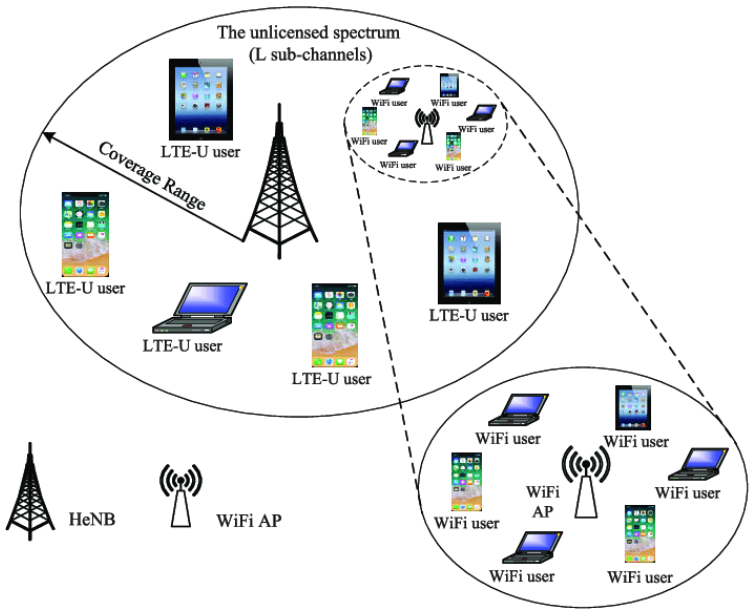

Figure 1.1: Coexistence of heterogeneous networks

1.1 Literature Review

1.1.1 Coexistence between homogeneous networks: WiFi-WiFi or LTE-LTE

Coexistence between two similar networks either WiFi-WiFi or LTE-LTE have been studied in the literature for both single and multi-carrier use of the spectrum as shown in Table 1.1. Effects of channel access mechanism and system parameters such as Contention

Window (CW) size for various WiFi and LTE density on coexistence performance such as throughput, idle time, collision time and risk factor have been studied under simulation and analytical models: Markov Chain (MC) and game theory.

Table 1.1: Coexistence between WiFi-WiFi or LTE-LTE

Number of carriers	**Study Parameter**	**Method**	**Performance metric**
Single-Carrier WiFi/WiFi	Wi-Fi density [1–3] CW size [1] No. contention stages [1] Channel access mechanism: [1]	Analytical - MC [1] Simulation [2,3]	Throughput [1–3] Idle time [1] Collision time [1] Risk Factor [2,3]
Multi-Carrier WiFi/WiFi	Wi-Fi Density: [3] No. of Channels: [3] Channel sense: [3]	Simulation [2,3]	Throughput [2,3] Risk Factor [2,3]
Single-Carrier LTE/LTE	LTE Density: [4]	Simulation [4]	Throughput [4]
Single-Carrier LAA/LAA	CW adaptation: [5]	Analytical - Game Theory [5]	Throughput [5]

Study on coexistence between WiFi-WiFi started with analytical evaluation of the saturation throughput based on 2D Markov chain model in [1] for finite number of terminals in ideal channel conditions using basic and RTS/CTS access. Studies in [2,3] have evaluated the coexistence between single carrier WiFi-WiFi and single carrier LTE-LTE using simulations to benchmark the base performance under homogeneous network coexistence in terms of the throughput and risk factor. Same studies have also been extended to a multi-carrier WiFi-WiFi coexistence. Single-carrier LAA-LAA coexistence have been studied in [5] using a game theory approach which adapts the CW sizes under buffer length constraint and leverages difference of buffer status for collision alleviation and throughput improvement.

Table 1.2: Coexistence between WiFi-LTE without modification

Number of carriers	**Study Parameter**	**Method**	**Performance metric**
Single-Carrier	***Impacts on WiFi and LTE*** Wi-Fi/LTE Density: [6, 7] Carrier Sense [7, 8] Packet Arrival Rate [9] Sensing Threshold [10, 11] No. of Antenna [12] Indoor-Outdoor [7] ***Fairness Issue*** Proportionate Fairness [8]	**Analytical** MC [11] Stochastic Geometry [10] **Simulation** [6, 7, 9, 10] **Measurement** [12]	Throughput [6–9, 11, 12] SINR [11] SINR Coverage Probability [10] Sucessful Links [10] Rate Coverage Probability [10] Airtime [6]
Multi-Carrier	***Impacts on WiFi and LTE*** No of Channels: [6, 7] Wi-Fi/LTE Density: [6, 7]	**Simulation** [6, 7]	Throughput [6, 7] Airtime [6]

1.1.2 Coexistence between heterogeneous networks: WiFi-LTE without modification

Impacts of LTE on WiFi without LBT and much modification to LTE system have been investigated for single and multi-carrier coexistence as shown in Table 1.2. For single-carrier, the effects of channel access mechanism [7, 8] and system parameters such as packet arrival rate [9] and carrier sensing threshold [10, 11] have been studied. Study in [11] provides an analytical framework based on MC that characterizes interference of WiFi and LTE for dense deployment scenarios with spatially overlapping coverage and demonstrates that WiFi is significantly degraded by a nearby LTE system without any modifications, while LTE degradation is minimal as long as the WiFi system is within carrier sense range. Other analytical methods include study in [10] where stochastic geometry is leveraged to characterize throughput and Signal to Interference Ratio (SINR) where locations for the WiFi APs and LTE eNBs are modeled as two independent homogeneous Poisson point processes. Studies based on simulations in [6, 7] show the impact of LTE on WiFi throughput and airtime for single and multi-carrier whereas [9, 10] show their impact on throughput, SINR

coverage probability, number of successful links and rate coverage probability. Measurement study in [12] leverages LTE and WiFi antennas already available on smartphones to let LTE and WiFi transmit together and successfully decode the interfered signals. Most of these study [6–9, 11, 12] focus on the throughput performance of each LTE and WiFi network to see how much LTE throughput gain is achieved at the expense of WiFi throughput. Proportionate fairness between LTE and WiFi throughput have also been investigated in [8]. For multi-carrier, only a few studies based on simulations [6,7] have reported the throughput and airtime performance over a number of available channels for various density of LTE-WiFi stations.

1.1.3 Coexistence between heterogeneous networks: WiFi-LTE-U

Numerous studies as shown in Table 1.3 and Table 1.4 have been done regarding the coexistence of LTE-U and WiFi where LTE does modify some system parameters to impact the WiFi network as little as possible.

In single-carrier, to minimize the degradation of WiFi performance due to introduction of LTE-U, analytical studies in [35, 35] have proposed modifying the LTE ON period. Study in [42] have adjusted the carrier sensing threshold and evaluated the effect of WiFi-LTE density on throughput performance based on analytical game theory models and decision tree based learning model. Decision models in [31] have proposed introducing muting period in transmission whereas transmit power have been adjusted in [21]. Study in [40] evaluate the airtime fraction and Jain's fairness using a coalition formation game framework based on Shapley value. Measurement studies based on transmit power [37], duty cycle patterns and packet size [28, 37], duty cycle [24, 26] have also been reported. Other parameter modifications include introduction of blank sub-frames [13, 29, 30], changing time duration for which LTE can send frames after it has gained contention for the transmission medium termed Transmit OPportunity (TXOP) [31], carrier sensing threshold [7, 10, 15, 27], channel sensing time [30], transmission time [30], number of iteration in strategic game theory evolution [33],

Table 1.3: Coexistence between WiFi-LTE-U (Single-Carrier)

Study Parameter	**Method**	**Performance metric**
Impact on WiFi and LTE	**Analytical**	Throughput [2, 3, 7, 13, 15–19, 21–23, 25, 28–31, 34–39, 41]
Wi-Fi/LTE Density [2, 3, 7, 13–21]	MC [35, 36]	Airtime Fraction [40]
Duty cycle [2, 7, 10, 21–27]	Game theory [33, 39, 40]	SINR [37]
Duty cycle Patterns [28]	Stochastic Geometry [10, 15, 18]	Latency [23, 34]
Blank sub-frames [13, 29, 30]	Others [14, 16, 19, 26, 37]	Jitter [28]
Muting period [31, 32]	**Simulation**	Packet Loss [28]
Transmit opportunity (TXOP) [31]	[2, 3, 7, 10, 13, 15, 17, 22, 23, 25, 27, 29, 30, 32, 35, 36, 38, 40, 41]	Spectrum utility [5]
Carrier sensing threshold [7, 10, 15, 27]	**Measurement**	Channel access probs. [14]
Sensing Time [30]	[24, 26, 28, 37]	Mean Back-off Delay [14]
Transmission time [30]	**Learning**	SINR Coverage probs [10]
No of Iteration [33]	Decision Tree [21, 31, 39]	Sucessful Links [10]
LTE ON period [19, 23, 26, 34–36]		Rate Coverage probs [10]
Tx Power [7, 13, 17, 21, 24, 28, 37, 38]		Served load [32]
Packet Size [14, 28]		Channel Utilization [25]
Modulation and Coding Scheme (MCS) [24, 28]		Jain's Fairness [40]
Indoor Outdoors [7, 17]		Entropy [40]
Spectral Efficiency [20]		No of beacons [26]
Fairness Issue		Collision Probability [35, 36]
Fairness in Throughput [2, 39]		Energy Efficiency [21]
Proportional Fairness [16]		Others [33]

Modulation and Coding Scheme (MCS) [24, 28], indoor-outdoor scenarios [7, 17] and spectral efficiency [20]. Throughput still remains the most dominant metric to be studied for WiFi-LTE-U coexistence. Other important metrics include latency [23,34], jitter [28], packet loss [28], spectrum utility [5], channel access probability [14], mean back-off delay [14], SINR coverage probability [10], number of sucessful links [10], rate coverage probabilities [10], served load [32], channel utilization [25], Jain's fairness [40], entropy [40], number of beacons [26], collision probability [35, 36] and energy efficiency [21] as listed in Table 1.3.

Table 1.4: Coexistence between WiFi-LTE-U (Multi-Carrier)

Study Parameter	**Method**	**Performance metric**
Impact on WiFi and LTE	**Simulation** [3, 7, 13, 15, 45]	Throughput [3, 7, 15, 43, 44]
Wi-Fi/LTE Density [7, 15]	**Learning**	
Duty cycle [7, 43]	Q learning [34, 43, 44]	
Channel Selection [13, 44, 45]		
Blank sub-frames [13, 45]		
No of Channels [3, 7, 15, 43]		
Channel sense [3]		
Sensing thresholds [7] [15]		
Indoor Outdoors [7]		
Tx Power [7]		

In multi-carrier, effects of channel selection [13,44,45], changing channel access mechanisms [3], channel sensing thresholds [7,15], and system parameters such as duty cycle [7,43], transmit power [7] and introducing blank-subframes [13, 45] have been studied as shown in Table 1.4. Q-learning based coexistence models have been popular recently. Study in [44] utilizes distributed Q-learning mechanism that exploits prior experience for channel selection functionality. [43] proposes alternating transfer data in LTE-U and WiFi taking into account both the fairness and the performance of the system to optimize the duty cycle, and [34] takes into account the latency imposed on WiFi activity by employing carrier sensing at the base station and aims to maximize it while maximizing unlicensed LTE utilization of the idle spectral resources.

1.1.4 Coexistence between heterogeneous networks: WiFi-LTE-LAA

Numerous studies as shown in Table 1.5 and Table 1.6 have been done regarding the coexistence of LTE-LAA and WiFi where LTE tries to sense the channel before transmission using LBT similar to WiFi's DCF and modifies some system parameters to impact the WiFi network as little as possible.

Table 1.5: Coexistence between WiFi-LTE-LAA (Single-Carrier)

Study Parameter	**Method**	**Performance metric**
Impact on WiFi and LTE	**Analytical**	Throughput [2, 3, 7, 18, 19, 23, 41, 42, 46, 48–61, 63, 64]
Wi-Fi/LTE density [2, 3, 7, 17–19, 42, 46–48]	MC [42, 46–48, 51, 55–57, 59]	Fractional airtime [48, 61, 62]
Duty cycle [2, 7, 10, 27, 49, 50]	Stochastic Geometry [10, 18]	WiFi-Throughput [48, 56]
Reference sub-frame [51]	Others [19]	Latency [23, 42, 50, 51, 58, 63]
Tx Power [7, 17]	**Simulation**	Success tx prob [46, 65]
Carrier sensing threshold [7, 10, 27]	[2, 3, 7, 10, 17, 23, 32, 41, 51, 52, 54, 57, 58, 61, 62]	Channel Access prob [59]
Wi-Fi energy detection threshold [47, 50, 52]	**Measurement**	Carrier Utilization rate [65]
LAA transmission time [53]	[47, 59, 63]	SINR [49, 63]
LBT category-types [41, 42, 48, 51]	**Learning**	QoS [57]
CW size [32, 47, 48, 51, 54–58]	Q learning [49, 53]	SINR Coverage Probability [10]
Retry count [51]	**Algorithmic** [61]	Sucessful Links [10]
Contention levels [47]		Rate Coverage Probability [10]
Max Delay [57]		Served Load [32]
COT [59]		Collision Avoidance [62]
Channel Idle time [59]		DOA [62]
TXOP [47]		TXOP [63]
Data rates [47]		Resource Block allocation [63]
Indoor Outdoors [7, 17]		
TON [19]		
Channel Bit Rate [59]		
Preamble Detect [60]		
Fairness Issue		
Fairness in Throughput [2]		
Jain's Fairness [61]		
Throughput and Airtime Fairness [48]		

In single-carrier, some additional parameters with respect to WiFi-LTE-U coexistence have been studied for WiFi-LAA coexistence such as WiFi energy detection threshold [47, 50, 52], LBT category-types [41, 42, 48, 51], CW size [32, 47, 48, 51, 54–58], contention levels [59], data-rates [47], preamble detect [60] etc. as shown in Table 1.3. From fairness point of view, study in [2] and [61] have discussed the throughput fairness and Jain's fairness index respectively. Analytical study include works in [10] which leverages stochastic geometry for LTE-LBT and random backoff to adopt short transmission duty cycle, lower channel access priority and more sensitive CCA thresholds to improve density of successful transmissions and rate coverage probability. Most of the analytical studies are based on MC [42, 46–48, 51, 55–57, 59]. Study in [46] introduces a MC for a simple LAA with two stages: high and low data rates to evaluate the coexistence performance in terms of channel access and successful transmission probabilities. Study in [42] extends the model in [46] to LAA-LBT Cat3 and Cat4 models at different packet arrival rates and discusses the throughput and delay performances. Study in [56] proposes optimizing the CW size of LAA for maximizing LAA throughput while guaranteeing WiFi throughput above a predefined threshold. Study in [55] also analyses the effect of CW size on throughput performance. Using MC, [59] establishes frame based equipment MAC protocol that is a good trade-off for throughput compromise between WiFi and LAA. Work in [57] guarantees the QoS for the users by optimizing the LTE-LAA transmission time, sub-carrier assignment and power allocation. Work in [47] explores the impact of various network parameters such as energy detection threshold, contention levels, CW size and data-rates on LTE and WiFi throughput whereas [51] redesigns the CW doubling policy and explores the maximum CW size retry count to analyze their effect in latency. Effect of other parameters such as reference subframes [51], transmit power and indoor-outdoor scenarios [7, 17] have been studied under simulation. Performance metrics such as SINR coverage probability, number of successful links, rate coverage probability [10], number of served load [32], collision avoidance [62] have also been explored under simulation. Performance metrics such as channel access probabili-

ties [59], throughput [47, 59], latency [63] and number of resource block allocation [63] have been studied using measurements. Study in [61] evaluate the fractional airtime performance based on algorithmic procedure of detecting WiFi traffic saturation and adapts the Channel Occupancy Time (COT). Q-learning based approaches such as in [49] adapt the duty cycle to manage throughput and SINR whereas [53] adapts the LAA transmission time.

Table 1.6: Coexistence between WiFi-LTE-LAA (Multi-Carrier)

Study Parameter	**Method**	**Performance metric**
Impact on WiFi and LTE LTE-WiFi Density [3, 4, 7, 66, 67] Channel Selection [64–66, 68] No. of Channel [3, 7, 66] Channel Aggregation [66] Carrier sense [3, 7] DTX [64] TPC [7, 64, 68] LBT Category [64] CW size [65, 69] Indoors Outdoors [7] Duty Cycle [7] Transmission mode [65] Energy Detection [65] Access Priority [65] ***Fairness Issue*** Fairness in Throughput [2, 66] Fairness in Airtime [66] Carrier Sensing [70] Carrier Grouping [68] Throughput-Airtime Fairness [67, 69]	**Analytical** MC [67, 69] **Simulation** [3,4,7,27, 64, 65, 70] **Learning** Q learning [64] LSTM [66] **Algorithmic** [68]	Throughput [3, 4, 7, 64, 66–70] Airtime [66, 67, 69] Distribution of aggregated carriers [68]

In multi-carrier, study based on algorithm [68] proposes a hybrid design of two LBT types and divides carriers into multiple groups with a guard band in between to avoid power leakage among groups and selects the primary carrier of each group to maximize LAA's carrier aggregation capacity. Simulation studies in [3, 4, 7, 65] show the dominant

effect of carrier sense mechanism, CW size and availability of number of channels over other parameters such as transmit power control and duty cycle on throughput performance of both LTE and WiFi. Study in [64] proposes a Q-learning mechanism for learning unlicensed band activity and proposes a double Q-learning method for carrier selection that takes into account both Discontinuous Transmission (DTX) and Transmit Power Control (TPC). Study in [66] utilizes Long Short Term Memory (LSTM), a recurrent learning based model, and proposes enabling LTE-LAA to proactively perform dynamic channel selection, carrier aggregation and fractional spectrum access while guaranteeing fairness with existing WiFi networks and other LTE-LAA operators.

In extension to studies of coexistence between LTE and WiFi presented from Table 1.1 to Table 1.6, surveys in [71–78] also address the impact of various parameters on performances of both LTE and WiFi, and highlight the fairness issue associated with it.

1.1.5 Coexistence of WiFi with other technologies

Besides LTE, coexistence of WiFi with other technologies have also been studied. Study in [79] examines the unlicensed spectrum splitting between femto-cell and WiFi by proposing a fair and QoS-based strategy. Coexistence of small-cells and WiFi in [62] shows that with direction of arrival estimation and null steering, LTE-LAA small-cells can transmit simultaneously with nearby WiFi devices without causing significant interference. Survey in [80] discusses how key features in next-generation WiFi are being designed to leverage the additional unlicensed bands, and sheds light on the foreseeable challenges that designers of unlicensed radio access technologies might face in the near future.

1.2 Motivation and Objective

LTE-U is known to severely degrade the performance of the incumbent WiFi system which relies on decentralized channel access with Carrier Sense Multiple Access-Collision Avoidance (CSMA-CA) protocol in single or multi-carrier unlicensed spectrum as shown in studies in Table 1.3 and Table 1.4. LTE-LAA has a mechanism of sensing the channel before

transmission similar to WiFi's DCF, and is more courteous towards the incumbent WiFi and is known to lower the degradation of WiFi performance as shown in studies in Table 1.5 and Table 1.6.

For LTE-LAA to coexist with WiFi in a way that maximizes its own performance and minimizes WiFi performance degradation, it needs to fairly access the common unlicensed spectrum so as to give equal opportunity to WiFi. This brings us to a discussion of fair access to the channel. While most of the previous studies analyze the effect on individual LTE-LAA and WiFi throughput, very limited studies have been conducted to examine the effect on airtime or Channel Occupancy Time (COT) defined as the time percentage that a system occupies the channel. We believe airtime is also an equally important performance metric from the fairness point of view. The fair coexistence system should be able to achieve the highest possible overall throughput maintaining both throughput and airtime fairness. While some studies have discussed the fair coexistence in terms of throughput fairness and proportional fairness metric, studies accounting the airtime fairness metric is limited. There have also not been any studies that extend this notion of fair access in terms of both throughput and airtime between LTE and WiFi in the case of Multi-Carrier LBT and Component Carrier (CC) aggregations. The capability of LTE to sense multiple free carriers in the unlicensed spectrum and having the ability to aggregate them to achieve higher bandwidth for transmission necessitates the extension of study of LAA-WiFi coexistence in multi-carrier LBT and aggregation scenarios.

The overall objective of our work is to ensure the maximum performance in LAA-WiFi coexistence taking into account the throughput and airtime fairness in single-channel, multi-channel and aggregated channel scenarios. Therefore, we aim to accomplish following tasks.

1. Establish contention window (CW) size as a key parameter that LAA stations can dynamically adjust to balance the channel access with WiFi and depict the inherent trade-off in achieving throughput fairness and airtime fairness.

2. Define a performance metric (fitness function) that takes into account total throughput and combined throughput-airtime fairness.

3. Compare adjustments of CW sizes for LAA-Cat4 and LAA-Cat3 to find which performs better fairness.

4. Find a better CW assignment technique for multi-channel scenario.

5. Find an optimal station distribution and system parameters (CW size and load intensity) for the dual-channel aggregation scenario.

1.3 Contributions and Outline

Chapter 2 introduces the concepts for the coexistence of heterogeneous wireless networks and channel access principles, discusses differences in channel access methods in LTE/WiFi and provides details on differences in WiFi CSMA-CA and LAA LBT protocol. It also describes the principles of multi-carrier LBT and component carrier aggregation.

Chapter 3 first demonstrates the unfair advantage to LAA when LAA (both LAA-Cat3 and LAA-Cat4) and WiFi coexist in a single channel without any CW size adjustments. It then establishes the CW size of LAA as an important system parameter that enables LAA to coexist fairly with WiFi. The main contribution of this chapter is to show that there exists an inherent trade-off while optimizing CW size for LAA for throughput and airtime fairness. We define a fitness function that takes into account both total throughput and combined fairness metric which can ensure fair coexistence. We compare the performances of LAA-Cat4 and LAA-Cat3 coexisting with WiFi on the basis of this fitness function.

Chapter 4 builds on the framework of Chapter 3 to optimize the coexistence of LAA and WiFi in the case of multi-carrier LBT with different data-rate specifications for each station in each channel. The main contribution of this chapter is to show that both total throughput and combined fairness metric in the case of multi-carrier LBT can be improved by optimizing the CW sizes of each LAA station separately. We show that adjusting these

CW sizes for each station could be done using a Genetic Algorithm (GA)-based assignment technique. We compare the performances of the GA assignment with the equal assignment and show that GA based assignment performs considerably better in terms of both total throughput and combined fairness.

Chapter 5 extends the coexistence study in Chapter 3 and Chapter 4 to a dual-carrier aggregation scenario. The main contribution of this chapter is to show that by configuring system parameters (CW size and load intensity) along with distribution of stations (partition) over the individual and aggregated channels, fair coexistence between different groups of stations can be achieved.

Finally chapter 6 concludes our work.

CHAPTER 2

COEXISTENCE OF HETEROGENEOUS WIRELESS NETWORKS

In this chapter, we introduce the concepts for the coexistence of heterogeneous wireless networks, their need and channel access principles.

2.1 Licensed and Unlicensed Spectrum

Radio spectrum is generally categorized into a) licensed and b) unlicensed spectrum. Licensed spectrum is a part of the radio spectrum that is assigned exclusively to operators for independent usage and cannot be used by others. In the licensed spectrum, an operator can exercise more flexibility in deploying networks without worrying about interference from other operators or systems. However, since the licensed spectrum is dedicated, no one else other than the licensee has the right to utilize the channel. This reservation of the spectrum makes it a scarce resource that other operators cannot use. Long-Term Evolution (LTE) bands and Fifth Generation-New Radio (5G-NR) frequency range FR1 and FR2 are some examples of wireless licensed spectrum.

On the contrary, an unlicensed spectrum is a part of the radio spectrum that is not exclusively assigned to any operators and is free to use for anyone. The channel usage in the unlicensed spectrum is uncoordinated with no regulatory restrictions other than a restriction in the transmission power. This makes interference management more difficult and requires some channel sensing mechanisms to coordinate. Bluetooth, WiFi, Near Field Communication (NFC) devices using Industrial, Scientific and medical (ISM) bands and WiGig (Gigabit WiFi) are examples of technologies in the unlicensed spectrum.

2.2 Centralized and Decentralized Channel Access

Depending on how a system allocates spectrum for data transmission, the channel access mechanism can be categorized into a) Centralized and b) Decentralized. In a centralized channel access mechanism, a central authority controls the channel assignment and has full control over the allocation of specific channels to specific users at a specific time. Whereas in a decentralized channel access mechanism, there is no central authority and everyone must contend with each other for channel access. Channel sensing methods such as Carrier Sense Multiple Access-Collision Avoidance (CSMA-CA) is required by each user to sense the empty channel before initiating a transmission.

2.2.1 Channel Access in LTE

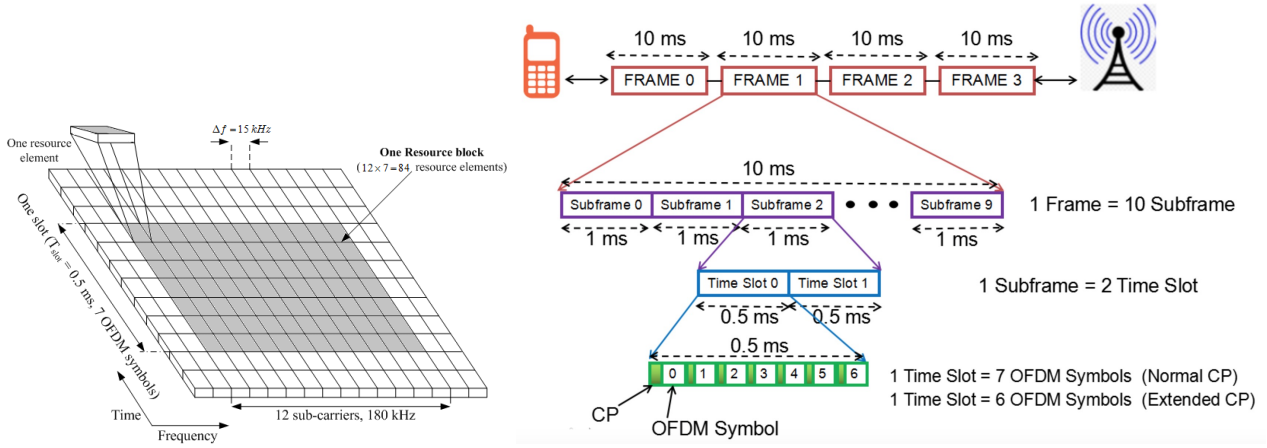

(a) Resource Block (b) Frame Structure

Figure 2.1: LTE Resource Block and Frame Structure, Courtesy (Techplayon)

LTE utilizes centralized channel access where a central entity allocates channel resources in terms of a basic Resource Block (RB). Each RB consists of 12 sub-carrier and 180 kHz bandwidth for a time period of one slot (0.5 ms) as shown in Fig. 2.1. Each time slot includes 7 Orthogonal Frequency Division Multiplexing (OFDM) symbols. Altogether 84 resource elements are allocated in a RB. LTE operates in a licensed band and schedules these resources to the users individually such that there is never a contention for resources.

2.2.2 Channel Access in WiFi

WiFi utilizes 802.11 protocol based on the CSMA-CA to access the medium. The re-transmission of collided packets is managed according to binary exponential backoff rules. The basic access mechanism in this protocol is characterized by the immediate transmission of positive acknowledgment (ACK) by the receiver when the packet sent by the transmitter is successfully received. Fig 2.2 briefly summarizes the Distributed Coordination Function (DCF) protocol described in 802.11 standard [81].

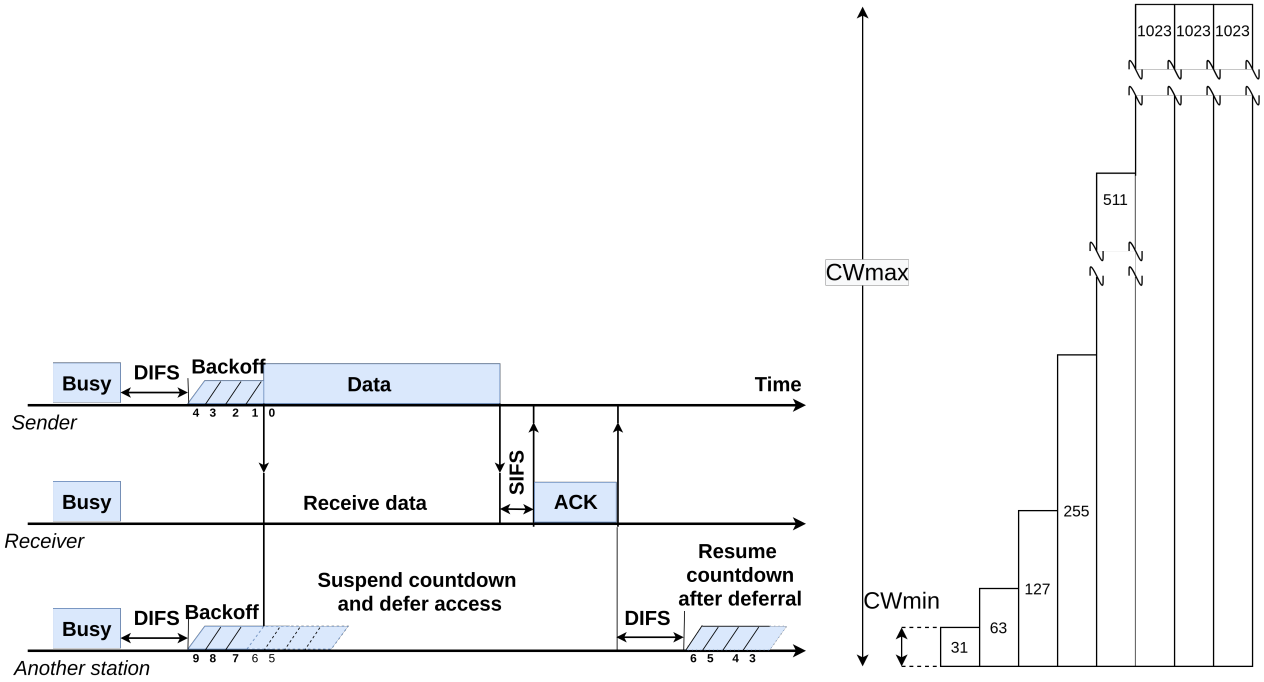

(a) Contention in channel (b) Exponential backoff

Figure 2.2: Exponential backoff

Clear Channel Assessment (CCA) is a mechanism to determine whether a channel is idle or busy using channel sensing and energy detection. Any station trying to transmit packet into the channel first checks if the channel is empty for Distributed Inter Frame Space (DIFS) using CCA. If the channel is sensed busy during DIFS, the station monitors the channel until the channel is empty for DIFS. If the channel is not busy during DIFS, the station generates a random backoff interval from a Contention Window (CW) size before

transmission to minimize the probability of collision with packets being transmitted by other stations. If the channel is not busy after the backoff timer expires, the packet gets transmitted and the receiver sends an ACK signal after Short Inter Frame Space (SIFS). The same procedure has to be followed for consecutive packet transmissions.

Any other station trying to transmit packet must also wait for DIFS and have a random backoff timer. If this station senses the channel to be busy within the backoff time, it must defer the countdown process until the channel is free and again wait for DIFS before resuming the countdown process as shown in Fig 2.2(a). After the countdown is over, if it finds the channel empty it will transmit otherwise it will re-generate the random backoff interval with twice the period as before. This exponential backoff would keep on happening if the channel is busy until a max CW size is reached and will stay at max until successful transmission occurs as shown in Fig 2.2(b). The CW size at each stage is twice that of the previous stage and ranges from the minimum to the maximum CW size.

2.2.3 Licensed Assisted Access

Access to higher spectrum such as 5G spectrum give opportunity to provide wider bandwidth for higher data-rates and support the exponentially increasing mobile traffic data demand. But much of these higher spectrum are reserved as licensed spectrum for either cellular, military or civil use worldwide. It is getting much harder and expensive for even the cellular operators to acquire such a limited and scarce resource. This has led licensed cellular operators such as Long-Term Evolution (LTE) and 5G to expand their operation into the unlicensed spectrum with LTE-LAA (LTE-Licensed Assisted Access). Other examples of such heterogeneous coexistence include: a) coexistence between IoT, Bluetooth and WiFi in 2.4 GHz b) coexistence of 5G/6G and WiFi-6E in 6 GHz and c) coexistence of New Radio-Unlicensed (NR-U) and Gigabit WiFi (WiGig) in 60 GHz.

LTE-LAA is a feature of Rel-13 [82] in 3GPP which uses carrier aggregation in the downlink to combine LTE in the licensed band with 5 GHz unlicensed band as shown in

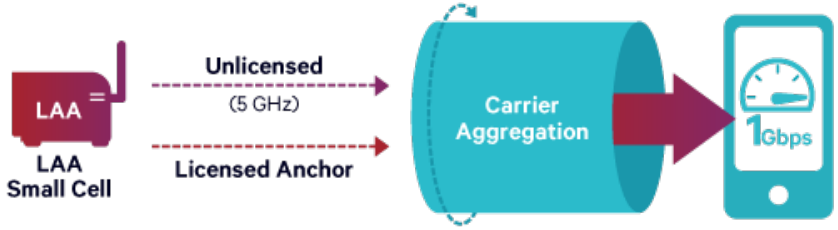

Figure 2.3: Licensed Assisted Access

Fig. 2.3. This aggregation of the spectrum provides a fatter pipe with faster data rates and more responsive user experiences. For each LTE eNB, in addition to using maximum 20 MHz bandwidth obtained using licensed band, aggregation can explore additional 100MHz bandwidth in unlicensed band. This allows operators to distribute traffic between licensed and unlicensed bands freeing up capacity on the licensed spectrum and offering faster LTE by utilizing chunks of unlicensed band opportunistically.

2.2.4 Listen Before Talk

Listen Before Talk (LBT) is a traffic driven contention-based channel sensing mechanism for LAA that is much similar to DCF of WiFi designed to address the coexistence issues described in Chapter 1. This protocol makes it possible for multiple stations to share the same channel and can also be used to find a free radio channel. LBT is considered as a global standard for LAA channel sensing and has been mandated in many parts of the world. This mechanism allows LTE to share an unlicensed spectrum with WiFi maintaining the performance of individual systems. There are four different categories of LBT.

- LBT-Cat1 (No LBT): No LBT is performed before any transmission, such as LTE-U system.
- LBT-Cat2 (LBT without random backoff): The duration of time between when the channel is sensed to be idle and when a station transmits is deterministic.

- LBT-Cat3 (LBT with random backoff contention window of fixed size): The duration of time between when the channel is sensed to be idle and when a station transmits is a random number within a fixed contention window size.

- LBT-Cat4 (LBT with random backoff CW of variable size): The backoff mechanism is similar to WiFi where a random number is drawn within a CW size and this CW size doubles every time the station finds the channel busy after countdown timer expires. This exponential backoff may happen for several stages until a maximum CW limit is reached. At this stage, the CW size will remain at the maximum size until the channel is sensed idle. Cat-4 takes a longer time and has a lower success rate as compared to other LBT procedures, but offers fairness with other unlicensed network nodes.

2.3 Multi-Carrier LBT

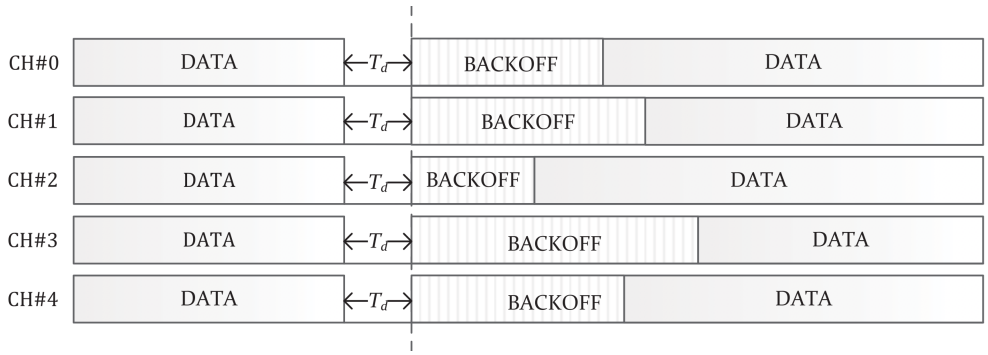

Figure 2.4: Multi-Carrier LBT

Multi-Carrier LBT is a process by which a station having an ability to sense multiples carriers can run LBT procedure in each channel and can utilize portions of whichever spectrum it finds free for transmission of data. Fig. 2.4 shows that in a multi-carrier LBT, a transmitter runs an independent backoff process for each carrier and can thus explore each channel opportunistically. After a carrier is sensed idle for DIFS period T_d, a different random backoff is generated for each carrier and the data transmission starts when the countdown expires and the corresponding channel is idle. A hybrid design of LBT that realizes carrier

grouping and can determine division of carriers into multiple groups with a guard band in between has been studied in [68].

2.4 Carrier Aggregation of Component Carriers

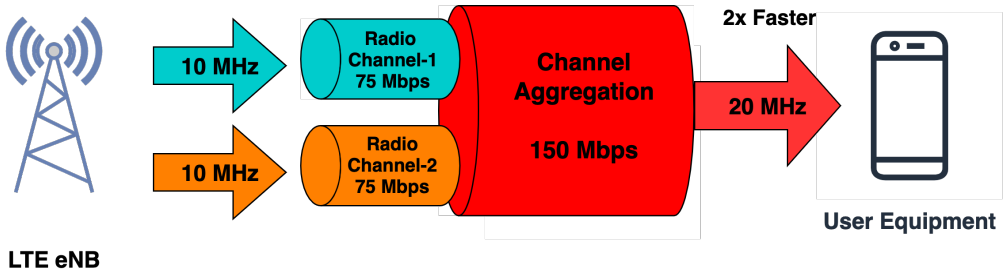

Figure 2.5: Carrier Aggregation of two carriers in Unlicensed Band

Carrier Aggregation (CA) is a feature of LTE-Advanced which allows LTE eNB to combine two or more LTE component carriers into a single data channel, which increases the overall capacity by exploiting fragmented spectrum. Each aggregated carrier is referred to as a Component Carrier (CC). Fig 2.5 shows a case where an LTE eNB is able to aggregate two 75 Mbps channels into a single 150 Mbps channel to provide two times faster speeds. There are two types of carrier aggregation as shown in Fig. 2.6. Type of carrier aggregation possible is limited by the transceiver design in the LTE and the availability of free CCs in single or different bands.

1. Intra-Band Carrier Aggregation: This type of carrier aggregation uses only a single band and can be further divided into:

    - Continuous: In this type of aggregation, CCs (for example two each with 5 MHz band) are adjacent to each other in a single-band (20 MHz), requiring only a single transceiver.
    - Non-Continuous: In this type of aggregation, CCs are not adjacent to each other in a single-band, requiring two transceivers which increases complexity and cost.

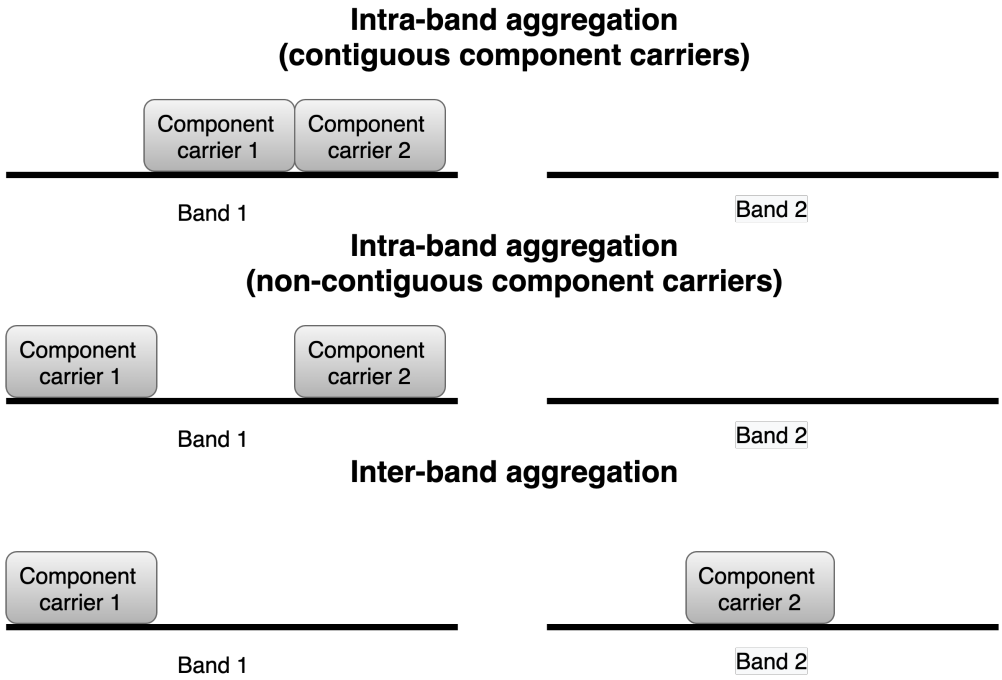

Figure 2.6: Carrier Aggregation

2. Inter-Band Carrier Aggregation: This type of carrier aggregation combined two CCs from two different bands (each 20 MHz) and also requires multiple transceivers to transmit/receive signals which increases cost, complexity and creates space constraints.

Basic LTE component carriers can have a bandwidth of 1.4, 3, 5, 10, 15 or 20 MHz. LTE-Advanced can aggregate a maximum of five component carriers with a maximum bandwidth of 100 MHz. Using five aggregated CCs, Multiple Input Multiple Output (MIMO) and 256 Quadrature Amplitude Modulation (QAM) allows theoretical data rates up to 2 Gbps. The capability of carrier aggregation is also utilized in the deployments of 5G and WiGig networks.

CHAPTER 3

THROUGHPUT AND AIRTIME/COT TRADE-OFF

We saw in Chapter 1 and Chapter 2 that LAA operating in an unlicensed band severely impacts the incumbent WiFi and figuring out how to obtain optimal coexistence between LAA and WiFi with acceptable fairness is a primary challenge. In this chapter, we lay out the necessary analytical framework for coexistence based on a steady-state analysis of the Markov Chain. We will show how a contention window size is an important parameter for LAA systems to adjust throughput and airtime fairness. We will show how an inherent trade-off exists between throughput fairness and airtime fairness while trying to adjust the contention window size parameter of LAA and that both fairness could not be met simultaneously. We will also show the extent of this trade-off for different cases and compare the performances of LAA-Cat4 and LAA-Cat3 coexisting with WiFi.

Section 3.2 models the coexistence of LAA and WiFi as a coupling between two MCs of LAA and WiFi. Section 3.3 derives the throughput and airtime of LAA and WiFi networks and describes different fairness metric to analyze the coexistence. Section 3.4 states the coexistence problem of optimizing the CW size of LAA stations to obtain a maximum fitness that accounts for total throughput and combined throughput-airtime fairness. Section 3.5 introduces the scenario under which the fair coexistence between LAA and WiFi is analyzed. Finally, the results are discussed in Section 3.6.

3.1 Terminologies

3.1.1 Throughput

A typical LTE that utilizes 10 MHz with 64 QAM modulation has a maximum data rate of 75 Mbps in downlink. LTE-Advanced with 3 component carrier aggregation with

same modulation can achieve a peak data rate of 300 Mbps in the downlink. Throughput refers to the amount of effective data that can be transferred in a given amount of time. In other words, even if the data is transmitted at a higher data rate, due to several factors like congestion, collision and channel quality, the perceived rate, i.e., the throughput, might be much less.

3.1.2 Airtime/COT

We define airtime or Channel Occupancy Time (COT) to be the percentage of time that a carrier occupies the channel for the successful transmission of the packets. Generally, WiFi APs have lower data-rates than LAA eNBs so that eNBs require a much shorter time duration than APs to transmit the same data packet size, resulting in much lower airtime for LAA than WiFi to transmit the same packet size.

3.1.3 Fairness Index

Jain's fairness index is one of the fairness metrics that determines whether users are receiving a fair share of system resources. In networking, the Jain's fairness index (3.1)

$$J(x_1, x_2, \ldots, x_n) = \frac{(\sum_{i=1}^{n} x_i)^2}{n \sum_{i=1}^{n} x_i^2} = \frac{\overline{\mathbf{x}}^2}{\overline{\mathbf{x}^2}} \tag{3.1}$$

rates the fairness of a set of values where there are n users, x_i is the throughput for the i^{th} user. The result ranges from $\frac{1}{n}$ (worst case) to 1 (best case), and is maximum when all users receive the same allocation i.e. x_i's are close to each other. The notion can be extended to incorporate not just throughput but also other measures of performance such as airtime.

3.2 System Model

We consider a scenario where N_l LAA eNBs and N_w WiFi APs share a channel in an unlicensed band as shown in Fig. 3.1. We further assume that each node can detect the presence of other nodes within a carrier sense threshold and there is no hidden node problem. As described in Section 2.2, LTE and WiFi systems adopt different channel access

schemes. WiFi uses the CSMA mechanism with exponential backoff counter to sense and yield the channel before any transmission. We consider two access mechanisms LBT-Cat3 and LBT-Cat4 for LAA. We consider two broad cases: 1) LAA-Cat4 eNBs coexisting with WiFi and 2) LAA-Cat3 eNBs coexisting with WiFi.

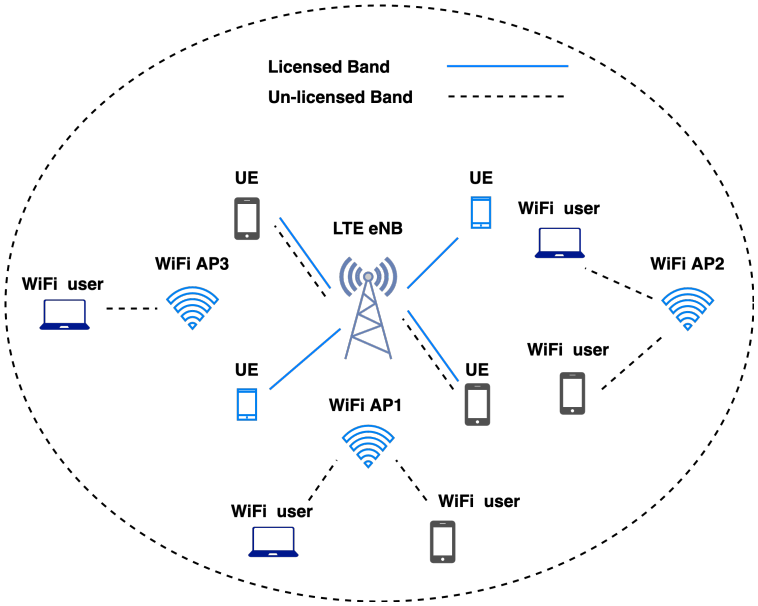

Figure 3.1: System Model for a Single Carrier

Throughput analysis of WiFi-DCF and LAA using Markov Chain (MC) steady-state analysis is well studied in the literature [1] [46] [42]. We will use the same model to analyze the effect of LTE CW size on throughput and airtime of individual WiFi and LTE network and determine the fairness achieved in different scenarios.

3.2.1 Markov Chain of WiFi

The channel access mechanism for WiFi as described in Section 2.2.2 is modeled as a 2D Markov process as shown in Fig. 3.2(a) characterized by states $(w(t), b(t))$ [1], where $w(t)$ represents the current contention window size and b(t) the backoff counter. Parameter q_w denotes the probability of packet availability for transmission and is used to indicate traffic load intensity. $q_w = 1$ refers to maximum load with transmit buffer always full and $q_w = 0$ refers to no load. $p_{f,w}$ is the probability of packet failure due to collision. The random

backoff starts with an initial contention window size of W_0 and increases exponentially at each stage $W_i = 2W_{i-1}$ to a maximum of $W_m = 2^m W_0$ at the final backoff stage m. The AP at the final backoff stage m will remain at the highest backoff stage in case of packet failure, or returns back to first stage in case of success.

With steady-state analysis described in (3.2), the probability that an AP transmits in a randomly chosen slot time is given by (3.3).

$$
\begin{cases}
b_{wait} = (1-q)b_{wait} + (1-p_{f,w})\sum_{i=0}^{m} b_{i,0} \quad , \quad i \in (0,m) \\
b_{0,W_0-1} = \frac{q}{W_0} b_{wait} + p_{f,w} b_{0,W_0-1} \\
b_{0,j} = \frac{q}{W_0} b_{wait} + p_{f,w} b_{0,j} + (1-p_{f,w}) b_{0,j+1} \quad , \quad j \in (1, W_0 - 1) \\
b_{0,0} = \frac{q}{W_0} b_{wait} (1-p_{f,w}) b_{0,1} \\
b_{i,W_i-1} = \frac{p_{f,w}}{W_i} b_{i-1,0} + p_{f,w} b_{i,W_i-1} \quad , \quad i \in (1, m-1) \\
b_{i,j} = \frac{p_{f,w}}{W_i} b_{i-1,0} + p_{f,w} b_{i,j} + (1-p_{f,w}) b_{i,j+1} \quad , \quad i \in (1, m-1), j \in (1, W_i - 2) \\
b_{i,0} = \frac{p_{f,w}}{W_i} b_{i-1,0} + (1-p_{f,w}) b_{i,1} \quad , \quad i \in (1, m-1) \\
b_{m,W_m} = \frac{p_{f,w}}{W_m} (b_{m-1,0} + b_{m,0}) + p_{f,w} b_{m,W_m-1}) \\
b_{m,j} = \frac{p_{f,w}}{W_m} (b_{m-1,0} + b_{m,0}) + p_{f,w} b_{m,j} + (1-p_{f,w}) b_{m,j+1} \quad , \quad j \in (1, W_m - 2) \\
b_{m,0} = \frac{p_{f,w}}{W_m} (b_{m-1,0} + b_{m,0}) + (1-p_{f,w}) b_{m,1} \\
b_{wait} + \sum_{i=0}^{m} \sum_{j=0}^{W_i} b_{i,j} = 1
\end{cases}
\tag{3.2}
$$

$$
\tau_w = \frac{2q_w(1-p_{f,w})(1-2p_{f,w})}{2(1-p_{f,w})^2(1-2p_{f,w}) + q_w[W_0 p_{f,w}(1-(2p_{f,w})^m) + (1+W_0-2p_{f,w})(1-2p_{f,w})]} \tag{3.3}
$$

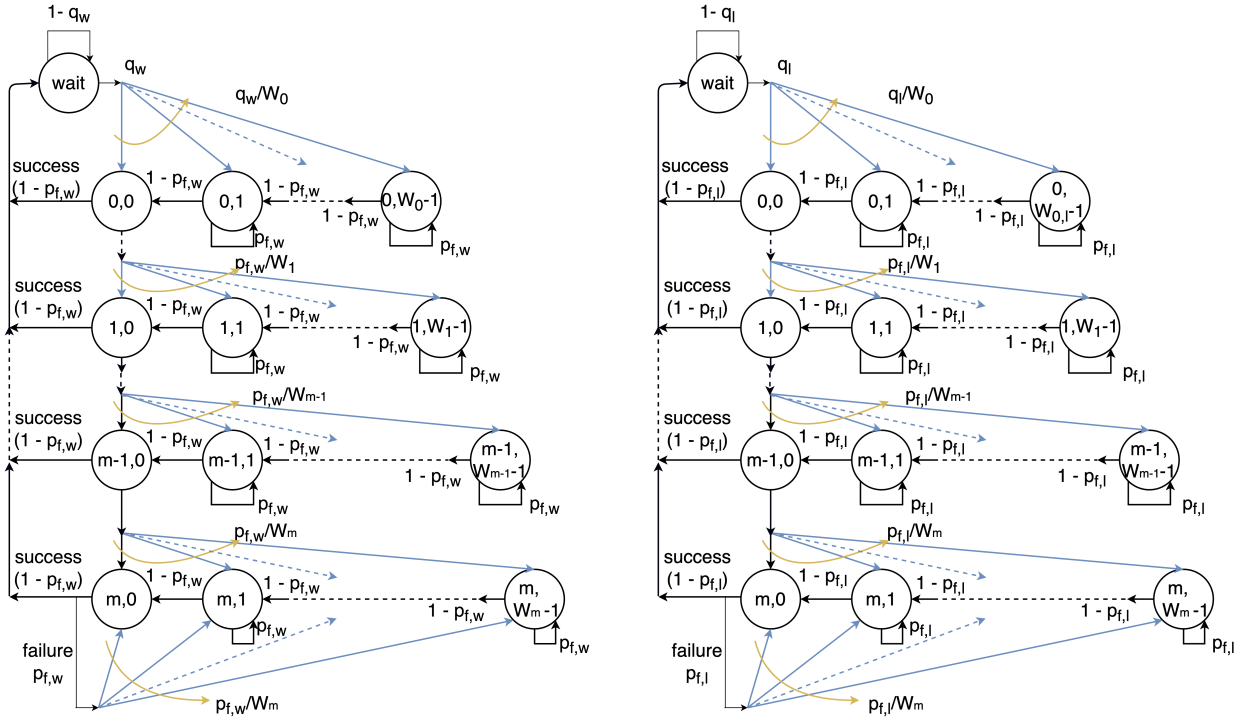

(a) WiFi Markov Chain (b) LAA-Cat4 Markov Chain

Figure 3.2: Markov Chain for WiFi and LAA-Cat4

3.2.2 Markov Chain of LAA-Cat4

Fig 3.2(b) shows the Markov Chain model for LAA-Cat4 channel access mechanism as described in Section 2.2.4. The LAA-Cat4 MC is similar to that of WiFi MC in the sense of having multiple stages with exponential backoff. But in contrast to WiFi which has a fixed initial contention window size of $W_0 = 16$, the initial contention window size W of LAA can be varied. Total number of stages m for LAA-Cat4 is still fixed at 6 similar to WiFi.

Similar to that of WiFi, the probability that an LAA-Cat4 eNB transmits in a randomly chosen slot time is given by (3.4).

$$\tau_l = \frac{2q_l(1-p_{f,l})(1-2p_{f,l})}{2(1-p_{f,l})^2(1-2p_{f,l}) + q_l[Wp_{f,l}(1-(2p_{f,l})^m) + (1+W-2p_{f,l})(1-2p_{f,l})]} \tag{3.4}$$

3.2.3 Markov Chain of LAA-Cat3

Fig 3.3 shows the Markov Chain model for LAA-Cat3 channel access mechanism as described in Section 2.2.4. In contrast to LBT-Cat4, there is no exponential backoff in LBT-Cat3. Similar to LAA-Cat4, the contention window size W can also be varied.

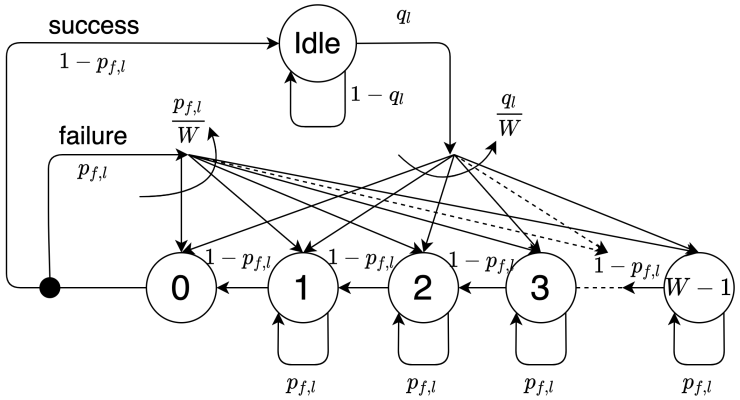

Figure 3.3: Markov Chain for LAA-Cat3

$$
\begin{cases}
b_{wait} = (1-p_{f,l})b_0 + (1-q_l)b_{wait} \\
b_{wait} = \dfrac{1-p_{f,l}}{q} b_0 \\
b_i = p_{f,l} b_i + \frac{q_l}{W} b_{wait} + \frac{p_{f,l}}{W} b_0 + (1-p_{f,l}) b_{i+1} \quad , i = 1, 2, \ldots, W-1 \\
b_i = b_{W-(W-i)} = \frac{W-i}{W} \frac{b_0}{(1-p_{f,l})} \\
1 = b_{wait} + b_0 + \sum_{i=1}^{W-1} b_i
\end{cases}
\tag{3.5}
$$

Using the steady-state analysis of the MC from (3.5), the probability that an LAA-Cat3 eNB transmits in a randomly chosen slot time is given by (3.6).

$$
\tau_l = \frac{2q_l(1-p_{f,l})}{2(1-p_{f,l})^2 + 2q_l(1-p_{f,l}) + q_l(W-1)} \tag{3.6}
$$

3.3 Performance Analysis

3.3.1 Probability of Transmission Failure

The probability of transmission failure for LAA and WiFi when both coexist is calculated from (3.7).

$$\begin{cases} p_{f,w} = 1 - (1 - \tau_w)^{N_w - 1}(1 - \tau_l)^{N_l} \\ p_{f,l} = 1 - (1 - \tau_l)^{N_l - 1}(1 - \tau_w)^{N_w} \end{cases} \tag{3.7}$$

Equations (3.4), (3.3) and (3.7) need to be solved iteratively to find the values of both transmission and failure probabilities in case of coexistence between LAA-Cat4 and WiFi. Similarly equations (3.6), (3.3) and (3.7) need to be solved for the coexistence between LAA-Cat3 and WiFi.

The iteration starts with an initial guess of $\tau_l = \tau_w = 0.1$ and $p_{f,w} = p_{f,l} = 0.1$. At each iteration, value of τ is refined with known value of p_f and value of p_f is further refined with new calculated value of τ. This is carried out for multiple iterations until the values of all unknown variables converge. The convergence and uniqueness of the solution is guaranteed by a monotonic function described in [1].

3.3.2 Probabilities of events

The throughput and airtime that a station eNB or AP achieves in a coexistence scenario can be characterized by what events take place in a randomly chosen slot time. Three events need to be considered.

1. Idle: The channel is not utilized by any eNB or AP.

2. Success: The channel is utilized for successful transmission if only one station; either an eNB or a WiFi, accesses the channel.

3. Collision: The channel is utilized for transmission but the packet fails due to collision;

either within WiFi network itself, or within LAA network itself, or between WiFi and LAA.

Given the transmission probability of LAA from (3.4) or (3.6) and WiFi from (3.3), the corresponding probability for

- channel being idle P_I,
- channel occupied by successful transmission by LAA (or WiFi) $P_{s,l}$ (or $P_{s,w}$),
- channel contains packet collisions within own system $P_{c,l}$ ($P_{c,w}$), and collision between WiFi and LAA $P_{c,wl}$

are calculated from (3.8).

$$\begin{cases} P_I = (1-\tau_w)^{N_w}(1-\tau_l)^{N_l} \\ P_{s,w} = N_w\tau_w(1-\tau_w)^{N_w-1}(1-\tau_l)^{N_l} \\ P_{s,l} = N_l\tau_l(1-\tau_l)^{N_l-1}(1-\tau_w)^{N_w} \\ P_{c,w} = (1-\tau_l)^{N_l}(1-(1-\tau_w)^{N_w} - N_w\tau_w(1-\tau_w)^{N_w-1}) \\ P_{c,l} = (1-\tau_w)^{N_w}(1-(1-\tau_l)^{N_l} - N_l\tau_l(1-\tau_l)^{N_l-1}) \\ P_{c,wl} = 1 - P_I - P_{s,w} - P_{s,l} - P_{c,w} - P_{c,l} \end{cases} \tag{3.8}$$

3.3.3 Average Time Duration of events

Fig. 3.4 shows the average duration of successful transmission and collision when average payload size $E[P]$ along with the headers are transmitted in a channel according to the protocol as described in Section 2.2.2.

The average time that the channel is occupied due to successful transmission by LAA (or WiFi) $T_{s,l}$ (or $T_{s,w}$) and the average time that the channel is busy due to transmission collision $T_{c,l}$ ($T_{c,w}$) is given by (3.9). $T_{c,wl}$ denotes the time duration of event when there is a collision between WiFi and LAA.

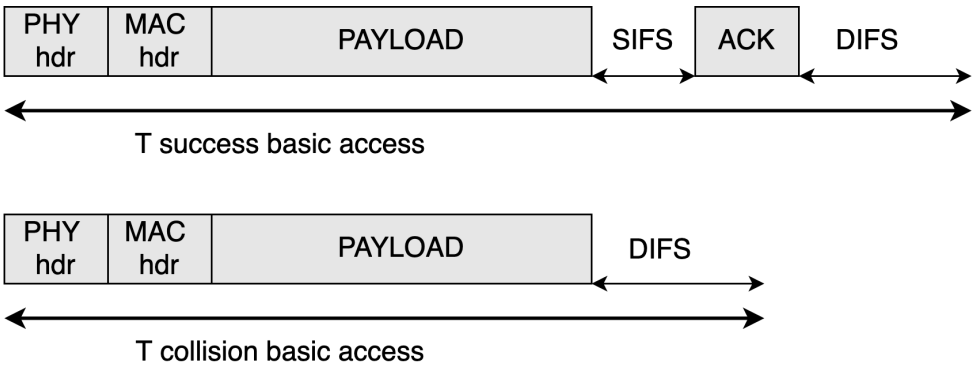

Figure 3.4: Average Time for successful transmission and collision in basic access

$$\begin{cases} T_{s,w} = \dfrac{\text{PHY}_{hdr} + \text{MAC}_{hdr} + E[P] + \text{ACK}}{R_w} + \delta + \text{SIFS} + \text{DIFS} + \delta \\ T_{c,w} = \dfrac{\text{PHY}_{hdr} + \text{MAC}_{hdr} + E[P]}{R_w} + \text{DIFS} + \delta \\ T_{s,l} = \dfrac{\text{PHY}_{hdr} + \text{MAC}_{hdr} + E[P] + \text{ACK}}{R_l} + \delta + \text{DIFS} + \delta \\ T_{c,l} = \dfrac{\text{PHY}_{hdr} + \text{MAC}_{hdr} + E[P]}{R_l} + \text{DIFS} + \delta \\ T_{c,wl} = \max(T_{c,w}, T_{c,l}) \end{cases} \tag{3.9}$$

where δ is the propagation delay and R_l and R_w are the peak data rates used by LAA and WiFi stations to transmit the data. The values for these system parameters differ depending on the access mechanism (basic or RTS/CTS) and modulation chosen. Table 3.1 shows a typical value of the system parameters we chose for our coexistence setup which is further discussed in Section 3.5.

LAA is assumed to use the same frame structure as WiFi but the ACK is sent immediately when the receiver receives the packet.

3.3.4 Throughput and Airtime

Having calculated the event probabilities in Section 3.3.2 and average time duration of the events in Section 3.3.3, the average event time duration $E[T]$ is calculated from (3.10).

$$E[T] = P_I\sigma + P_{s,l}T_{s,l} + P_{s,w}T_{s,w} + P_{c,l}T_{c,l} + P_{c,w}T_{c,w} + P_{c,wl}T_{c,wl} \tag{3.10}$$

Throughput of LAA and WiFi is given by (3.11).

$$S_l = \frac{P_{s,l}}{E[T]}E[P_l] \quad , \quad S_w = \frac{P_{s,w}}{E[T]}E[P_w] \tag{3.11}$$

Airtime of LAA and WiFi is given by (3.12)

$$A_l = \frac{P_{s,l}T_{s,l}}{E[T]} \quad , \quad A_w = \frac{P_{s,w}T_{s,w}}{E[T]} \tag{3.12}$$

where $E[P_l]$ and $E[P_w]$ denote the average packet size for LAA and WiFi correspondingly.

3.3.5 Fairness Metric

As described in Section 3.1.3, fairness in channel access and performance output of different stations is measured in terms of Jain's fairness index (3.1). We consider three different fairness indices:

1. Throughput fairness F_S determines the fair share of throughput between LAA and WiFi

2. Airtime fairness F_A determines the fair share of channel airtime between LAA and WiFi

3. Throughput-Airtime fairness F_{SA} which is a harmonic mean between two metrics F_S and F_A, captures the notion of trade-off optimization of both fairness in combination. The harmonic mean cannot be made arbitrarily large by changing some values to bigger ones while having at least one value unchanged. Jain's fairness index ensures that all throughput (or airtime) are similar while the harmonic mean ensures that both

throughput and airtime fairness are high. All fairness metrics have a maximum value of 1 and a higher value indicates a better fairness.

For only two networks LAA and WiFi, these are calculated from (3.13).

$$\begin{cases} F_S = \dfrac{(S_L + S_W)^2}{2(S_L^2 + S_W^2)} \\ F_A = \dfrac{(A_L + A_W)^2}{2(A_L^2 + A_W^2)} \\ F_{SA} = 2\dfrac{F_S \times F_A}{F_S + F_A} \end{cases} \tag{3.13}$$

3.3.6 Fitness Metric

Besides fair sharing resources, we also want to get maximum throughput achievable in a given coexistence scenario. Hence, we define a fitness metric J in (3.14) which takes into consideration both fairness and overall throughput.

$$J = F_{SA}(S_W + S_L) \tag{3.14}$$

3.4 Problem Statement

For a fair coexistence of LAA (Cat4 or Cat3) with WiFi, we want to find the optimized value of contention window size W_{opt} from different choices $\mathcal{W} = [W_1, W_2, \ldots, W_k]$ that maximizes the fitness metric in (3.14) which depends on number of LAA eNBs and WiFi APs.

$$W_{opt} = \arg \underset{W \in \mathcal{W}}{\text{maximize}}\ J(N_L, N_W, W) \tag{3.15}$$

Since the search space is small, we use exhaustive brute-force to search for the best CW size with time complexity $O(|\mathcal{W}|)$.

Table 3.1: System Parameters

Packet Size, $E[P_w] = E[P_l]$	12800 bits
MAC header	272 bits
PHY header	128 bits
ACK	112 bits + PHY header
Wi-Fi Bit Rate, R_w	40 Mbps
LAA Bit Rate, R_l	75 Mbps
Slot Time σ	9 μs
SIFS	16 μs
DIFS	34 μs
Propagation Delay, δ	1 μs
CW-Cat4	[8:1:24]
CW-Cat3	[8:1:80]
Initial CW size Wi-Fi, W_0	16
CW Stages Wi-Fi & Cat4, m	6
load intensity, q	1.0

3.5 Scenario-Setup

We consider two scenarios: 1) when LAA-Cat4 coexist with WiFi and 2) when LAA-Cat3 coexist with WiFi. In both scenarios we consider $N_l = \{1, 2, \ldots, 7\}$ LAA eNBs contending with $N_w = 3$ WiFi APs on a single channel with system parameters from Table 3.1. Different choices for CW sizes are $\mathcal{W} = \{8, 9, \ldots, 24\}$ and $\mathcal{W} = \{8, 9, \ldots, 80\}$ for LAA-Cat4 and LAA-Cat3 respectively. Since Cat3 is linear and Cat4 is exponential in back-off nature, the maximum value for Cat3-CW size of 80 is chosen to be much higher than the maximum value for Cat4-CW size of 24.

3.6 Results and Discussion

3.6.1 Coexistence of LAA-WiFi without CW adjustment

We first establish a baseline with reference to which we will compare our optimized results. With no CW adjustments, both LAA-Cat3 and LAA-Cat4 would contend on a channel with incumbent WiFi, with a CW size of 16 which matches WiFi's initial CW size.

For LAA-Cat4-WiFi coexistence, with fixed number of WiFi APs $N_w = 3$, increase

in the number of LAA eNBs N_l improves both the throughput and airtime of LAA at the expense of WiFis performance as shown in Fig. 3.5(a). For lower values of N_l than N_w, LAA has both low airtime and throughput, and has low impact on WiFi. But for higher values of N_l, the channel is significantly occupied by LAA transmissions and the WiFi performance degrades further. Since we are not adjusting the CW sizes, all stations are similar and the network that has more number of stations dominates the channel.

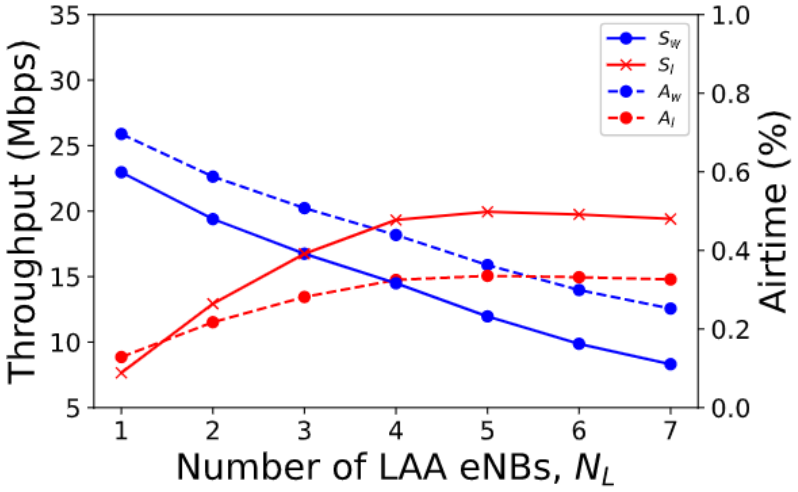

(a) LAA-Cat4-WiFi

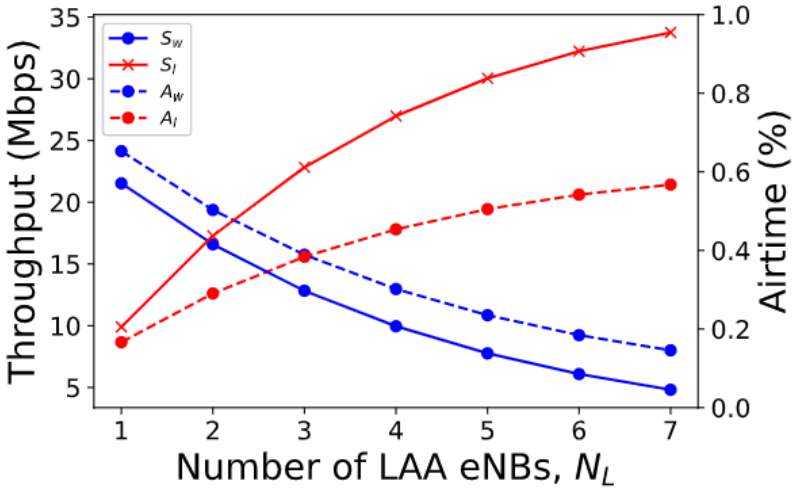

(b) LAA-Cat3-WiFi

Figure 3.5: Throughput and Airtime of LAA-WiFi coexistence without CW adjustment for $N_w = 3$

For LAA-Cat3-WiFi coexistence with similar setup, we observe similar impacts on the performance of WiFi as shown in Fig. 3.5(b). Since LAA-Cat3 doesn't have any exponential backoff stages, it is more aggressive in accessing the channel and degrades the performance of WiFi even greater than LAA-Cat4. For the case of contention without CW adjustment, it is known in the study that LAA-Cat4 coexists with WiFi more fairly than LAA-Cat3 [42]. This is also evident from Fig. 3.6 where the combined fairness performance from (3.13) remains fairly high for LAA-Cat4 than LAA-Cat3 for higher N_l.

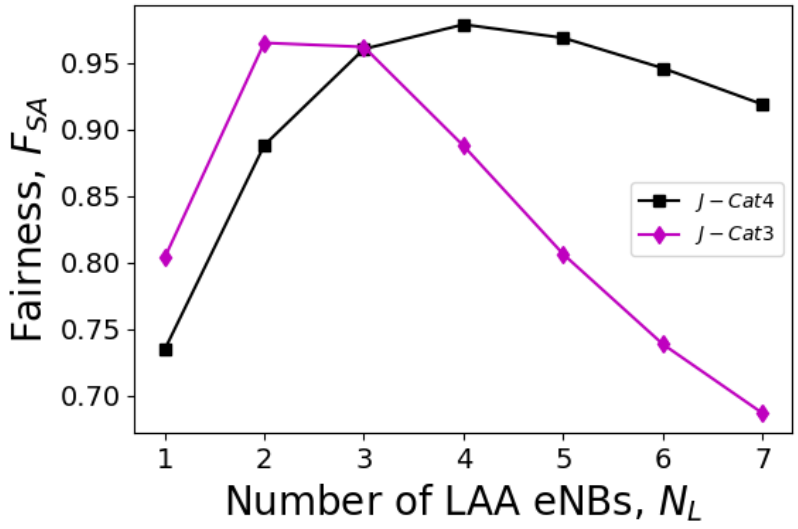

Figure 3.6: Performance of LAA-Cat4 and LAA-Cat3

3.6.2 Coexistence performance for specific scenario (N_l, N_w) with adjustable CW sizes

We analyze the performance of coexistence when the CW is dynamic and adjustable depending upon the scenario (N_l, N_w). We consider a coexistence scenario ($N_l = 4$, $N_w = 3$) where CW size W can be varied among different choices $\mathcal{W}$ for LAA-Cat4 and LAA-Cat3 respectively as discussed in Section 3.5. The CW size for LAA-Cat3 is longer since it only has a single stage for linear backoff while LAA-Cat4 has exponential backoff with m stages.

We first consider a scenario where $N_l = 4$ LAA-Cat4 eNBs contend with $N_w = 3$ APs using various adjustable CW sizes. Fig 3.7(a) shows the throughput and airtime achieved for this scenario. Smaller values of CW sizes give more chance for LAA than WiFi to access the

channel which in turn increases the airtime and throughput for LAA and decreases both for WiFi. Larger values of CW sizes give more opportunity for WiFi to access the channel which increases the airtime and throughput of WiFi but the LAA network is not able to access the channel enough to maintain its airtime and throughput. There exists an optimized value of CW which gives more or less equal access to channel for both LAA and WiFi. This equal access to channel could be defined either in-terms of similar throughput or similar airtime.

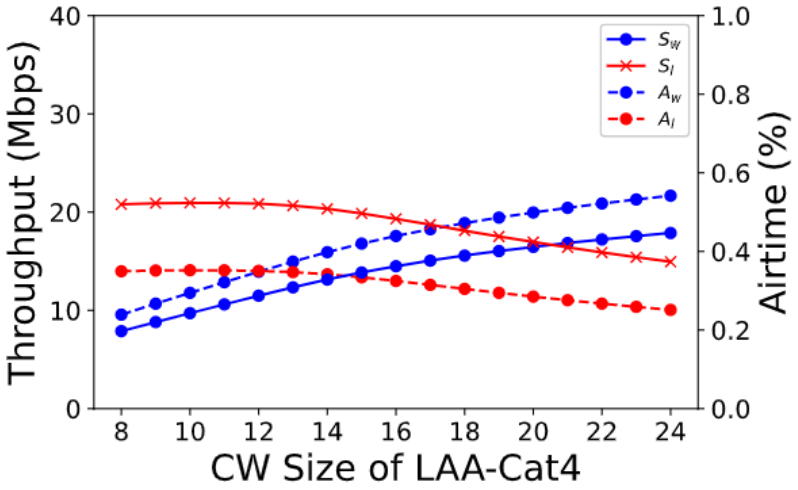

(a) LAA-Cat4-WiFi

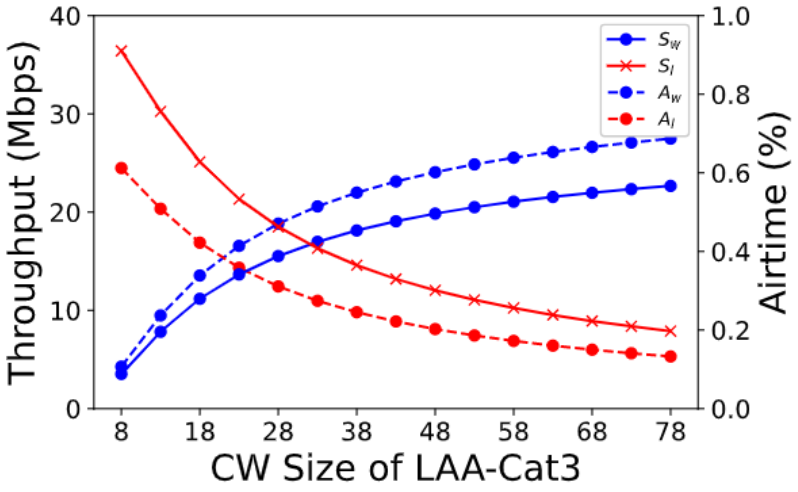

(b) LAA-Cat3-WiFi

Figure 3.7: Throughput and Airtime of LAA-WiFi coexistence with CW adjustment for $N_l = 4, N_w = 3$

It can be seen from Fig. 3.7(a) that throughput for WiFi and LAA is similar at a CW size of 21 whereas airtime for WiFi and LAA is similar at a CW size of 12. This happens mainly because of the higher data rate for LAA in comparison to WiFi. LAA obtains higher throughput at a relatively lower time than WiFi. Hence there inherently exists a trade-off while trying to optimize the CW size for throughput and airtime fairness between LAA and WiFi. Both fairness cannot be achieved generally at the same CW size.

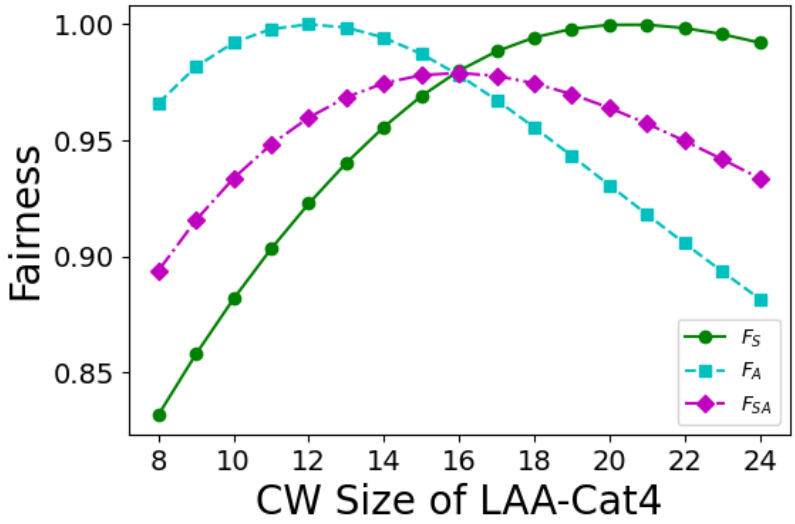

(a) LAA-Cat4-WiFi

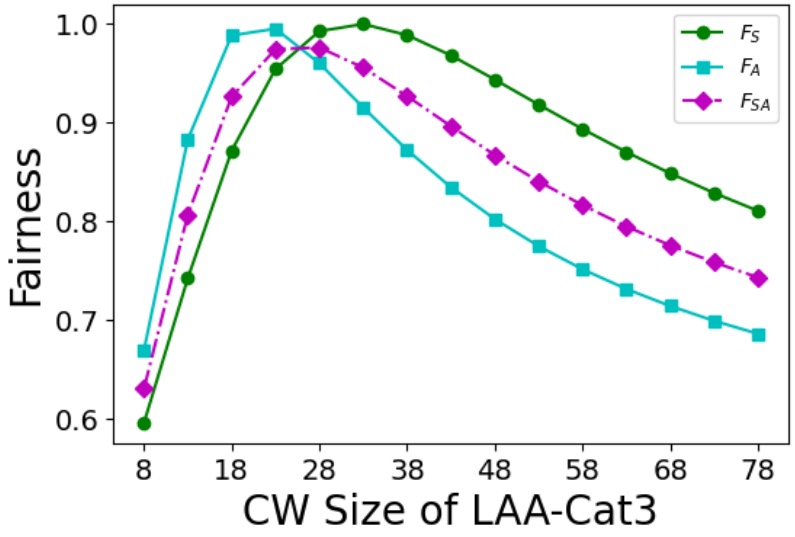

(b) LAA-Cat3-WiFi

Figure 3.8: Fairness of LAA-WiFi coexistence with CW adjustment for $N_l = 4, N_w = 3$

This is also evident from Fig. 3.8(a), where we can see the maximum value of throughput fairness and airtime fairness from (3.13) does not occur at the same CW size. Thus we consider the fitness metric from (3.14) which takes into account both fairness and total throughput. Thus an optimized CW size of 16 is chosen to be the best CW size for scenario ($N_l = 4$, $N_w = 3$) that maximizes the fitness and is shown in Fig 3.9(a). Optimization of CW for general scenario (N_l, $N_w = 3$) is further discussed in Section 3.6.3.

A similar trade-off for choosing the best CW size is also observed in LAA-Cat3-WiFi coexistence. Throughput-Airtime in Fig. 3.7(b), fairness in Fig. 3.8(b) and fitness in Fig. 3.9(b) show that the best values of CW sizes that maximizes the throughput fairness, airtime fairness and overall fitness are achieved at 32, 21 and 22 respectively.

3.6.3 Optimization of CW for different scenarios

We find the best CW size for different scenarios (N_l, $N_w = 3$), $N_l = 1, 2, \ldots, 7$ similarly as was done for specific scenario ($N_l = 4$, $N_w = 3$) in Section 3.6.2. The best CW sizes for Cat4 and Cat3 are tabulated in Table 3.2. Fig. 3.9 shows fitness performances of Cat4 and Cat3 for various CW sizes for three specific scenarios ($N_l = 2, 3, 4$, $N_w = 3$). It is observed from the Fig. 3.9(a) that depending on scenario (N_l, N_w), the best CW size that maximizes the fitness changes. It is also observed that the best CW size 16 for larger number of LAA eNBs($N_l = 4$, $N_w = 3$) is higher than the best CW size 8 for smaller number of LAA eNBs ($N_l = 2$, $N_w = 3$). This happens because for smaller N_l, LAA tries to aggressively access the channel more with smaller CW size and for larger N_l, LAA gives more opportunity for WiFi to access the channel with larger CW size. LAA does this to obtain maximum fitness. It is to be noted that smaller CW sizes of LAA do decrease the fairness but yield higher total throughput effectively causing higher fitness, which is defined to incorporate both fairness and total throughput.

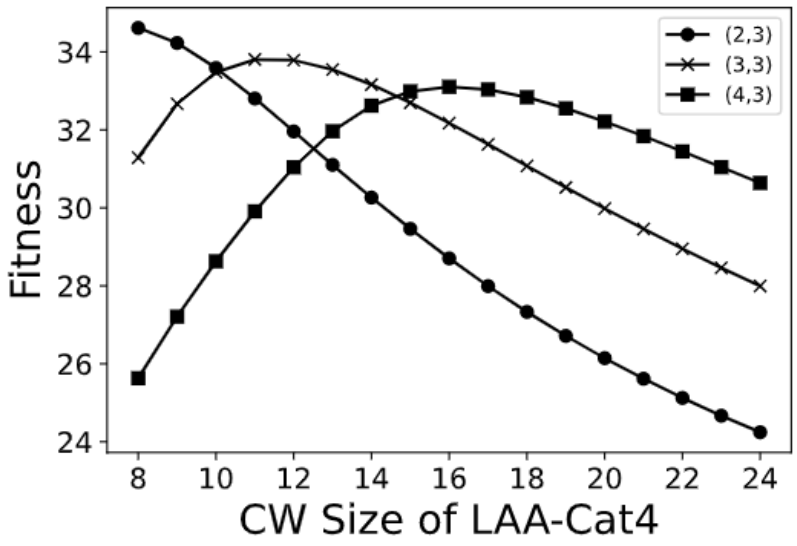

(a) LAA-Cat4-WiFi

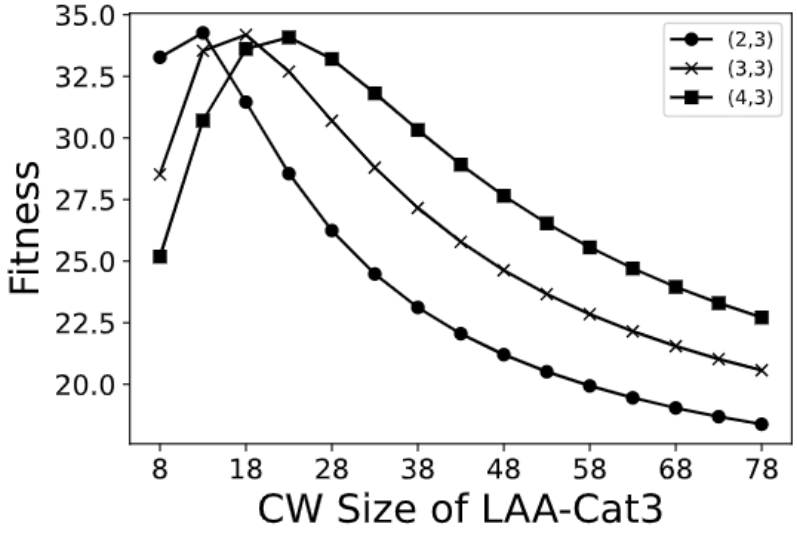

(b) LAA-Cat3-WiFi

Figure 3.9: Optimized CW for different scenarios (N_l, $N_w = 3$)

Table 3.2: Optimized CW for different scenarios (N_l, $N_w = 3$)

N_l	CW-Cat4	CW-Cat3
1	8	8
2	8	11
3	11	16
4	16	22
5	21	27
6	24	32
7	24	38

3.6.4 Improvement on the impact of LAA on WiFi by adjusting the CW size

With best CW size determined for a scenario (N_l, N_w) as described in Section 3.6.3, we are able to optimize the fitness for any number of LAA eNBs coexisting with WiFi APs. Figs. 3.10, 3.11 and 3.12 show the improvement of fitness, throughput and airtime we get by optimizing the CW size with respect to the case without CW adjustments.

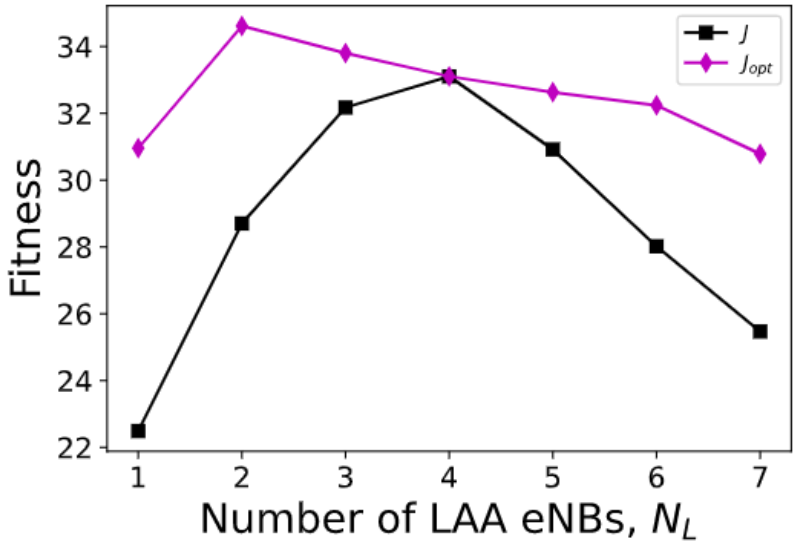

(a) LAA-Cat4-WiFi

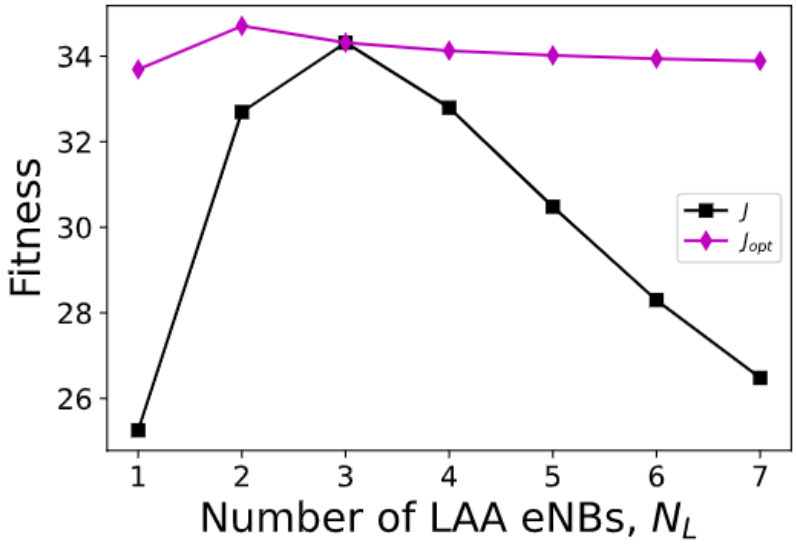

(b) LAA-Cat3-WiFi

Figure 3.10: Fitness improvement of optimizing CW size for various scenarios (N_l, $N_w = 3$)

It is seen from Fig. 3.10 that both LAA-Cat3 and Cat4 achieve more fitness when we optimize the value of CW size in comparison to the case without CW adjustment. LAA-Cat3 achieves more stable fitness than LAA-Cat4. This happens mainly because the CW adjustment is linear in Cat3 and exponential in Cat4. This gives Cat3 more granular control over the adjustment of CW.

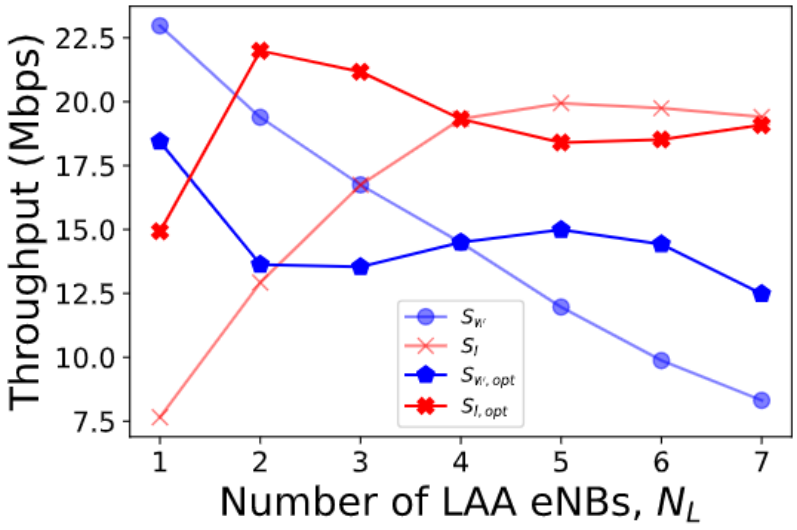

(a) LAA-Cat4-WiFi

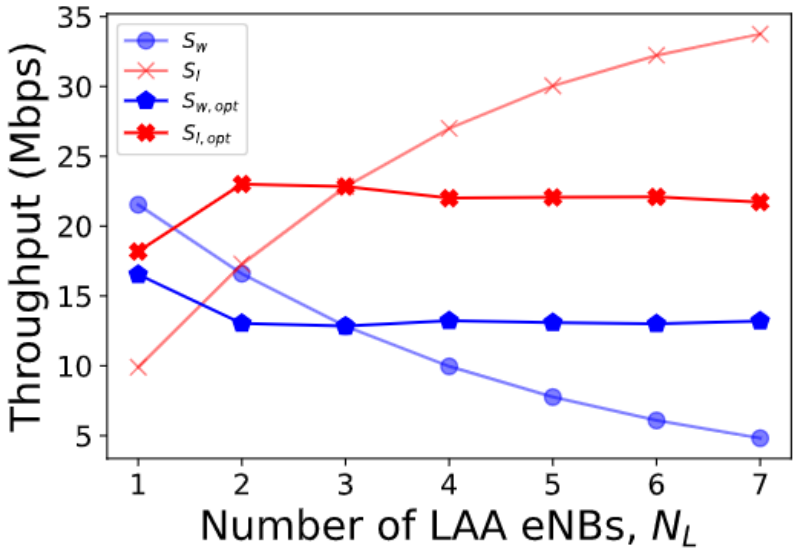

(b) LAA-Cat3-WiFi

Figure 3.11: Throughput improvement for various scenarios (N_l, $N_w = 3$)

Figs. 3.11 and 3.12 show that by optimizing CW size as obtained from Table 3.2, LAA-Cat4 and Cat3 balance out the throughput and airtime of both LAA and WiFi with respect to the case without CW adjustment.

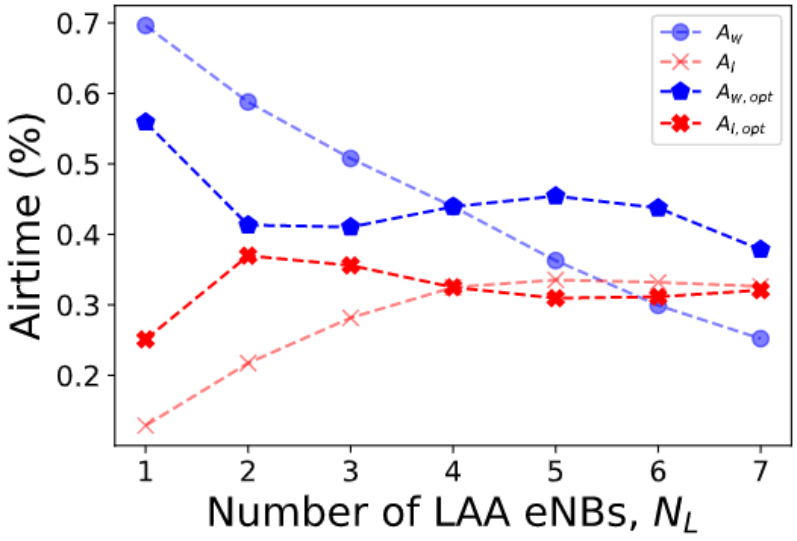

(a) LAA-Cat4-WiFi

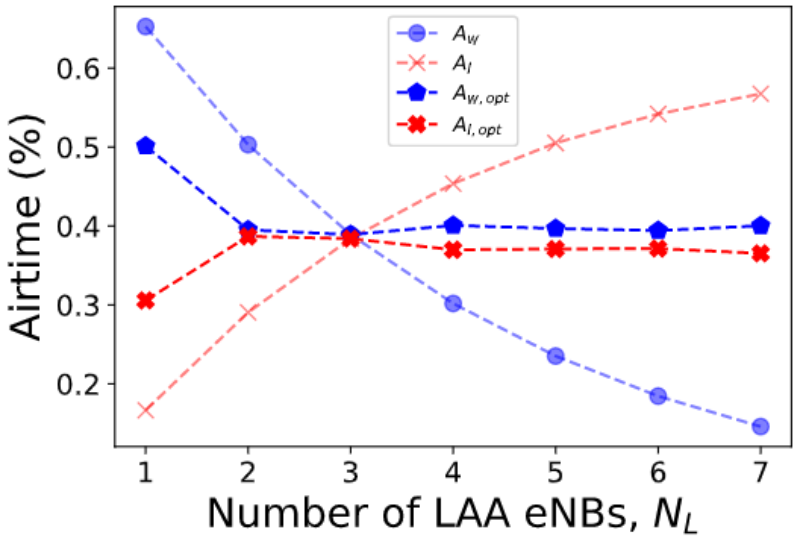

(b) LAA-Cat3-WiFi

Figure 3.12: Airtime improvement for various scenarios (N_l, $N_w = 3$)

3.6.5 Comparison of LAA-Cat4-WiFi coexistence with LAA-Cat3-WiFi coexistence

For a given same scenario (N_l, $N_w = 3$), we compare the coexistence of LAA-Cat3-WiFi and LAA-Cat4-WiFi. Fig. 3.13 shows that LAA-Cat3 achieves a higher fitness value than LAA-Cat4. It is seen from Fig. 3.14(a) and Fig. 3.15(a) that throughput fairness for Cat4 is higher than Cat3. Whereas the airtime fairness for Cat3 is higher than Cat4 as can be seen from Fig. 3.14(a) and Fig. 3.15(b). Also, the total throughput of the combined LAA and WiFi is higher for Cat3 than Cat4 as can be seen from Fig. 3.14(b). The net cumulative effect of total throughput and combined fairness is that the fitness for LAA-Cat3 is higher than LAA-Cat4 as seen in Fig. 3.13.

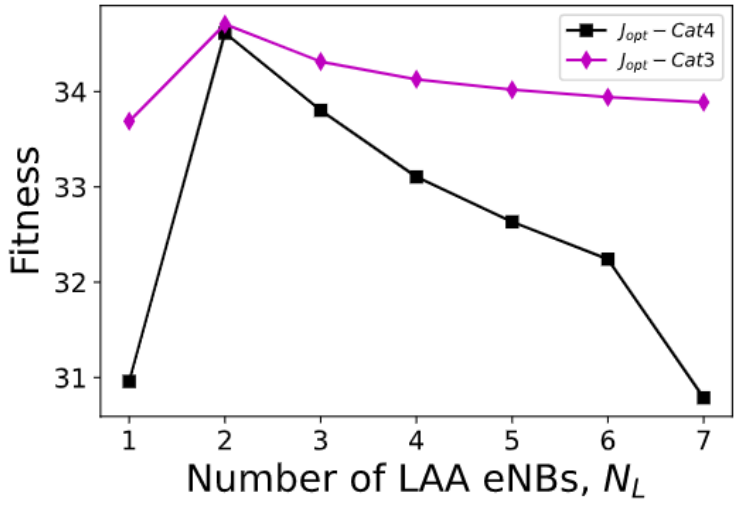

Figure 3.13: Fitness Comparison when Cat4 or Cat3 coexist with WiFi

In this chapter, we established that CW size is an important parameter in the LAA system for both LAA-Cat3 and LAA-Cat4 that enables LAA to coexist fairly with WiFi. We discussed the trade-off that exists while trying to optimize the throughput and airtime fairness. We defined a fitness function that takes into account total throughput and both fairness and tried to find out the best CW size that maximizes the fitness. We showed the effects of LAA on WiFi with and without CW size adjustments. We compared the performances of LAA-Cat4 and LAA-Cat3 coexisting with WiFi, and determined that even though LAA-

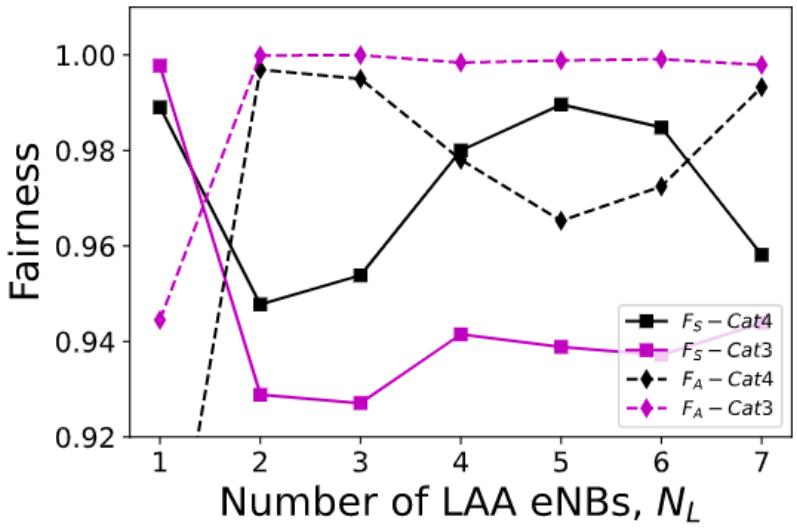

(a) Fairness

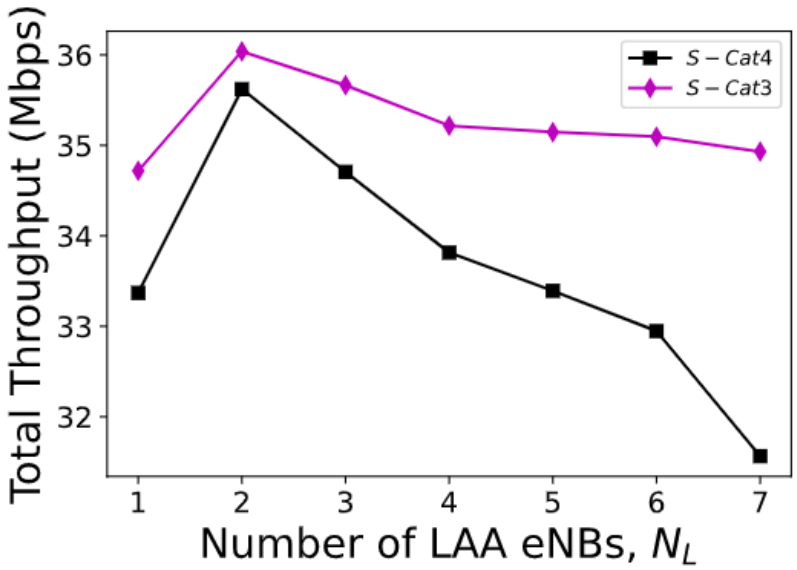

(b) Total Throughput

Figure 3.14: Fairness and Total throughput Comparison when Cat4 or Cat3 coexist with WiFi

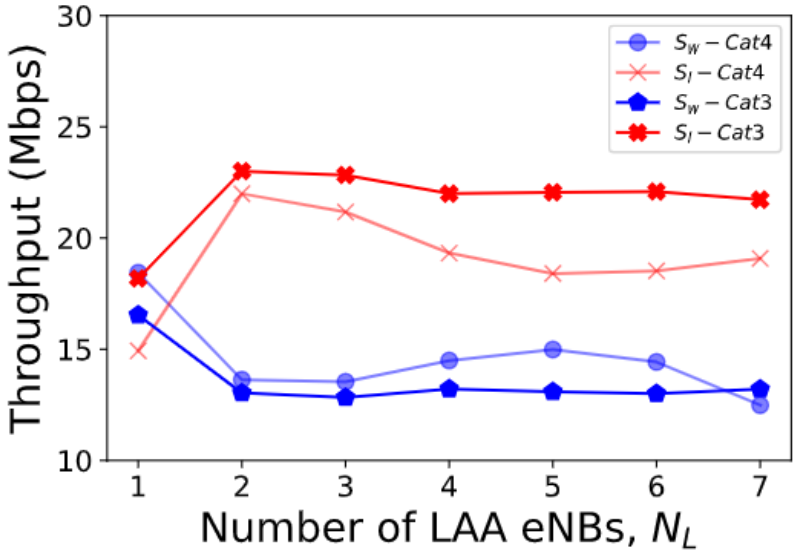

(a) Throughput

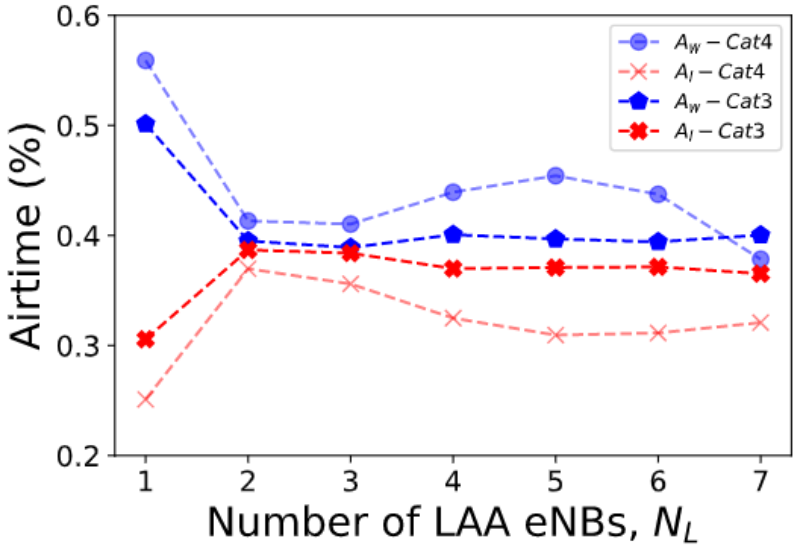

(b) Airtime

Figure 3.15: Throughput and Airtime Comparison when Cat4 or Cat3 coexist with WiFi

Cat4 achieves better throughput fairness, LAA-Cat3 does a better job in obtaining a higher fitness by having higher airtime fairness and total throughput.

CHAPTER 4

COEXISTENCE IN MULTI-CARRIER LBT

Multi-Carrier LBT, as described in Chapter 2 Section 2.3, is a process by which a station having an ability to sense multiples carriers can run LBT procedure in different channels and can utilize portions of whichever spectrum it finds free for use. LAA stations use various modulations (QPSK, 16QAM, 64QAM, 128QAM) and MIMO (SISO, MIMO 2x2, MIMO 4x4) techniques to vary the transmission-rate depending on the channel conditions. In this chapter, we will study the coexistence of LAA especially LAA-Cat3 with WiFi in a multi-channel scenario. We will show how an optimized CW size can be configured for each station at each channel to get the best throughput out of the combination of channels taking into account the throughput and airtime fairness. We will compare two CW assignment techniques based on equal CW size and Genetic Algorithm (GA).

Section 4.1 formulates the multi-carrier LBT system with LAA eNBs with specified data-rates and configurable CW sizes coexisting with WiFi APs on multi-channels. Section 4.2 derives the total throughput and total airtime of different stations based on Section 3.3 in Chapter 3. Section 4.3 describes the fairness indices in multi-carrier LBT which is similar to Section 3.3.5 in Chapter 3. Section 4.11 states the problem of optimizing the CW sizes of all LAA stations over all channels to maximize the combined throughput-airtime fairness. Section 4.5 describes the equal and genetic algorithm based CW assignment technique that ensures maximum fairness. Lastly the results are discussed in Section 4.7.

4.1 System Model

We consider a model as shown in Table 4.1 where N_l LAA-Cat3 eNBs contend with N_w WiFi APs for channel access on N_c different channels. WiFi being a legacy system

Table 4.1: System Model: Different Data Rates and Contention-Window sizes

Channels	**eNB-1**	**eNB-2**	...	**eNB-N_l**	**WiFi-AP**
CH-1	$R_l^{[1,1]}, W^{[1,1]}$	$R_l^{[1,2]}, W^{[1,2]}$	...	$R_l^{[1,N_l]}, W^{[1,N_l]}$	R_w, W_0
CH-2	$R_l^{[2,1]}, W^{[2,1]}$	$R_l^{[2,2]}, W^{[2,2]}$	...	$R_l^{[2,N_l]}, W^{[2,N_l]}$	R_w, W_0
$\vdots$	$\vdots$	$\vdots$	$\ddots$	$\vdots$	R_w, W_0
CH-N_c	$R_l^{[N_c,1]}, W^{[N_c,1]}$	$R_l^{[N_c,2]}, W^{[N_c,2]}$	...	$R_l^{[N_c,N_l]}, W^{[N_c,N_l]}$	R_w, W_0

has a fixed CW size W_0 and fixed data-rate R_w across all channels. Each LAA station as mentioned before can employ different data-rates $R_l^{[h,j]}$, for different channels $h = 1, 2, \ldots, N_c$ and different stations $j = 1, 2, \ldots, N_l$. $W^{[h,j]}$ is a configurable CW size of each eNB on each channel which needs to be optimized to obtain best possible total throughput of the system with fair allocations.

We assume both LAA-eNBs and WiFi APs have the ability to sense all channels simultaneously, use an independent back-off processes in each channel and utilize portions of whichever spectrum it finds free for use. WiFis employ CSMA-CA as described by the WiFi Markov chain in Section 3.2.1 on all channels. LAAs also employ LAA-LBT-Cat3 procedure as described by the LBT-Cat3 Markov chain in Section 3.2.3 on all channels. The only difference is that each WiFi runs the backoff process with the same CW size W_0 and fixed data-rate R_w across all channels whereas each LAA runs the backoff process with configurable CW size $W^{[h,j]}$ on each channel given specified data-rates $R_l^{[h,j]}$, for different channels $h = 1, 2, \ldots, N_c$ and different stations $j = 1, 2, \ldots, N_l$. $W^{[h,j]}$ needs to be optimized to obtain best possible total throughput of the system with fair allocations that ensures joint fairness of throughput and airtime.

We evaluate the performance of the coexistence in multi-channel as an aggregation of performances in each individual channel. A set of equations (3.6) and (3.7) have to be modified to (4.1) and (4.2) to describe the coexistence in single-channel with different CW sizes for each LAA station. Both of these equations are solved iteratively to find the

transmission probability for each WiFi station τ_w and LAA station $\tau_{l,j}$ for a single channel.

$$\begin{cases} \tau_w = \dfrac{2q_w(1-p_{f,w})(1-2p_{f,w})}{2(1-p_{f,w})^2(1-2p_{f,w}) + q_w[W_0 p_{f,w}(1-(2p_{f,w})^m) + (1+W_0-2p_{f,w})(1-2p_{f,w})]} \\ p_{f,w} = 1-(1-\tau_w)^{N_w-1}\prod_{j=1}^{N_l}(1-\tau_l^{[j]}) \end{cases} \tag{4.1}$$

$$\begin{cases} \tau_l^{[j]} = \dfrac{2q_l^{[j]}(1-p_{f,l}^{[j]})}{2(1-p_{f,l}^{[j]})^2 + 2q_l^{[j]}(1-p_{f,l}^{[j]}) + q_l^{[j]}(W^{[j]}-1)} \\ p_{f,l}^{[j]} = 1 - \prod_{k=1,k\neq j}^{N_l}(1-\tau_l^{[k]})(1-\tau_w)^{N_w} \quad , \quad j = 1,2,\ldots,N_l \end{cases} \tag{4.2}$$

4.2 Performance Analysis

We evaluate the performance of the coexistence in multi-channel as an aggregation of performances in each individual channel.

4.2.1 Single Channel

The event probabilities (idle, success and collision) in (3.8) and subsequent event average time duration in (3.9) discussed in Section 3.3 needs to be modified to (4.3) and (4.4) to account for different CW size of LAA $W^{[j]}$ for station j in a single channel. The subscripts w, l and wl denote WiFi, LAA and combination. The subscripts I, s and c denote idle, success and collision events. Given these two quantities, the average event duration, throughput and airtime from (3.10), (3.11) and (3.12) have to be modified to (4.5), (4.6) and (4.7) respectively.

$$
\begin{cases}
P_I = (1-\tau_w)^{N_w} \prod_{k=1}^{N_l}(1-\tau_l^{[k]}) \\
P_{s,w}^{[i]} = \tau_w(1-\tau_w)^{N_w-1} \prod_{k=1}^{N_l}(1-\tau_l^{[k]}) \quad , \quad i = 1,2,\ldots,N_w \\
P_{s,l}^{[j]} = \tau_l^{[j]} \prod_{k=1,k\neq j}^{N_l} (1-\tau_l^{[k]})(1-\tau_w)^{N_w} \quad , \quad j = 1,2,\ldots,N_l \\
P_{c,w} = \prod_{k=1}^{N_l}(1-\tau_l^{[k]}) \Big[1-(1-\tau_w)^{N_w} - N_w\tau_w(1-\tau_w)^{N_w-1}\Big] \\
P_{c,l} = (1-\tau_w)^{N_w} \Big[1 - \prod_{k=1}^{N_l}(1-\tau_l^{[k]}) - \sum_{j=1}^{N_l}\tau_l^{[j]} \prod_{k=1,k\neq j}^{N_l}(1-\tau_l^{[k]})\Big] \\
P_{c,wl} = 1 - P_I - \sum_{i=1}^{N_w} P_{s,w}^{[i]} - \sum_{j=1}^{N_l} P_{s,l}^{[j]} - P_{c,w} - P_{c,l}
\end{cases}
\tag{4.3}
$$

$$
\begin{cases}
T_{s,w} = \dfrac{\mathrm{PHY}_{hdr} + \mathrm{MAC}_{hdr} + E[P] + \mathrm{ACK}}{R_w} + \delta + \mathrm{SIFS} + \mathrm{DIFS} + \delta \\
T_{c,w} = \dfrac{\mathrm{PHY}_{hdr} + \mathrm{MAC}_{hdr} + E[P]}{R_w} + \mathrm{DIFS} + \delta \\
T_{s,l}^{[j]} = \dfrac{\mathrm{PHY}_{hdr} + \mathrm{MAC}_{hdr} + E[P] + \mathrm{ACK}}{R_l^{[j]}} + \delta + \mathrm{DIFS} + \delta \\
T_{c,l}^{[j]} = \dfrac{\mathrm{PHY}_{hdr} + \mathrm{MAC}_{hdr} + E[P]}{R_l^{[j]}} + \mathrm{DIFS} + \delta \\
T_{c,l} = \max(T_{c,l}^{[j]}) \\
T_{c,wl} = \max(T_{c,w}, T_{c,l})
\end{cases}
\tag{4.4}
$$

$$
E[T] = P_I\delta + \sum_{j=1}^{N_l} P_{s,l}^{[j]} T_{s,l}^{[j]} + \sum_{i=1}^{N_w} P_{s,w}^{[j]} T_{s,w} + P_{c,l}T_{c,l} + P_{c,w}T_{c,w} + P_{c,wl}T_{c,wl} \tag{4.5}
$$

Throughput of individual LAA and WiFi stations in a single channel h,

$$\begin{cases} S_l^{[h,j]} = \dfrac{P_{s,l}^{[j]}}{E[T]} E[P_l] \quad , \quad j = 1, 2, \ldots, N_l \\ S_w^{[h,i]} = \dfrac{P_{s,w}^{[i]}}{E[T]} E[P_w] \quad , \quad i = 1, 2, \ldots, N_w \end{cases} \tag{4.6}$$

Airtime of individual LAA and WiFi stations in a single channel h,

$$\begin{cases} A_l^{[h,j]} = \dfrac{P_{s,l}^{[j]} T_{s,l}^{[j]}}{E[T]} \quad , \quad j = 1, 2, \ldots, N_l \\ A_w^{[h,i]} = \dfrac{P_{s,w}^{[i]} T_{s,w}}{E[T]} \quad , \quad i = 1, 2, \ldots, N_w \end{cases} \tag{4.7}$$

4.2.2 Multiple Channel

We aggregate the performance of LAA and WiFi stations across all channel $h = 1, 2, \ldots, N_c$ to find the aggregated throughput (4.8) and aggregated airtime (4.9) of each LAA and WiFi station.

$$\begin{cases} S_l^{[j]} = \displaystyle\sum_{h=1}^{N_c} S_l^{[h,j]} \quad , \quad j = 1, 2, \ldots, N_l \\ S_w^{[i]} = \displaystyle\sum_{h=1}^{N_c} S_w^{[h,i]} \quad , \quad i = 1, 2, \ldots, N_w \end{cases} \tag{4.8}$$

$$\begin{cases} A_l^{[j]} = \displaystyle\sum_{h=1}^{N_c} A_l^{[h,j]} \quad , \quad j = 1, 2, \ldots, N_l \\ A_w^{[i]} = \displaystyle\sum_{h=1}^{N_c} A_w^{[h,i]} \quad , \quad i = 1, 2, \ldots, N_w \end{cases} \tag{4.9}$$

4.3 Fairness and Fitness

Different to fairness between LAA and WiFi networks as described in Section 3.3.5, we explore the fairness across stations. The throughput, airtime, combined fairness and overall fitness are calculated in (4.10) using Jain's fairness index described in Section 3.1.3.

$$
\begin{cases}
F_S = \dfrac{\Big(\sum_{j=1}^{N_l} S_l^{[j]} + \sum_{i=1}^{N_w} S_w^{[i]}\Big)^2}{\Big(N_l + N_w\Big)\Big(\sum_{j=1}^{N_l}(S_l^{[j]})^2 + \sum_{i=1}^{N_w}(S_w^{[i]})^2\Big)} \\
F_A = \dfrac{\Big(\sum_{j=1}^{N_l} A_l^{[j]} + \sum_{i=1}^{N_w} A_w^{[i]}\Big)^2}{\Big(N_l + N_w\Big)\Big(\sum_{j=1}^{N_l}(A_l^{[j]})^2 + \sum_{i=1}^{N_w}(A_w^{[i]})^2\Big)} \\
F_{SA} = 2\dfrac{F_S \times F_A}{F_S + F_A} \\
J = F_{SA}(S_W + S_L)
\end{cases}
\tag{4.10}
$$

4.4 Problem Statement

For a fair coexistence of N_l LAA eNBs with N_w WiFis , given different transmission data-rates of LAA stations in different channels $R_l^{[h,j]}$, we want to find the optimized value of CW size $W_{opt}^{[h,j]}$ for each LAA eNB station j in each channel h from different choices $\mathcal{W} = [W_1, W_2, \ldots, W_k]$ that maximizes the fitness metric J in (4.10).

$$
\Big[\boldsymbol{W_{opt}}\Big]_{N_c \times N_l} = \arg\underset{W \in \mathcal{W}}{\text{maximize}}\ J(N_L, N_W, \boldsymbol{W}) \tag{4.11}
$$

For example, fair coexistence between $N_l = 4$ eNBs and $N_w = 3$ APs on $N_c = 3$ different channels with each eNBs data-rate specification on each channel R_{3x4} as described in Table 4.2 should produce an optimized CW size of each eNB on each channel $\Big[W_{opt}\Big]_{3\times4}$ as shown in Table 4.4.

The time complexity for searching over all possible configurations of CW sizes is $O(|\mathcal{W}|^{N_c \times N_l})$ which is exponential in N_c and N_l, and cannot be brute-forced exhaustively. The optimization problem is non-convex and requires some clever CW assignment technique to achieve this optimization. We utilize the Genetic Algorithm (GA) to find the optimized CW size for the optimization problem.

4.5 CW Assignment Technique

4.5.1 Equal CW Assignment

Equal assignment technique is a simple technique where an equal value of CW size is configured for all LAA stations in all channels. We will use this technique as a base to compare our results later.

$$W^{[h,j]} = \text{constant} \qquad \forall h, \forall j$$

4.5.2 GA Assignment

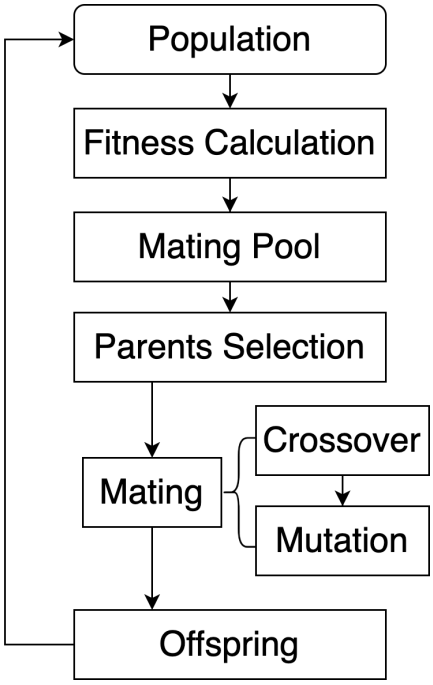

Figure 4.1: Genetic Algorithm

The Genetic Algorithm (GA) is a method for solving both constrained and non-constrained optimization problems that is based on natural selection, the process that drives biological evolution. The genetic algorithm repeatedly modifies a population of individual solutions. At each step, the genetic algorithm selects individuals at random from the current population to be parents and uses them to produce the children for the next generation. Over successive generations, the population evolves toward an optimal solution.

GA assignment utilizes three main rules to create new generations of CW sizes from the current population. GA assignment starts with an initial population of CW sizes. In each iteration, it uses these three main rules to modify the population for the next generation.

1. Selection: Based on the fitness value, individuals called parents are selected which contribute to the population at the next generation

2. Crossover: Parts of CW sizes of two parents are combined to form children for the next generation

3. Mutation: Applies a random change in CW sizes of individual parent to form children.

4.6 Scenario-Setup

We consider a scenario where $N_l = 4$ LAA eNBs contend with $N_w = 3$ WiFi APs on $Nc = 3$ different channels with full traffic load $q_l = q_w = 1$. The transmission data-rates of each LAA station on each channel $R_l^{[h,j]}$ is specified as in Table 4.2. Note that the transmission data-rate for WiFi is fixed. The system parameters for LAA-Cat-3 and WiFi are same as that in Table 3.1 with different choices for CW sizes $\mathcal{W} = [8{:}1{:}128]$.

Table 4.2: Data-Rate (Mbps) specification for LAA eNBs and WiFi APs

Channels	**eNB-1**	**eNB-2**	**eNB-3**	**eNB-4**	**WiFi-AP**
CH-1	75	100	50	25	40
CH-2	25	50	75	25	40
CH-3	100	150	75	25	40

4.7 Results and Discussion

4.7.1 Equal Assignment

For equal assignment, the maximum fitness occurs at an optimal CW size of $W_{opt}^{[h,j]} = 27$ as shown in Fig. 4.2. We use this technique as a base to compare our results from GA later.

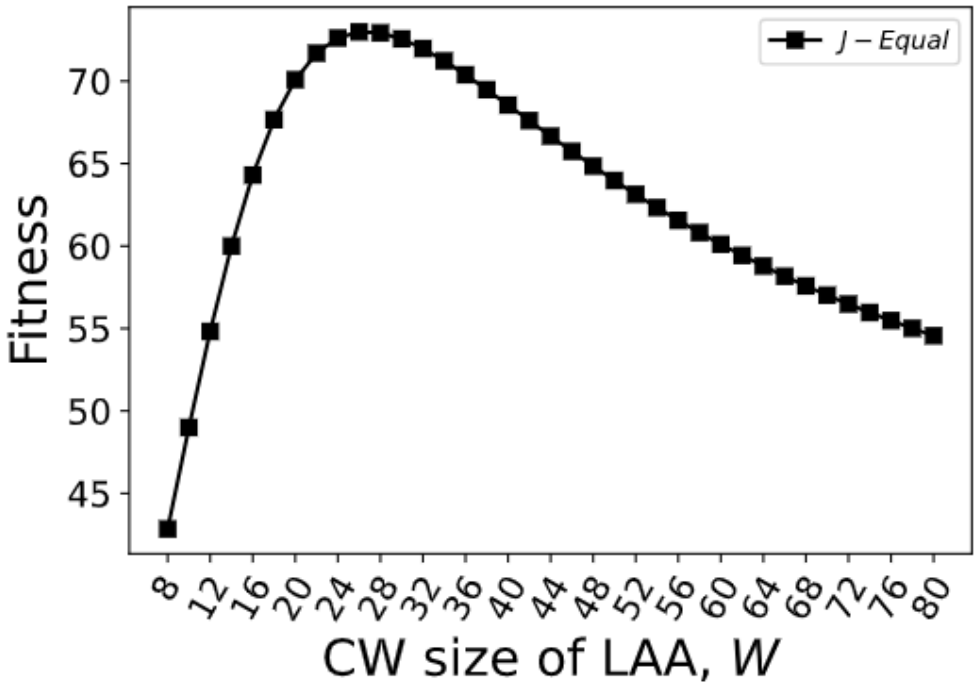

Figure 4.2: Optimal CW size for Equal Assignment

4.7.2 GA Assignment

Fig. 4.3 shows the improvement of both mean and best fitness (penalty = - fitness) in different generations. The parameters of GA iteration are tabulated in Table 4.3. We see that in each generation GA generates a new population that has better fitness than the previous generation. The iteration is stopped at a max generation of 500. At the end of the iteration, we get optimal CW sizes for each station in each channel as shown in Table 4.4.

Table 4.3: GA Parameters

Parameter	**Value**
Max Generations	500
Max Stall Generations	200
Population Size	1000
Function Tolerance	1e-6
Crossover Fraction	0.8

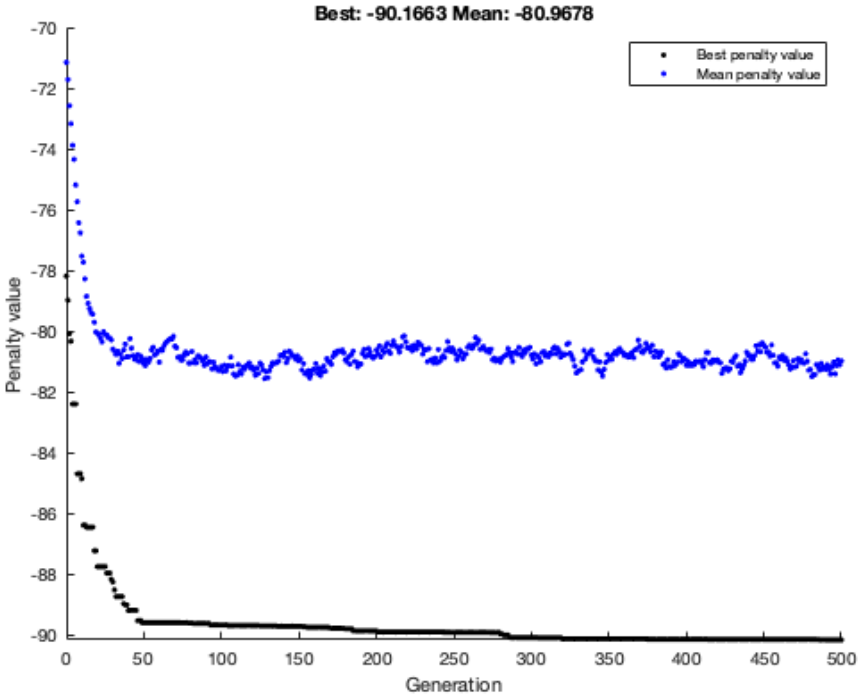

Figure 4.3: Fitness improvement of GA over generations

Table 4.4: Optimal CW size configuration using GA

Channels	**eNB-1**	**eNB-2**	**eNB-3**	**eNB-4**
CH-1	54	8	113	128
CH-2	101	112	8	128
CH-3	18	17	20	41

4.7.3 Comparison of Equal and GA Assignment

Table 4.5 shows the comparison of performances between equal CW = 27 and GA assignments in terms of Fitness (J), Total Throughput (S), Throughput Fairness (F_S), Airtime Fairness (F_A) and combined Throughput-Airtime Fairness (F_{SA}).

Table 4.5: Comparison of Equal and GA Assignment

Assignment	J	S	F_S	F_A	F_{SA}
Equal	73.0	80.63	0.999	0.828	0.905
GA	90.3	95.85	0.924	0.96	0.942

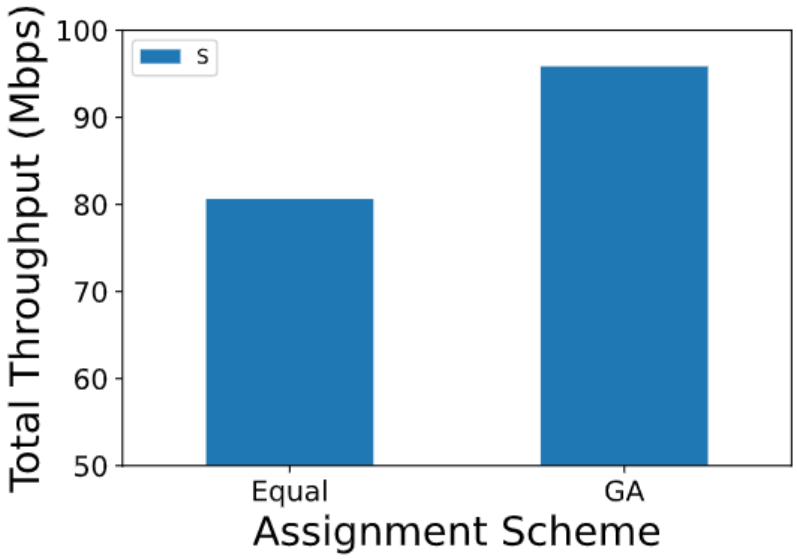

(a) Total Throughput

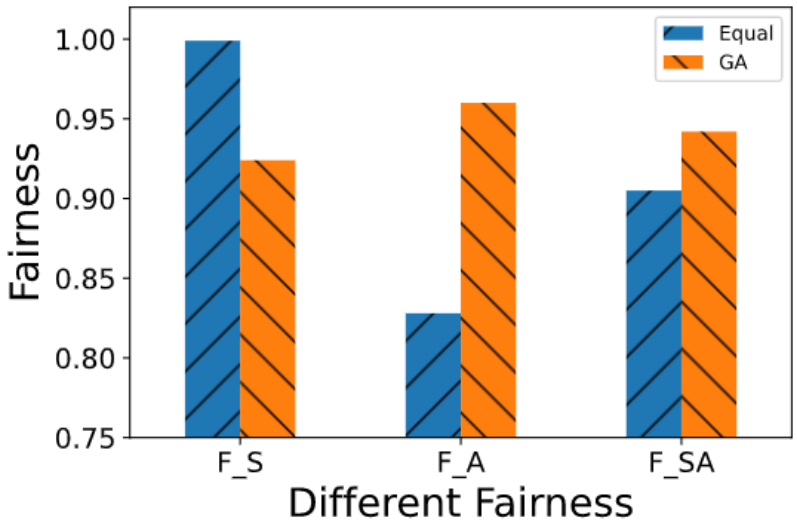

(b) Fairness

Figure 4.4: Comparison of total throughput and fairness of the system between Equal and GA assignments

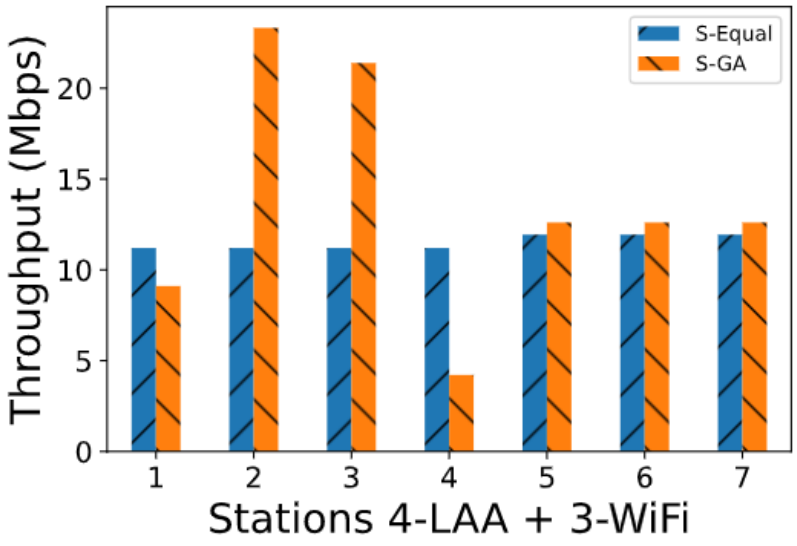

(a) Throughput

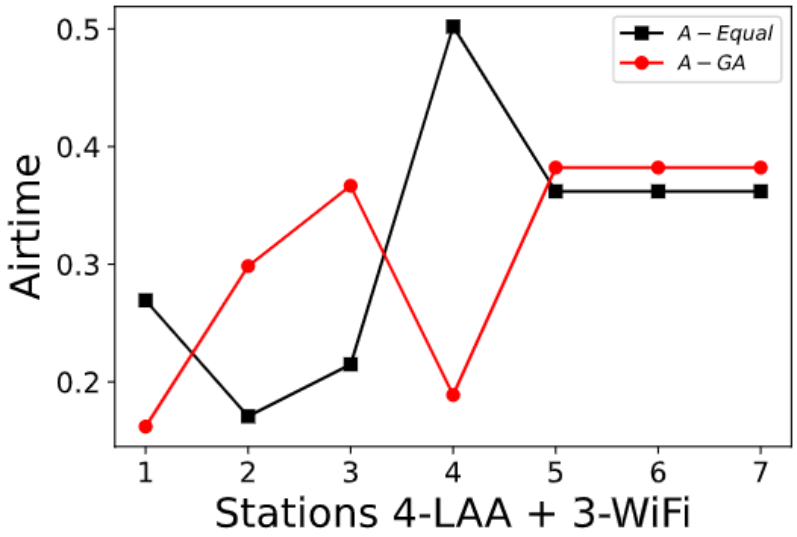

(b) Airtime

Figure 4.5: Comparison of throughput and fairness of individual stations between Equal and GA assignments

Table 4.5 and Fig 4.4 shows the total throughput and fairness achieved by the system for equal and GA assignments. It is seen that GA achieves a higher fitness, total throughput and combined fairness (F_{SA}). It seems in Fig. 4.4(b) as though the throughput fairness for equal assignment is higher than GA but it happens only because the equal assignment is not able to achieve higher throughput for LAAs effectively causing it to lose throughput and become much similar to that of WiFi stations. This is also evident in throughput distribution of 4 LAA eNBs (indexed 1, 2, 3, 4) in Fig. 4.5(a). Throughput and airtime for station #4 is significantly lower since the specified data-rate for station #4 is the least in all channels in Table 4.2. The equal assignment does particularly worse in-terms of airtime-fairness as can be seen from Figs. 4.4(b) and 4.5(b).

It is to be noted that the aggregated data-rate of individual LAA from Table 4.2 is (200, 300, 200, 75) Mbps. This reflects on the aggregated throughput distribution of LAA stations in Fig. 4.5(a). It can also be seen from Fig. 4.5(b) that the airtime for low data rate LAAs are penalized due to airtime fairness scheme.

On the other hand, GA performs better in terms of the total throughput and its airtime-fairness is far better than the equal assignment. GA also performs reasonably well in terms of throughput-fairness. Overall, GA sacrifices some throughput fairness in order to achieve better combined fairness and yields higher total throughput. This effectively causes GA to have higher fitness value than equal CW assignment.

It is to be noted in Fig. 4.5 that regardless of the assignment, throughput and airtime are equal for all stations in WiFi. It is because we consider WiFi to be a legacy system so there is no difference between any WiFi stations and every station acts similarly. For the equal assignment, throughput for individual stations in LAA are the same but airtime varies. In the GA assignment, both throughput and airtime for individual stations in LAA vary. By configuring the optimal CW size of each station in each channel, the GA assignment is able to vary the throughput and airtime of individual stations in such an optimized way that the total throughput and combined fairness of the system are higher than equal assignment.

Moreover, the analysis assumes that LAA knows the number of WiFi N_w in the system, which can be achieved either in cooperative sensing or having a WiFi-interface in LAA eNB station. We also ignored the number of users associated with each eNB and AP since the dominant transmission in a wireless network is through WiFi-AP or LAA-eNB.

In this chapter, considering the coexistence of LAA-Cat3 and WiFi, we showed that a dynamic contention window size assignment based on combined fairness of throughput and airtime achieves better fairness than equal contention window size assignment for coexistence in a multi-channel scenario. We utilized the genetic algorithm to assign the optimized contention window size of each LAA station in each channel based on the fitness function that takes into account the total throughput and joint fairness. Fair coexistence with WiFi 802.11ac, 802.11ax capable of variable Modulation and Coding Scheme (MCS) needs to be further studied.

CHAPTER 5

COEXISTENCE IN DUAL CARRIER AGGREGATION

Carrier Aggregation (CA) is a feature of LTE-Advanced which allows LTE eNB to combine one or more LTE component carriers into a single data channel which increases the overall capacity by exploiting fragmented spectrum as described in Chapter 2 Section 2.4. CA allows stations in primary channel to be able to sense the secondary channel and use it in aggregation to primary channel to boost its throughput if the secondary channel is empty. In this chapter, we will discuss the coexistence of LAA stations with CA ability with those without CA ability. By modeling the coexistence using Markov Chains, we will first see how dual-channel sensing stations affect the performance of other single-channel sensing stations and then secondly we will see how we can find an optimal distribution (partition) of stations with system parameters including CW size and load intensity that maximize different fairness indices and their effects on secondary CH-2 throughput.

Section 5.1 models the dual-carrier aggregation as a coupling between MCs and Section 5.2 formulates it to derive the individual throughput and airtime of different groups of stations, including a) sensing only primary channel CH-1, b) sensing only secondary channel CH-2 and c) sensing both channels CH-1 and CH-2 for channel aggregation opportunity. Based on this, the total throughput and different fairness indices similar to those described in Section 3.3.5 of Chapter 3 are analyzed. Section 5.3 describes the effect of partition (distribution of stations in primary and aggregated channel) in the dual channel coexistence. Section 5.3.3 describes the optimization problem with fixed CW size and load intensity but configurable partition, and analyses the distribution of optimized partitions, throughput and airtime over different fairness metrics. This section also describes the effect of different fairness metrics on the total throughput and the secondary CH-2 throughput. Section 5.4

describes the effect of CW size and load intensity on the single and dual channel coexistence. Section 5.4.3 states the final optimization problem of optimizing the partition, CW size and load intensity in combination to achieve a fair coexistence between different groups in dual carrier aggregation.

5.1 System Model

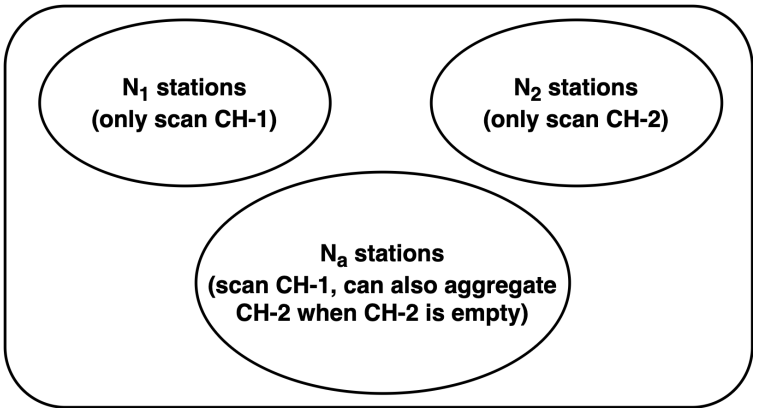

Figure 5.1: System Model: Dual Carrier Aggregation

We consider a pool of stations that have the capability of sensing either a single channel or multiple channels as shown in Fig. 5.1. We consider a scenario where

- $\mathcal{N}_1$ group consisting of N_1 stations that only sense primary channel CH-1.
- $\mathcal{N}_2$ group consisting of N_2 stations that only sense secondary channel CH-2.
- $\mathcal{N}_2$ group consisting of N_a stations that sense primary channel CH-1 normally as $\mathcal{N}_1$ stations but also have the capability of sensing secondary channel CH-2 for dual-carrier aggregation.

Note that $\mathcal{N}_a$ stations cannot separately use only secondary channel CH-2 without using the primary channel CH-1.

The Markov Chain for LAA-LBT Cat3 channel access as described in Section 3.2.3 is still valid for each individual station but coupling between two channel access will have to be modified which is discussed in Section 5.2.2.

There are a couple of differences between this model and the models which were described in previous chapters.

1. Coexistence: We only consider the coexistence between LAA eNBs assuming no WiFis are present.

2. Contention Window CW: We assume that CW is fixed for the entire system such that each LAA eNB will be configured to exactly the same CW size.

3. Load Intensity q: We assume that q is fixed for the entire system such that each LAA eNB will be configured to exactly the same value. In previous models, we always assumed a full traffic load. But for this model, we assume that after a packet has been transmitted successfully, we deliberately make stations wait with probability q before allowing them to actively participate in the contention again. Along with the CW size W, load intensity q will also play a significant role in reducing the contention in the channel whenever there are too many stations in the channel.

5.2 Performance Analysis in Dual-Carrier Aggregation

5.2.1 On Primary Channel: CH-1

Since stations in $\mathcal{N}_1$ and $\mathcal{N}_a$ all sense primary channel CH-1, the transmission probability (τ_1, τ_a) and the failure probability (p_{f1}, p_{fa}) of each group is given by (5.1) from Sections 3.2.3 and 3.3 of Chapter 3.

$$\begin{cases} \tau_1 = \tau_a = \dfrac{2q(1-p_{f1})}{2(1-p_{f1})^2 + 2q(1-p_{f1}) + q(W-1)} \\ p_{f1} = p_{fa} = 1 - (1-\tau_1)^{N_1+N_a-1} \end{cases} \tag{5.1}$$

The channel probabilities are given by (5.2).

$$\begin{cases} \text{Idle: } p_{I1} = (1-\tau_1)^{N_1+Na} \\ \text{Success per station: } p_{s1} = \tau_1(1-\tau_1)^{N_1+N_a-1} \\ \text{Collision: } p_{c1} = 1 - p_{I1} - (N_1+N_a)p_{s1} \end{cases} \tag{5.2}$$

It is to be noted here that p_{s1} describes the probability of successful transmission for a single station unlike $p_{s,l}$ in previous chapters which denoted the successful transmission for all LTE stations. From equation 5.2, the total successful transmission for all LTE stations in CH-1 would be given by $(N_1+N_a)p_{s1}$. This had to be done so as to condition the probability of successful transmission of a single LAA on an event Y which will be further described in Section 5.2.2.

Let X denote the event that at least one station in $\mathcal{N}_2$ transmits in CH-2 with $p(X) = 1-(1-\tau_2)^{N_2}$. The associated throughput and airtime for the stations in $\mathcal{N}_1$ and $\mathcal{N}_a$ groups are given by (5.3).

$$\begin{cases} S_1|X = S_1 = \dfrac{N_1\ p_{s1}\ E[P]}{E[T_1]} & \text{, single primary channel mode for } \mathcal{N}_1 \text{ stations} \\ A_1|X = A_1 = \dfrac{N_1\ p_{s1}\ T_{s1}}{E[T_1]} & \\ S_a|X = \dfrac{N_a\ p_{s1}\ E[P]}{E[T_a]} & \text{, single primary channel mode for } \mathcal{N}_a \text{ stations} \\ A_a|X = \dfrac{N_a\ p_{s1}\ T_{s1}}{E[T_1]} & \\ S_a|X^c = 2\ S_a|X & \text{, carrier aggregation mode for } \mathcal{N}_a \text{ stations} \\ A_a|X^c = A_a|X & \\ S_a = E[S_a|X] = S_a|X\ P(X) + S_a|X^c\ (1-P(X)) & \text{, Average Throughput} \\ A_a = E[A_a|X] = A_a|X\ P(X) + A_a|X^c\ (1-P(X)) & \text{, Average Airtime} \end{cases} \tag{5.3}$$

5.2.2 On Secondary Channel: CH-2

Stations in $\mathcal{N}_2$ and $\mathcal{N}_a$ all sense secondary channel CH-2. Stations in $\mathcal{N}_2$ can use secondary channel CH-2 in standalone while stations in $\mathcal{N}_2$ cannot. Stations in $\mathcal{N}_a$ only use secondary channel CH-2 opportunistically when primary and secondary are both empty. If Y denote the event that at least one station in $\mathcal{N}_a$ transmits in CH-2 such that $p(Y) = 1-(1-\tau_a)^{N_a}$. Then the transmission probability τ_2 and failure probability p_{f2} for stations in $\mathcal{N}_2$ is given by (5.4).

$$\begin{cases} \tau_2 = \dfrac{2q(1-p_{f2})}{2(1-p_{f2})^2 + 2q(1-p_{f2}) + q(W-1)} \\ p_{f2} = p_{f2|Y^c}\ P(Y^c) + p_{f2|Y}\ P(Y) = (1-(1-\tau_2)^{N_2-1})\ P(Y^c) + 1\ P(Y) \end{cases} \tag{5.4}$$

Equations (5.1) and (5.4) describe the coupling of two Markov chains in CH-1 and CH-2. These equations represent non-linear and dependent relationship between one another and needs to be calculated using numerical iterations.

The channel probabilities are given by (5.5).

$$\begin{cases} \text{Idle: } p_{I2} = (1-\tau_2)^{N_2}\ P(Y^c) \\ \text{Success per station: } p_{s2} = p_{s2|Y^c}\ P(Y^c) = \tau_2(1-\tau_2)^{N_2-1}\ P(Y^c) \\ \text{Collision: } p_{c2} = 1 - p_{I2} - (N_2)p_{s2} \end{cases} \tag{5.5}$$

The associated single channel throughput and airtime for the stations in $\mathcal{N}_2$ group is given by (5.6).

$$\begin{cases} S_2 = \dfrac{N_2\ p_{s2}\ E[P]}{E[T_2]} \\ A_2 = \dfrac{N_2\ p_{s2}\ T_{s2}}{E[T_1]} \end{cases} \tag{5.6}$$

The average time duration $E[T_1]$, $E[T_a]$ and $E[T_2]$ are given by (5.7) and time duration for idle, success and collision events are same as described in previous chapters.

$$\begin{cases} E[T_1] = p_{I1}T_{I1} + N_1 p_{s1}T_{s1} + p_{c1}T_{c1} \\ E[T_2] = p_{I2}T_{I2} + p_{s2}T_{s2} + p_{c2}T_{c2} \end{cases} \tag{5.7}$$

5.3 Results: Effect of number of stations, partition

5.3.1 In Single Channel

As we saw in the previous chapters, both the throughput and airtime for a single channel first rises with increase in total number of stations because the channel is under-utilized and more stations can be accommodated. But after a certain number of stations ($N_2 = 5$ in Fig. 5.2), both throughput and airtime begin to decline because of the over-utilization of the channel and collision.

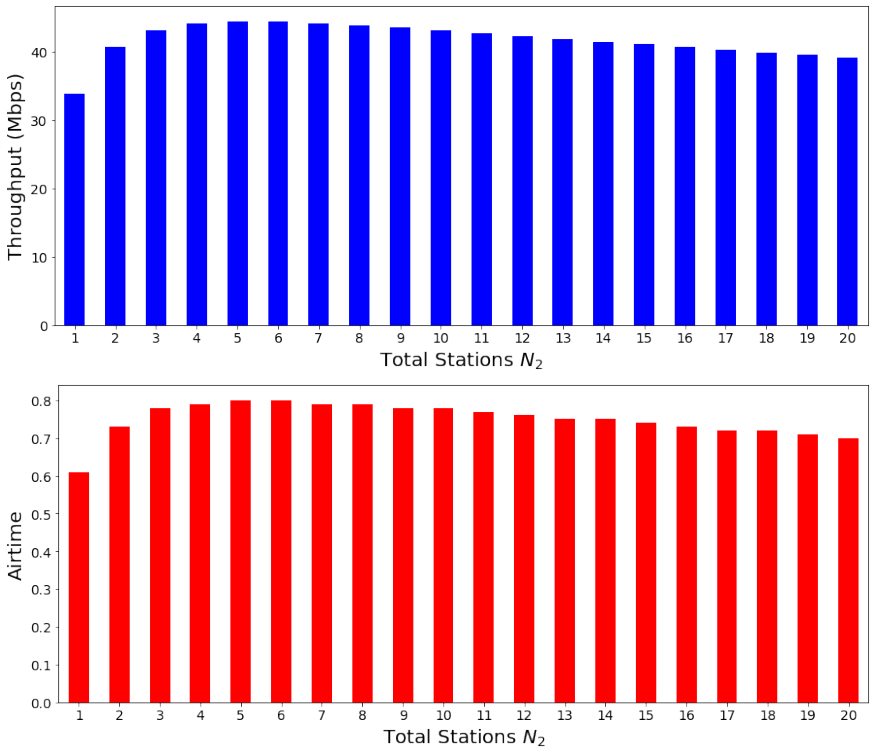

Figure 5.2: Effect of stations in single channel

5.3.2 In Dual Channel with partition ($\mathcal{N}_1$, $\mathcal{N}_a$, $\mathcal{N}_2$)

To understand the effect of partition of stations, we consider $N_1 = 5$ stations in CH-1 and $N_2 = 5$ stations in CH-2 with fixed CW size $W = 32$ and load intensity $q = 1.0$. Depending on the scenario we analyze different cases when stations in $\mathcal{N}_1$ start migrating to $\mathcal{N}_a$ such that we have different scenarios ($\mathcal{N}_1$, $\mathcal{N}_a$, $\mathcal{N}_2$): {(5, 0, 5), (4, 1, 5), (3, 2, 5), (2, 3, 5), (1, 4, 5), (0, 5, 5)}.

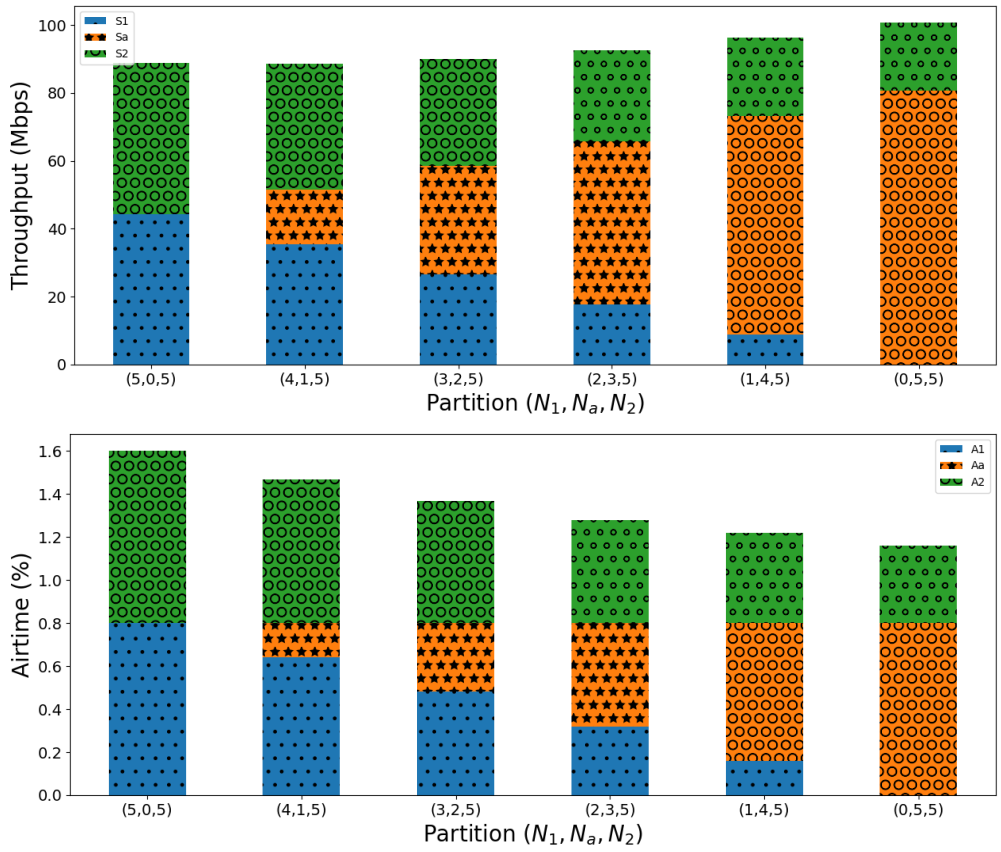

Figure 5.3: Partition effect of stations in dual carrier aggregation

The results for the effect of partitions are shown in Fig. 5.3 and Table 5.1. Starting from the scenario (5, 0, 5), there are no users in $\mathcal{N}_a$ group so that the carrier aggregation does not happen and the distribution of throughput and airtime for $N_1 = 5$ and $N_2 = 5$ stations in CH-1 and CH-2 are the same as can be seen in the first row of the table.

For the scenario (4, 1, 5) as shown in second row of the table, since there is only one

Table 5.1: Partition effect of stations in dual carrier aggregation

N	N1	Na	N2	W	q	J	S1	Sa	S2	A1	Aa	A2	S	A
5	5	0	5	32	1	0.67	44.41	0	44.41	0.8	0	0.8	88.82	1.6
5	4	1	5	32	1	0.86	35.53	15.88	37.17	0.64	0.16	0.67	88.58	1.47
5	3	2	5	32	1	0.97	26.65	31.89	31.45	0.48	0.32	0.57	89.99	1.37
5	2	3	5	32	1	0.91	17.77	48.02	26.85	0.32	0.48	0.48	92.64	1.28
5	1	4	5	32	1	0.72	8.88	64.27	23.09	0.16	0.64	0.42	96.24	1.22
5	0	5	5	32	1	0.53	0	80.64	19.98	0	0.8	0.36	100.62	1.16

station in $\mathcal{N}_a$, the station is able to aggregate both channels to achieve a throughput of 15.88. It is seen that throughput for both $\mathcal{N}_1$ and $\mathcal{N}_2$ groups have reduced compared to earlier case (5, 0, 5) but the throughput is reduced more for $\mathcal{N}_1$ than $\mathcal{N}_2$ because of lesser number of stations in $\mathcal{N}_1$ than $\mathcal{N}_2$. Similar behavior is also seen for the airtime distribution. For the case $(N_1, N_a, N_2) = (4, 1, 5)$, the airtime distribution of $(A_1, A_a, A_2) = (0.64, 0.16, 0.67)$ indicates that $\mathcal{N}_1$ group is able to utilize CH-1 64% of time, $\mathcal{N}_2$ group is able to utilize CH-2 67% of time and $\mathcal{N}_a$ group is able to utilize both channels CH-1 and CH-2 only 16% of time for successful transmission of their packets.

For the rest of the scenarios, migration of stations in $\mathcal{N}_1$ into $\mathcal{N}_a$ allows for more number of stations to exploit the aggregated band to achieve higher overall throughput. But this aggregation by $\mathcal{N}_a$ stations has negative impact on $\mathcal{N}_2$ stations as their contribution shrinks because of packet collision with $\mathcal{N}_a$ stations. This is also particularly bad from the perspective of fairness. For the extreme case scenario (0, 5, 5), we can see that the stations in $\mathcal{N}_2$ have been heavily impacted by stations in $\mathcal{N}_a$ raising an issue of fair allocation among stations in different group.

5.3.3 Optimizing Partitions: Problem Statement

For a system that has fixed N_2 number of LAA stations in secondary channel, we want to find the optimal partition $\{(N_1, N_a)|N_1 + N_a = N\}$ for given N which maximizes our objective J. We consider results for different objectives a) Total Throughput, b) Airtime Fairness, c) Throughput Fairness and d) combined Throughput-Airtime Fairness. We

consider a fixed CW size $W = 32$ and fixed load intensity $q = 1.0$. For the limited search space of (N_1, N_a), we find the optimal solution through exhaustive brute force search.

$$\begin{aligned} \underset{N_1, N_a}{\text{maximize}} \quad & J \\ \text{subject to} \quad & N_1 + N_a = N \end{aligned} \tag{5.8}$$

5.3.3.1 Optimizing Total Throughput

Optimizing the total throughput forces all stations to be assigned in $\mathcal{N}_a$ and no station in $\mathcal{N}_1$ so as to obtain maximum throughput irrespective of impact that $\mathcal{N}_a$ has on $\mathcal{N}_2$ as shown in Fig. 5.4. The behavior of total throughput is similar to single channel case in Fig. 5.2 but the behavior of airtime is different.

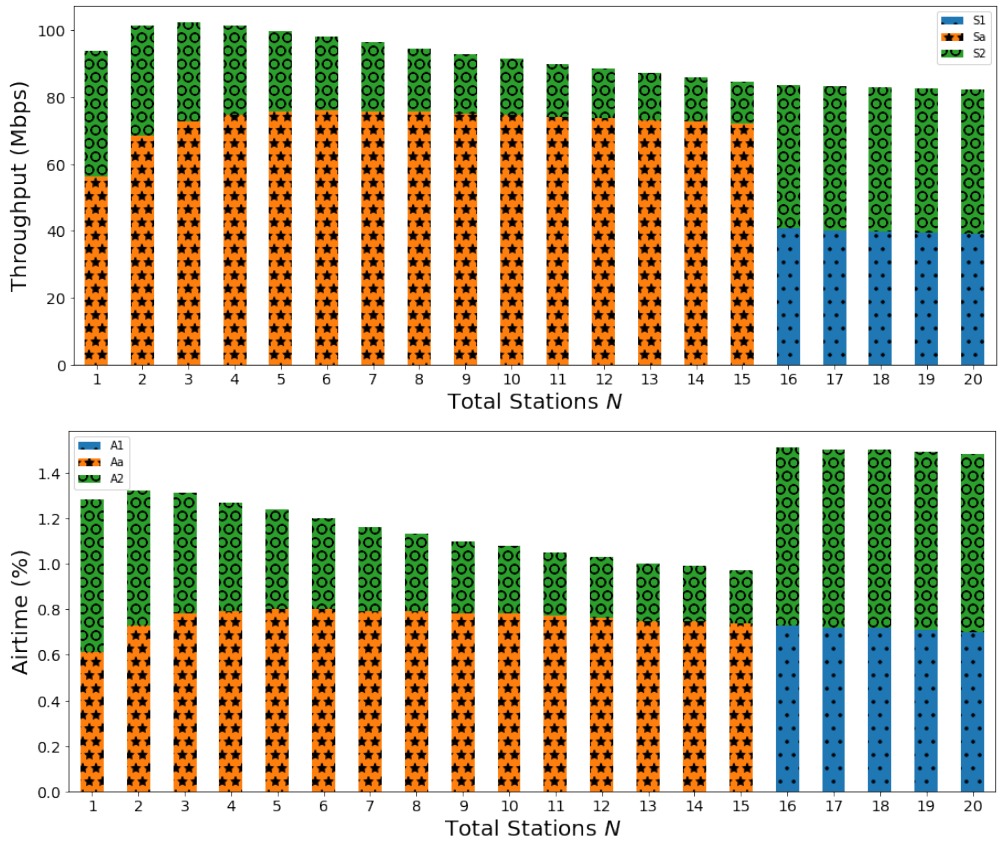

Figure 5.4: Optimizing Total Throughput

It is observed from Table A1 in the Appendix, with increase in the total number of

stations N, more stations keep on being assigned to $\mathcal{N}_a$ group causing the throughput and airtime for stations in secondary channel CH-2 to decline as can be seen for cases $N = 1$ to 15. Beyond $N = 15$, the collision impact on CH-2 is so severe that it is more beneficial to have all the stations in $\mathcal{N}_a$ transferred to $\mathcal{N}_1$. This forces all the stations in $\mathcal{N}_a$ to only sense CH-1, which lowers the collision in CH-2 and increases the airtime for $\mathcal{N}_2$ stations, hence yielding more total throughput.

5.3.3.2 Optimizing Airtime Fairness

Optimizing the airtime fairness ensures that the airtime distribution across different groups ($\mathcal{N}_1, \mathcal{N}_a, \mathcal{N}_2$) are similar but the distribution of throughput is quite different as shown in Fig. 5.5.

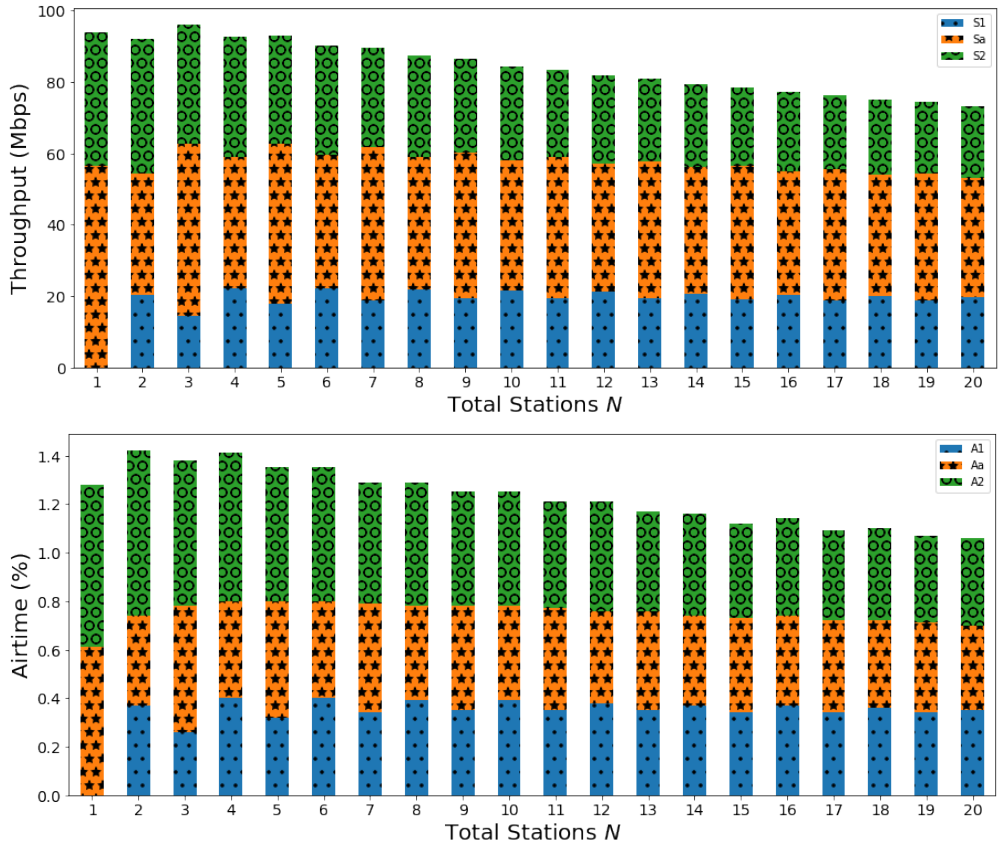

Figure 5.5: Optimizing Airtime Fairness

An interesting pattern for optimal partition (N_1, N_a) is observed in Table A2 where an

additional station is first assigned to $\mathcal{N}_a$ group and then other additional station is assigned to $\mathcal{N}_1$ group. For example, when $N = 6$, equal number of stations $N_1 = 3, N_a = 3$ are assigned. When $N = 7$, the optimal partition is (3, 4) and for $N = 8$, the optimal partition is (4, 4). Similar behavior is observed for higher values of N. This hints at the possibility of greedy assignment that is equivalent to optimizing airtime fairness.

5.3.3.3 Optimizing Throughput Fairness

Optimizing the throughput fairness ensures the throughput distribution across different groups ($\mathcal{N}_1$, $\mathcal{N}_a$, $\mathcal{N}_2$) are similar but the distribution of airtime is slightly different as shown in Fig. 5.6.

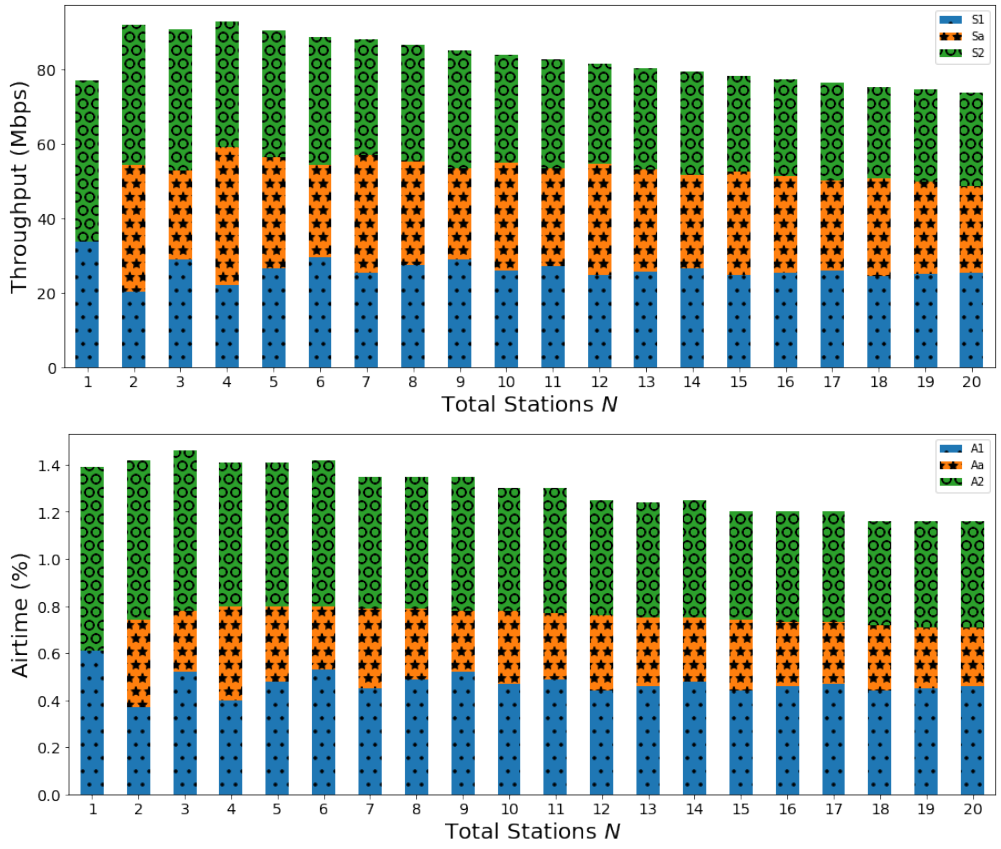

Figure 5.6: Optimizing Throughput Fairness

In contrast to the optimizing airtime fairness, optimizing throughput fairness would add the stations in $\mathcal{N}_a$ very conservatively as shown in Table A3. Additional stations are first

added to $\mathcal{N}_1$ group as can be seen in scenarios $N = 5, 6$. Extra stations are added to $\mathcal{N}_a$ only when they can be accommodated as can be seen in scenario $N = 7$. The pattern continues for higher values of N. This conservative assignment into $\mathcal{N}_a$ group happens because any introduction of additional station into $\mathcal{N}_a$ group would give that station ability to aggregate channel and obtain higher throughput and further imbalance the throughput fairness.

5.3.3.4 Optimizing Throughput-Airtime Fairness

Optimizing the combined fairness ensures the fair distribution of both throughput and airtime across different groups ($\mathcal{N}_1$, $\mathcal{N}_a$, $\mathcal{N}_2$) as shown in Fig. 5.7.

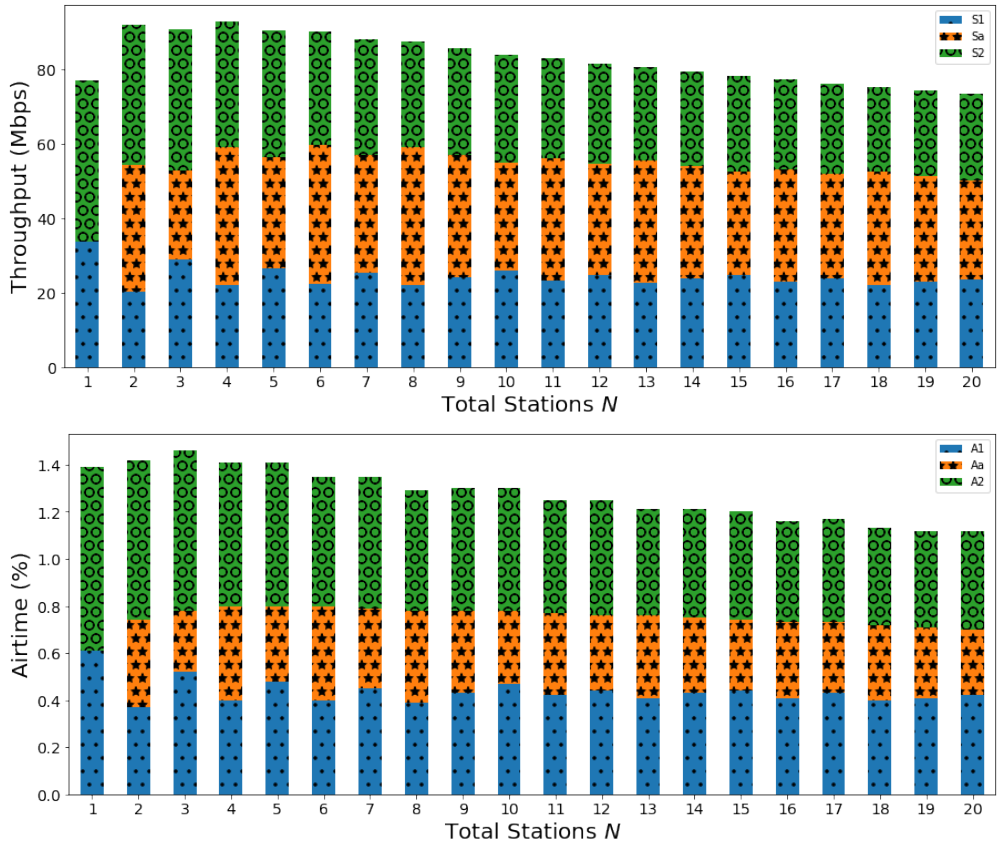

Figure 5.7: Optimizing Throughput-Airtime Fairness

Optimizing combined fairness would also add the stations in $\mathcal{N}_a$ conservatively as shown in Table A4 but not as conservatively as for the case of optimizing throughput fairness. For example, for $N = 9$, the optimal partitions for airtime, throughput and combined

fairness are (4, 5), (6, 3) and (5, 4) respectively. Assignment based on airtime fairness is the most liberal in assigning new stations in $\mathcal{N}_a$ group while the fair throughput assignment is the most conservative. Assignment based on combined throughput-airtime fairness offers a compromise between the throughput and airtime trade-off.

5.3.3.5 Optimizing Partition: Effect on secondary channel

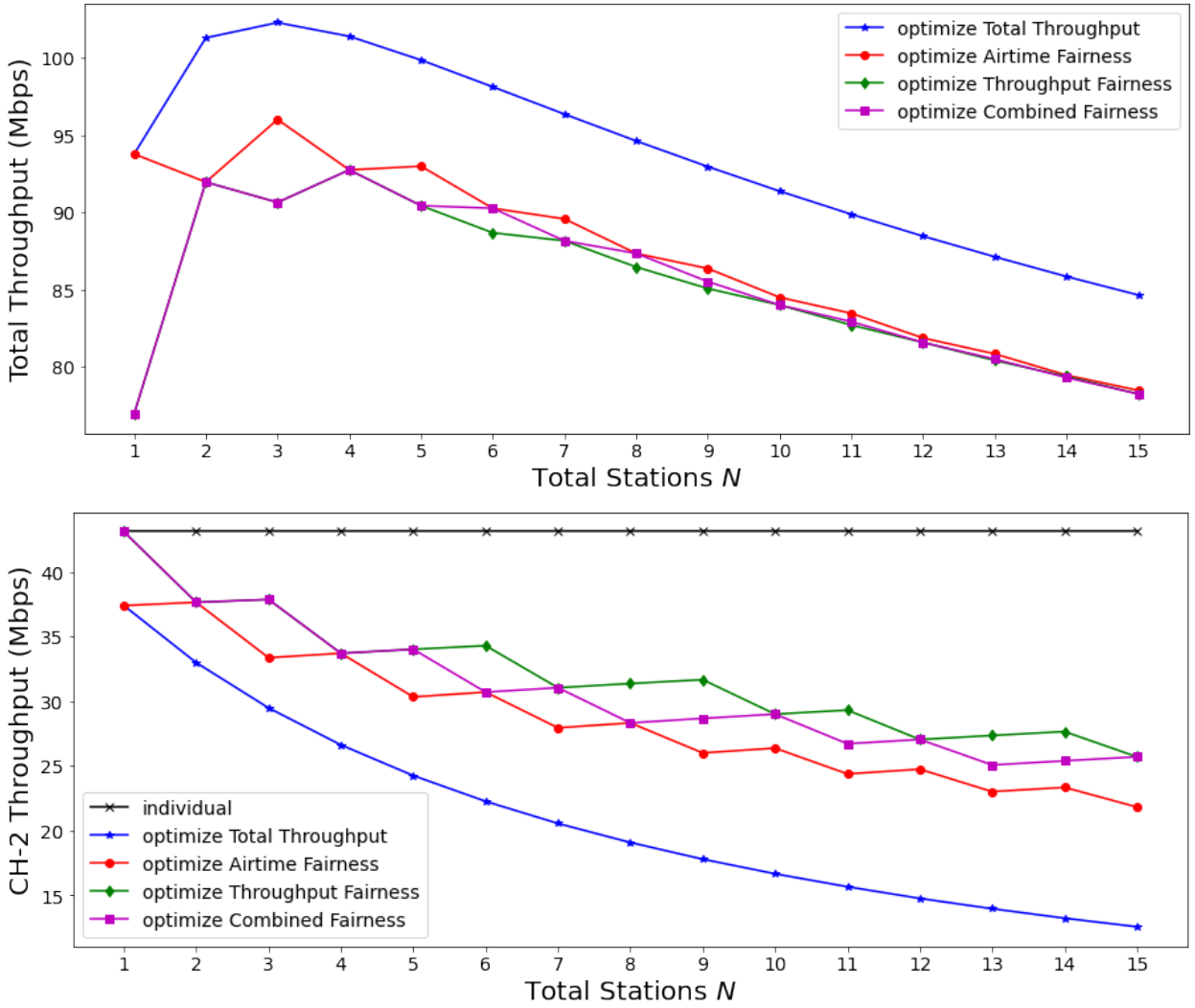

Figure 5.8: Effect on secondary channel

It is seen from Fig. 5.8 that even though optimizing total throughput achieves highest throughput than other objectives, it causes the most severe impact in secondary channel throughput compared to the individual case where there are no stations in $\mathcal{N}_a$. Optimiz-

ing throughput fairness impacts the secondary channel the least but yields the lowest total throughput. Optimizing airtime fairness yields higher total throughput than any other fairness optimization but still significantly impacts the secondary channel. The compromise is obtained with optimizing combined throughput-airtime fairness where a reasonable total throughput is obtained with acceptable impact to secondary channel.

5.4 Results: Effect of CW size W and load intensity q

5.4.1 Effect of W and q in a single channel

For a single channel, as the number of stations N increases, the system throughput initially rises, saturates and then starts to decline as shown in Fig. 5.9. This happens for any contention window size W and load intensity q because for low N, the channel is unsaturated and increasing N gives more chances to transmit. But as N increases further, collision starts dominating and then the throughput declines.

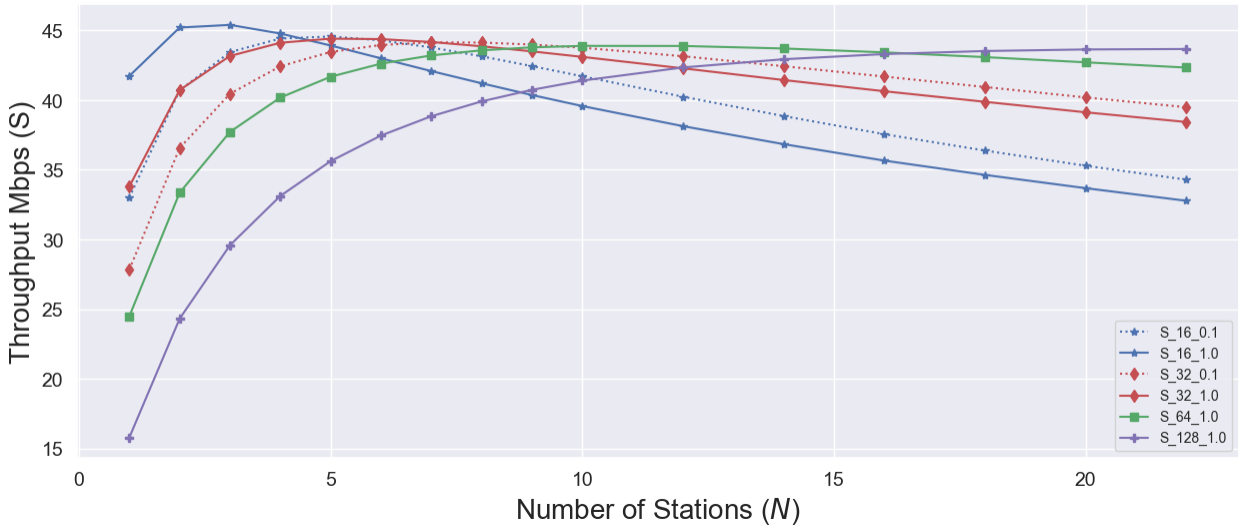

Figure 5.9: Impact of CW and load intensity on Single Channel

Contention window size W has a higher impact on throughput than load intensity. For a given $q = 1.0$, at lower N, larger W yields lower throughput. This is because when contention is low, increasing CW size results in stations waiting significantly on countdowns. However at larger N, larger W yields higher throughput. This is because when contention

is high, increasing CW gives extra waiting periods for stations not to collide during transmission.

Load intensity q has lower impact in throughput. For a given $W = 32$, at lower N, $q = 1.0$ yields higher throughput than $q = 0.1$. This happens because at lower N, there is less contention for channel access and increasing q increases throughput. But at higher N, there is already high contention for channel access and decreasing q to 0.1 lowers contention in the channel leading to slightly higher throughput. This also happens for $W = \{64, 128\}$ but is not shown in the Fig. 5.9 to reduce clutter.

5.4.2 Effect of W and q in dual channel

Effect of CW size and load intensity on total throughput, combined fairness and secondary CH-2 throughput are shown in Fig. 5.10. Higher CW sizes lower the contention in the channel so that higher load intensity can be utilized. Conversely in lower CW size the contention is too high so that load intensity has to be lowered. For this purpose we analyze load intensity $q = \{0.1, 1.0\}$ for lower CW sizes $W = \{16, 32\}$ and $q = 1.0$ for higher CW sizes $W = \{64, 128\}$.

- For too small CW size such as $W = 16$, lower value of load intensity ($q = 0.1$) reduces the contention in the channel and thus yields higher total throughput in any partition. For large CW sizes such as $W = 32$ and above, the load intensity q has opposite effects in low and high aggregation scenarios. In low aggregation scenario such as in (4, 1, 5), a higher value of $q = 1.0$ gives more opportunity to aggregate and hence increases the throughput while in high aggregation scenario such as in (1, 4, 5), a lower value of $q = 0.1$ reduces the contention. From CW point of view, maximum total throughput is generally achieved at moderate CW size $W = 32$, neither the smallest nor the largest.

- The CW size and load intensity don't seem to affect the fairness index too much at low aggregation but has some noticeable effect at high aggregation scenarios. From

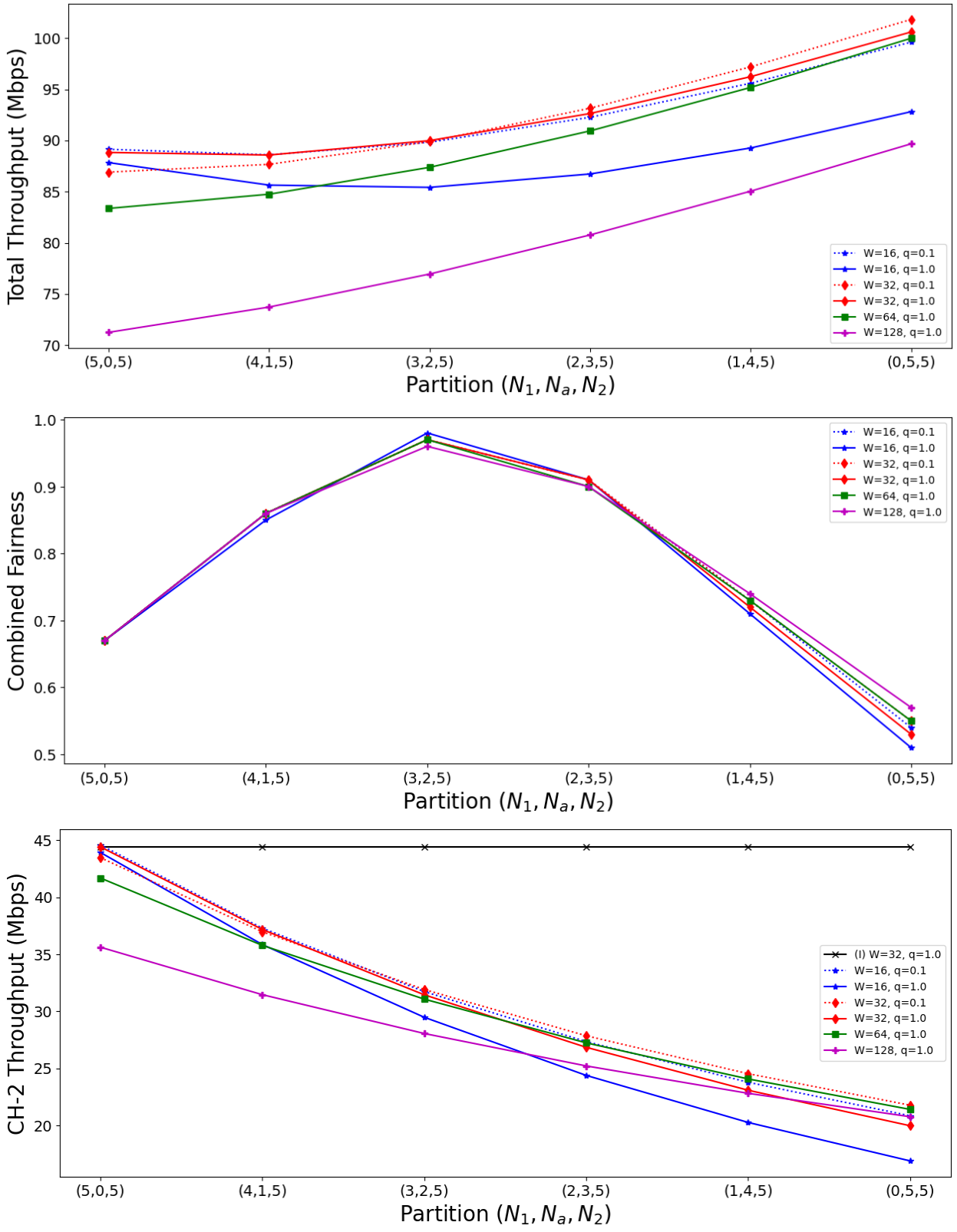

Figure 5.10: Effect of W and q in dual channel

fairness point of view, for high aggregation scenarios, larger CW sizes with reduced load intensity are preferred to reduce contention as much as possible.

- CH-2 throughput seem to be impacted similarly in lower and higher values of load intensity for low aggregation scenario such as (4, 1, 5). But at high aggregation scenario such as (1, 4, 5), having a lower load intensity protects secondary stations from over contentions and impacts the CH-2 throughput the least compared to individual (I) case where there are no stations in $\mathcal{N}_a$ group. From the perspective of CW size, at low aggregation scenario, small values of CW sizes give more opportunity for stations in $\mathcal{N}_2$ group causing CH-2 throughput to not degrade too much. At high aggregation scenario, large values of CW sizes reduces the chance of collision between stations in $\mathcal{N}_a$ and $\mathcal{N}_2$ group which also causes CH-2 throughput to not degrade too much.

Hence apart from partition, other system parameters CW size and load intensity also affect the fairness in the system and can also manage the impact of $\mathcal{N}_a$ stations to the secondary channel group $\mathcal{N}_2$.

5.4.3 Optimizing Partitions, CW and load intensity: Problem Statement

For a system that has fixed N_2 number of LAA stations in secondary channel, we want to find the optimal partition $\{(N_1, N_2)|N_1 + N_a = N\}$, system parameters: CW size $W \in [16 : 1 : 128]$ and load intensity $q \in [0.1 : 0.1 : 1.0]$ for given N which maximizes our combined fairness objective J. The search space of (N_1, N_a, W, q) is still limited enough to find the optimal solution through exhaustive brute force search.

$$\begin{aligned} \underset{N_1,N_a,W,q}{\text{maximize}} \quad & J \\ \text{subject to} \quad & N_1 + N_a = N \end{aligned} \tag{5.9}$$

Table A5 shows the results for optimizing combined fairness with partition, CW size and load intensity. Compared to the optimization without CW and load intensity in Table A4, it can be seen that the partition (N_1, N_a) plays a dominant role than the CW size and

load intensity. The partition is more or less similar to that of case without W and q. CW plays the least role with all values set at $W = 16$. System would rather adjust the partition and load intensity than CW size. The effect of load intensity q is seen only at higher values of $N > 17$, where the channel is saturated as was seen in Section 5.4.2.

In this chapter, we saw the effects of the partition and system parameters: contention window size and load intensity on total throughput, combined fairness and secondary channel throughput in case of dual-channel aggregation. It was shown that while optimizing the partition, maximizing total throughput objective impacts the throughput of the stations in secondary channel the most. Ensuring the combined throughput-airtime fairness protects the secondary channel users at the expense of some total throughput. It was also shown that the partition plays a dominating role than CW size and load intensity in maximizing the combined fairness. The effect of CW size is the least and the load intensity parameter only affects at channel saturation cases. Fair coexistence with dual carrier aggregation in presence of WiFi APs needs to be further studied.

CHAPTER 6

CONCLUSION

The main goal of this study was to address the importance of airtime/COT fairness along with the throughput fairness in the coexistence of LAA with incumbent WiFi in an unlicensed spectrum. We looked at the effects of groupings of users and system parameters such as CW size and load intensity on the performance of the coexistence system in terms of total throughput, throughput fairness and airtime fairness. We provide solutions to dynamically change system parameters of LAA stations to achieve maximum total throughput from the overall system taking into account fair allocation of throughput and airtime across different networks and stations.

In chapter 3, for the case of single-carrier LBT, we saw how LAA (both LAA-Cat3 and LAA-Cat4) implemented in an unlicensed spectrum along with WiFi without any contention window adjustment, would give an unfair advantage to LAA over WiFi. We established that adjusting the CW size of LAA plays an important role that enables LAA to coexist fairly with WiFi. We discussed the trade-off that exists while trying to optimize the throughput and airtime fairness. We showed that a fitness function that takes into account both total throughput and fairness metrics can ensure fair coexistence between LAA and WiFi. We compared the performances of LAA-Cat4 and LAA-Cat3 coexisting with WiFi and determined that even though LAA-Cat4 achieves better throughput fairness, LAA-Cat3 does a better job in obtaining a higher fitness by having higher airtime fairness and overall total throughput.

In chapter 4, for the case of multi-carrier LBT, we showed that the total throughput and fair allocation of resources among the LAA and WiFi stations in the case of multi-carrier LBT can be made better by optimizing the CW sizes of each LAA stations separately, which

was accomplished using a genetic algorithm based assignment technique. We compared the performances of the GA based assignment with the equal contention window assignment and showed that GA based assignment performed considerably better in terms of both total throughput and combined fairness.

In chapter 5, for the case of dual-carrier aggregation we explored the effects of system parameters: contention window size and load intensity parameter, and the partition of stations in different groups: single and dual channel sensing on total throughput, combined fairness and secondary channel throughput. It was shown that while optimizing the partition, maximizing total throughput objective would impact the throughput of the stations in secondary channel significantly. Ensuring the combined throughput-airtime fairness protects the secondary channel users at the expense of some total throughput. It was also shown that the partition plays a dominating role than contention window size and load intensity in maximizing the combined fairness. The effect of contention window size is the least and the load intensity parameter only affects at channel saturation cases.

Hence in this study, it was shown that the LAA would be able to fairly allocate resources while coexisting with WiFi in a common unlicensed spectrum by dynamically changing its system parameters, mainly contention window sizes, in case of single and multi-carrier LBT. For dual-carrier aggregation it was shown that the partition played the major role in affecting the fairness and secondary channel throughput. Load intensity and contention window contributed only a little in comparison to the partition.

BIBLIOGRAPHY

BIBLIOGRAPHY

[1] Giuseppe Bianchi. Performance analysis of the ieee 802.11 distributed coordination function. *IEEE Journal on selected areas in communications*, 18(3):535–547, 2000.

[2] Andra M Voicu, Ljiljana Simić, J Pierre de Vries, Marina Petrova, and Petri Mähönen. Analysing wi-fi/lte coexistence to demonstrate the value of risk-informed interference assessment. In *2017 IEEE International Symposium on Dynamic Spectrum Access Networks (DySPAN)*, pages 1–10. IEEE, 2017.

[3] Andra M Voicu, Ljiljana Simić, Jean Pierre De Vries, Marina Petrova, and Petri Mähönen. Risk-informed interference assessment for shared spectrum bands: A wi-fi/lte coexistence case study. *IEEE Transactions on Cognitive Communications and Networking*, 3(3):505–519, 2017.

[4] Rapeepat Ratasuk, Nitin Mangalvedhe, and Amitava Ghosh. Lte in unlicensed spectrum using licensed-assisted access. In *2014 IEEE Globecom Workshops (GC Wkshps)*, pages 746–751. IEEE, 2014.

[5] Xiaojing Yan, Hui Tian, Cheng Qin, and Arogyswami Paul. Constrained stochastic game in licensed-assisted access for dynamic contention window adaptation. *IEEE Communications Letters*, 22(6):1232–1235, 2017.

[6] Andre M Cavalcante, Erika Almeida, Robson D Vieira, Sayantan Choudhury, Esa Tuomaala, Klaus Doppler, Fabiano Chaves, Rafael CD Paiva, and Fuad Abinader. Performance evaluation of lte and wi-fi coexistence in unlicensed bands. In *2013 IEEE 77th Vehicular Technology Conference (VTC Spring)*, pages 1–6. IEEE, 2013.

[7] Ljiljana Simić, Andra M Voicu, Petri Mähönen, Marina Petrova, and Jean Pierre De Vries. Lte in unlicensed bands is neither friend nor foe to wi-fi. *IEEE Access*, 4:6416–6426, 2016.

[8] Cristina Cano, Douglas J Leith, Andres Garcia-Saavedra, and Pablo Serrano. Fair coexistence of scheduled and random access wireless networks: Unlicensed lte/wifi. *IEEE/ACM Transactions on Networking*, 25(6):3267–3281, 2017.

[9] Nadisanka Rupasinghe and İsmail Güvenç. Licensed-assisted access for wifi-lte coexistence in the unlicensed spectrum. In *2014 IEEE Globecom Workshops (GC Wkshps)*, pages 894–899. IEEE, 2014.

[10] Yingzhe Li, François Baccelli, Jeffrey G Andrews, Thomas D Novlan, and Jianzhong Charlie Zhang. Modeling and analyzing the coexistence of wi-fi and lte in unlicensed spectrum. *IEEE Transactions on Wireless Communications*, 15(9):6310–6326, 2016.

[11] Shweta Sagari, Ivan Seskar, and Dipankar Raychaudhuri. Modeling the coexistence of lte and wifi heterogeneous networks in dense deployment scenarios. In *2015 IEEE international conference on communication workshop (ICCW)*, pages 2301–2306. IEEE, 2015.

[12] Sangki Yun and Lili Qiu. Supporting wifi and lte co-existence. In *2015 IEEE Conference on Computer Communications (INFOCOM)*, pages 810–818. IEEE, 2015.

[13] Fuad M Abinader, Erika PL Almeida, Fabiano S Chaves, André M Cavalcante, Robson D Vieira, Rafael CD Paiva, Angilberto M Sobrinho, Sayantan Choudhury, Esa Tuomaala, Klaus Doppler, et al. Enabling the coexistence of lte and wi-fi in unlicensed bands. *IEEE Communications Magazine*, 52(11):54–61, 2014.

[14] Alireza Babaei, Jennifer Andreoli-Fang, Yimin Pang, and Belal Hamzeh. On the impact of lte-u on wi-fi performance. *International Journal of Wireless Information Networks*, 22(4):336–344, 2015.

[15] Abhijeet Bhorkar, Christian Ibars, and Pingping Zong. Performance analysis of lte and wi-fi in unlicensed band using stochastic geometry. In *2014 IEEE 25th Annual International Symposium on Personal, Indoor, and Mobile Radio Communication (PIMRC)*, pages 1310–1314. IEEE, 2014.

[16] Cristina Cano and Douglas J Leith. Coexistence of wifi and lte in unlicensed bands: A proportional fair allocation scheme. In *2015 IEEE international conference on communication workshop (ICCW)*, pages 2288–2293. IEEE, 2015.

[17] Andra M Voicu, Ljiljana Simić, and Marina Petrova. Coexistence of pico-and femtocellular lte-unlicensed with legacy indoor wi-fi deployments. In *2015 IEEE international conference on communication workshop (ICCW)*, pages 2294–2300. IEEE, 2015.

[18] Jiandong Li, Xijun Wang, Daquan Feng, Min Sheng, and Tony QS Quek. Share in the commons: Coexistence between lte unlicensed and wi-fi. *IEEE Wireless Communications*, 23(6):16–23, 2016.

[19] Cristina Cano and Douglas J Leith. Unlicensed lte/wifi coexistence: Is lbt inherently fairer than csat? In *2016 IEEE International Conference on Communications (ICC)*, pages 1–6. IEEE, 2016.

[20] Ahmed K Sadek, Tamer Kadous, Kai Tang, Heechoon Lee, and Mingxi Fan. Extending lte to unlicensed band-merit and coexistence. In *2015 IEEE International Conference on Communication Workshop (ICCW)*, pages 2344–2349. IEEE, 2015.

[21] MGS Sriyananda, Imtiaz Parvez, Ismail Güvene, Mehdi Bennis, and Arif I Sarwat. Multi-armed bandit for lte-u and wifi coexistence in unlicensed bands. In *2016 IEEE Wireless Communications and Networking Conference*, pages 1–6. IEEE, 2016.

[22] Timo Nihtilä, Vitaliy Tykhomyrov, Olli Alanen, Mikko A Uusitalo, Antti Sorri, Martti Moisio, Sassan Iraji, Rapeepat Ratasuk, and Nitin Mangalvedhe. System performance of lte and ieee 802.11 coexisting on a shared frequency band. In *2013 IEEE Wireless Communications and Networking Conference (WCNC)*, pages 1038–1043. IEEE, 2013.

[23] Zoraze Ali, Biljana Bojovic, Lorenza Giupponi, and Josep Mangues Bafalluy. On fairness evaluation: Lte-u vs. laa. In *Proceedings of the 14th ACM International Symposium on Mobility Management and Wireless Access*, pages 163–168, 2016.

[24] Ismael Gomez-Miguelez, Andres Garcia-Saavedra, Paul D Sutton, Pablo Serrano, Cristina Cano, and Doug J Leith. srslte: An open-source platform for lte evolution and experimentation. In *Proceedings of the Tenth ACM International Workshop on Wireless Network Testbeds, Experimental Evaluation, and Characterization*, pages 25–32, 2016.

[25] Yubing Jian, Uma Parthavi Moravapalle, Chao-Fang Shih, and Raghupathy Sivakumar. Duet: An adaptive algorithm for the coexistence of lte-u and wifi in unlicensed spectrum. In *2017 International Conference on Computing, Networking and Communications (ICNC)*, pages 19–25. IEEE, 2017.

[26] Vanlin Sathya, Morteza Mehrnoush, Monisha Ghosh, and Sumit Roy. Association fairness in wi-fi and lte-u coexistence. In *2018 IEEE Wireless Communications and Networking Conference (WCNC)*, pages 1–6. IEEE, 2018.

[27] Andra M Voicu, Ljiljana Simić, and Marina Petrova. Inter-technology coexistence in a spectrum commons: A case study of wi-fi and lte in the 5-ghz unlicensed band. *IEEE Journal on Selected Areas in Communications*, 34(11):3062–3077, 2016.

[28] C Capretti, Francesco Gringoli, Nicolò Facchi, and Paul Patras. Lte/wi-fi co-existence under scrutiny: An empirical study. In *Proceedings of the Tenth ACM International Workshop on Wireless Network Testbeds, Experimental Evaluation, and Characterization*, pages 33–40, 2016.

[29] Erika Almeida, André M Cavalcante, Rafael CD Paiva, Fabiano S Chaves, Fuad M Abinader, Robson D Vieira, Sayantan Choudhury, Esa Tuomaala, and Klaus Doppler. Enabling lte/wifi coexistence by lte blank subframe allocation. In *2013 IEEE International Conference on Communications (ICC)*, pages 5083–5088. IEEE, 2013.

[30] Baoan Jia and Meixia Tao. A channel sensing based design for lte in unlicensed bands. In *2015 IEEE international conference on communication workshop (ICCW)*, pages 2332–2337. IEEE, 2015.

[31] Vasilis Maglogiannis, Dries Naudts, Adnan Shahid, and Ingrid Moerman. A q-learning scheme for fair coexistence between lte and wi-fi in unlicensed spectrum. *IEEE Access*, 6:27278–27293, 2018.

[32] Jeongho Jeon, Huaning Niu, Qian Clara Li, Apostolos Papathanassiou, and Geng Wu. Lte in the unlicensed spectrum: Evaluating coexistence mechanisms. In *2014 IEEE Globecom Workshops (GC Wkshps)*, pages 740–745. IEEE, 2014.

[33] Ahmed A Alabdel Abass, Ratnesh Kumbhkar, Narayan B Mandayam, and Zoran Gajic. Wifi/lte-u coexistence: An evolutionary game approach. *IEEE transactions on cognitive communications and networking*, 5(1):44–58, 2018.

[34] Nazanin Rastegardoost and Bijan Jabbari. A machine learning algorithm for unlicensed lte and wifi spectrum sharing. In *2018 IEEE International Symposium on Dynamic Spectrum Access Networks (DySPAN)*, pages 1–6. IEEE, 2018.

[35] Amr Abdelfattah and Naceur Malouch. Modeling and performance analysis of wi-fi networks coexisting with lte-u. In *IEEE INFOCOM 2017-IEEE Conference on Computer Communications*, pages 1–9. IEEE, 2017.

[36] Amr Abdelfattah and Naceur Malouch. Studying the impact of lte-u on wi-fi downlink performance. In *2016 IEEE 12th International Conference on Wireless and Mobile Computing, Networking and Communications (WiMob)*, pages 1–9. IEEE, 2016.

[37] Shweta Sagari, Samuel Baysting, Dola Saha, Ivan Seskar, Wade Trappe, and Dipankar Raychaudhuri. Coordinated dynamic spectrum management of lte-u and wi-fi networks. In *2015 IEEE International Symposium on Dynamic Spectrum Access Networks (DySPAN)*, pages 209–220. IEEE, 2015.

[38] Fabiano S Chaves, Erika PL Almeida, Robson D Vieira, Andre M Cavalcante, Fuad M Abinader, Sayantan Choudhury, and Klaus Doppler. Lte ul power control for the improvement of lte/wi-fi coexistence. In *2013 IEEE 78th Vehicular Technology Conference (VTC Fall)*, pages 1–6. IEEE, 2013.

[39] Yuehong Gao, Lei Cheng, Lin Sang, Dacheng Yang, et al. Spectrum sharing for lte and wifi coexistence using decision tree and game theory. In *2016 IEEE Wireless Communications and Networking Conference*, pages 1–6. IEEE, 2016.

[40] Cengis Hasan, Mahesh K Marina, and Ursula Challita. On lte-wifi coexistence and inter-operator spectrum sharing in unlicensed bands: Altruism, cooperation and fairness. In *Proceedings of the 17th ACM International Symposium on Mobile Ad Hoc Networking and Computing*, pages 111–120, 2016.

[41] Abhijeet Bhorkar, Christian Ibars, Apostolos Papathanassiou, and Pingping Zong. Medium access design for lte in unlicensed band. In *2015 IEEE Wireless Communications and Networking Conference Workshops (WCNCW)*, pages 369–373. IEEE, 2015.

[42] Yuan Gao, Xiaoli Chu, and Jie Zhang. Performance analysis of laa and wifi coexistence in unlicensed spectrum based on markov chain. In *2016 IEEE Global Communications Conference (GLOBECOM)*, pages 1–6. IEEE, 2016.

[43] Yuhan Su, Xiaojiang Du, Lianfen Huang, Zhibin Gao, and Mohsen Guizani. Lte-u and wi-fi coexistence algorithm based on q-learning in multi-channel. *IEEE Access*, 6:13644–13652, 2018.

[44] Oriol Sallent, Jordi Pérez-Romero, Ramon Ferrús, and Ramón Agustí. Learning-based coexistence for lte operation in unlicensed bands. In *2015 IEEE international conference on communication workshop (ICCW)*, pages 2307–2313. IEEE, 2015.

[45] Jie Xiao and Jun Zheng. An adaptive channel access mechanism for lte-u and wifi coexistence in an unlicensed spectrum. In *2016 IEEE International Conference on Communications (ICC)*, pages 1–6. IEEE, 2016.

[46] Cheng Chen, Rapeepat Ratasuk, and Amitava Ghosh. Downlink performance analysis of lte and wifi coexistence in unlicensed bands with a simple listen-before-talk scheme. In *2015 IEEE 81st Vehicular Technology Conference (VTC Spring)*, pages 1–5. IEEE, 2015.

[47] Morteza Mehrnoush, Vanlin Sathya, Sumit Roy, and Monisha Ghosh. Analytical modeling of wi-fi and lte-laa coexistence: Throughput and impact of energy detection threshold. *IEEE/ACM Transactions on Networking*, 26(4):1990–2003, 2018.

[48] Sudat Tuladhar, Lei Cao, and Ramanarayanan Viswanathan. Throughput and channel occupancy time fairness trade-off for downlink laa-cat4 and wifi coexistence based on markov chain (poster). In *2018 IEEE Conference on Cognitive and Computational Aspects of Situation Management (CogSIMA)*, pages 129–134. IEEE, 2018.

[49] Nadisanka Rupasinghe and İsmail Güvenç. Reinforcement learning for licensed-assisted access of lte in the unlicensed spectrum. In *2015 IEEE Wireless Communications and Networking Conference (WCNC)*, pages 1279–1284. IEEE, 2015.

[50] Vanlin Sathya, Morteza Mehrnoush, Monisha Ghosh, and Sumit Roy. Wi-fi/lte-u coexistence: Real-time issues and solutions. *IEEE Access*, 8:9221–9234, 2020.

[51] Harim Lee, Hyoil Kim, Hyun Jong Yang, Jeong Tak Kim, and SeungKwon Baek. Performance analysis of license assisted access lte with asymmetric hidden terminals. *IEEE Transactions on Mobile Computing*, 17(9):2141–2154, 2018.

[52] Lorenza Giupponi, Thomas Henderson, Biljana Bojovic, and Marco Miozzo. Simulating lte and wi-fi coexistence in unlicensed spectrum with ns-3. *arXiv preprint arXiv:1604.06826*, 2016.

[53] Junjie Tan, Lin Zhang, Ying-Chang Liang, and Dusit Niyato. Deep reinforcement learning for the coexistence of laa-lte and wifi systems. In *ICC 2019-2019 IEEE International Conference on Communications (ICC)*, pages 1–6. IEEE, 2019.

[54] Fanrong Hao, Chang Yongyu, Hongdou Li, Jian Zhang, and Wei Quan. Contention window size adaptation algorithm for laa-lte in unlicensed band. In *2016 International Symposium on Wireless Communication Systems (ISWCS)*, pages 476–480. IEEE, 2016.

[55] Yujae Song, Ki Won Sung, and Youngnam Han. Coexistence of wi-fi and cellular with listen-before-talk in unlicensed spectrum. *IEEE Communications Letters*, 20(1):161–164, 2015.

[56] Yuan Gao, Bolin Chen, Xiaoli Chu, and Jie Zhang. Resource allocation in lte-laa and wifi coexistence: A joint contention window optimization scheme. In *GLOBECOM 2017-2017 IEEE Global Communications Conference*, pages 1–6. IEEE, 2017.

[57] Junjie Tan, Sa Xiao, Shiying Han, Ying-Chang Liang, and Victor CM Leung. Qos-aware user association and resource allocation in laa-lte/wifi coexistence systems. *IEEE Transactions on Wireless Communications*, 18(4):2415–2430, 2019.

[58] Tao Tao, Feng Han, and Yong Liu. Enhanced lbt algorithm for lte-laa in unlicensed band. In *2015 IEEE 26th annual international symposium on personal, indoor, and mobile radio communications (PIMRC)*, pages 1907–1911. IEEE, 2015.

[59] Amr Abdelfattah, Naceur Malouch, and Jonathan Ling. Analytical evaluation and potentials of frame based equipment for lte-laa/wi-fi coexistence. In *2019 IEEE Symposium on Computers and Communications (ISCC)*, pages 1–7. IEEE, 2019.

[60] Polina Kutsevol, Vyacheslav Loginov, Evgeny Khorov, and Andrey Lyakhov. New collision detection method for fair lte-laa and wi-fi coexistence. In *2019 IEEE 30th Annual International Symposium on Personal, Indoor and Mobile Radio Communications (PIMRC)*, pages 1–6. IEEE, 2019.

[61] Kangjin Yoon, Taejun Park, Jihoon Kim, Weiping Sun, Sunwook Hwang, Ingab Kang, and Sunghyun Choi. Cota: Channel occupancy time adaptation for lte in unlicensed spectrum. In *2017 IEEE International Symposium on Dynamic Spectrum Access Networks (DySPAN)*, pages 1–10. IEEE, 2017.

[62] Long Li, Amir Hossein Jafari, Xiaoli Chu, and Jie Zhang. Simultaneous transmission opportunities for lte-laa smallcells coexisting with wifi in unlicensed spectrum. In *2016 IEEE International Conference on Communications (ICC)*, pages 1–7. IEEE, 2016.

[63] Vanlin Sathya, Muhammad Iqbal Rochman, and Monisha Ghosh. Measurement-based coexistence studies of laa & wi-fi deployments in chicago. *IEEE Wireless Communications*, 28(1):136–143, 2020.

[64] Apostolos Galanopoulos, Fotis Foukalas, and Theodoros A Tsiftsis. Efficient coexistence of lte with wifi in the licensed and unlicensed spectrum aggregation. *IEEE Transactions on Cognitive Communications and Networking*, 2(2):129–140, 2016.

[65] Beixiong Zheng, Miaowen Wen, Shaoe Lin, Wen Wu, Fangjiong Chen, Shahid Mumtaz, Fei Ji, and Hua Yu. Design of multi-carrier lbt for laa&wifi coexistence in unlicensed spectrum. *IEEE Network*, 34(1):76–83, 2019.

[66] Ursula Challita, Li Dong, and Walid Saad. Proactive resource management for lte in unlicensed spectrum: A deep learning perspective. *IEEE transactions on wireless communications*, 17(7):4674–4689, 2018.

[67] Sudat Tuladhar, Lei Cao, and Ramanarayanan Viswanathan. Markov chain based performance analysis of laa and wifi coexistence in dual carrier aggregation. In *2019 IEEE 4th International Conference on Signal and Image Processing (ICSIP)*, pages 504–508. IEEE, 2019.

[68] Long Hoang Vu and Ji-Hoon Yun. Multi-carrier listen before talk with power leakage awareness for lte-laa in unlicensed spectrum. *IEEE Transactions on Cognitive Communications and Networking*, 5(3):678–689, 2019.

[69] Sudat Tuladhar, Lei Cao, and Ramanarayanan Viswanathan. Fair coexistence of laa and wifi in multi-carrier lbt based on joint throughput and airtime fairness. In *2021 IEEE International Symposium on Dynamic Spectrum Access Networks (DySPAN)*, pages 147–152. IEEE, 2021.

[70] Jianguo Liu and Gang Shen. Performance of multi-carrier lbt mechanism for lte-laa. In *2016 IEEE 83rd Vehicular Technology Conference (VTC Spring)*, pages 1–5. IEEE, 2016.

[71] Andra M Voicu, Ljiljana Simić, and Marina Petrova. Survey of spectrum sharing for inter-technology coexistence. *IEEE Communications Surveys & Tutorials*, 21(2):1112–1144, 2018.

[72] Yan Huang, Yongce Chen, Y Thomas Hou, Wenjing Lou, and Jeffrey H Reed. Recent advances of lte/wifi coexistence in unlicensed spectrum. *IEEE Network*, 32(2):107–113, 2017.

[73] Haixia Cui, Victor CM Leung, Shaoqian Li, and Xianbin Wang. Lte in the unlicensed band: Overview, challenges, and opportunities. *IEEE Wireless Communications*, 24(4):99–105, 2017.

[74] Bolin Chen, Jiming Chen, Yuan Gao, and Jie Zhang. Coexistence of lte-laa and wi-fi on 5 ghz with corresponding deployment scenarios: A survey. *IEEE Communications Surveys & Tutorials*, 19(1):7–32, 2016.

[75] Xuyu Wang, Shiwen Mao, and Michelle X Gong. A survey of lte wi-fi coexistence in unlicensed bands. *GetMobile: Mobile Computing and Communications*, 20(3):17–23, 2017.

[76] Stefania Zinno, Giovanni Di Stasi, Stefano Avallone, and Giorgio Ventre. On a fair coexistence of lte and wi-fi in the unlicensed spectrum: A survey. *computer communications*, 115:35–50, 2018.

[77] Ran Zhang, Miao Wang, Lin X Cai, Zhongming Zheng, Xuemin Shen, and Liang-Liang Xie. Lte-unlicensed: The future of spectrum aggregation for cellular networks. *IEEE Wireless Communications*, 22(3):150–159, 2015.

[78] Gaurang Naik, Jinshan Liu, and Jung-Min Jerry Park. Coexistence of wireless technologies in the 5 ghz bands: A survey of existing solutions and a roadmap for future research. *IEEE Communications Surveys & Tutorials*, 20(3):1777–1798, 2018.

[79] Sima Hajmohammad and Halima Elbiaze. Unlicensed spectrum splitting between femtocell and wifi. In *2013 IEEE International Conference on Communications (ICC)*, pages 1883–1888. IEEE, 2013.

[80] Gaurang Naik, Jung-Min Park, Jonathan Ashdown, and William Lehr. Next generation wi-fi and 5g nr-u in the 6 ghz bands: Opportunities and challenges. *IEEE Access*, 8:153027–153056, 2020.

[81] IEEE Standard Association et al. Ieee standard for wireless lan medium access control (mac) and physical layer (phy) specification. *http://standards. ieee. org/getieee802/802.11. html*, 1999.

[82] TS ETSI. 136 213 v13. 0.0. *ETSI standard*, 2016.

APPENDICES

We tabulate the results for optimization of partitions, CW size and load intensity in Chapter 5.

Table A1: Optimizing Total Throughput

N	N1	Na	N2	J	S1	Sa	S2	A1	Aa	A2	S	A
1	0	1	10	93.777	0	56.38	37.4	0	0.61	0.67	93.78	1.28
2	0	2	10	101.3227	0	68.33	32.99	0	0.73	0.59	101.32	1.33
3	0	3	10	102.3114	0	72.83	29.49	0	0.78	0.53	102.31	1.31
4	0	4	10	101.4186	0	74.79	26.63	0	0.79	0.48	101.42	1.27
5	0	5	10	99.8842	0	75.62	24.26	0	0.8	0.44	99.88	1.24
6	0	6	10	98.1418	0	75.87	22.27	0	0.8	0.4	98.14	1.2
7	0	7	10	96.365	0	75.8	20.56	0	0.79	0.37	96.37	1.16
8	0	8	10	94.6276	0	75.54	19.09	0	0.79	0.34	94.63	1.13
9	0	9	10	92.9603	0	75.16	17.8	0	0.78	0.32	92.96	1.1
10	0	10	10	91.3745	0	74.7	16.67	0	0.78	0.3	91.37	1.08
11	0	11	10	89.8722	0	74.2	15.67	0	0.77	0.28	89.87	1.05
12	0	12	10	88.4509	0	73.68	14.77	0	0.76	0.27	88.45	1.03
13	0	13	10	87.1063	0	73.14	13.97	0	0.75	0.25	87.11	1
14	0	14	10	85.8332	0	72.59	13.24	0	0.75	0.24	85.83	0.98
15	0	15	10	84.6265	0	72.05	12.58	0	0.74	0.23	84.63	0.96
16	16	0	10	83.7494	40.64	0	43.11	0.73	0	0.78	83.75	1.51
17	17	0	10	83.3593	40.25	0	43.11	0.72	0	0.78	83.36	1.5
18	18	0	10	82.9785	39.87	0	43.11	0.72	0	0.78	82.98	1.49
19	19	0	10	82.6072	39.5	0	43.11	0.71	0	0.78	82.61	1.49
20	20	0	10	82.2456	39.14	0	43.11	0.7	0	0.78	82.25	1.48

Table A2: Optimizing Airtime Fairness

N	N1	Na	N2	J	S1	Sa	S2	A1	Aa	A2	S	A
1	0	1	10	0.665	0	56.38	37.4	0	0.61	0.67	93.78	1.28
2	1	1	10	0.9113	20.36	33.95	37.65	0.37	0.37	0.68	91.96	1.41
3	1	2	10	0.9087	14.39	48.27	33.37	0.26	0.52	0.6	96.02	1.38
4	2	2	10	0.9571	22.06	36.98	33.71	0.4	0.4	0.61	92.75	1.4
5	2	3	10	0.9571	17.77	44.89	30.34	0.32	0.48	0.55	92.99	1.34
6	3	3	10	0.9749	22.19	37.36	30.71	0.4	0.4	0.55	90.26	1.35
7	3	4	10	0.9759	18.93	42.69	27.95	0.34	0.45	0.5	89.57	1.3
8	4	4	10	0.9846	21.93	37.07	28.33	0.39	0.39	0.51	87.33	1.3
9	4	5	10	0.9855	19.33	41.01	26.01	0.35	0.43	0.47	86.35	1.25
10	5	5	10	0.9905	21.55	36.55	26.38	0.39	0.39	0.47	84.48	1.25
11	5	6	10	0.9909	19.41	39.64	24.39	0.35	0.42	0.44	83.44	1.21
12	6	6	10	0.9942	21.14	35.96	24.75	0.38	0.38	0.45	81.84	1.21
13	6	7	10	0.9943	19.32	38.48	23.02	0.35	0.41	0.41	80.81	1.17
14	7	7	10	0.9967	20.72	35.35	23.35	0.37	0.37	0.42	79.43	1.17
15	7	8	10	0.9963	19.15	37.46	21.83	0.34	0.39	0.39	78.44	1.13
16	8	8	10	0.9983	20.32	34.75	22.15	0.37	0.37	0.4	77.22	1.13
17	8	9	10	0.9975	18.94	36.55	20.79	0.34	0.38	0.37	76.28	1.1
18	9	9	10	0.9993	19.94	34.17	21.1	0.36	0.36	0.38	75.2	1.1
19	9	10	10	0.9982	18.71	35.74	19.87	0.34	0.37	0.36	74.32	1.07
20	10	10	10	0.9998	19.57	33.61	20.16	0.35	0.35	0.36	73.35	1.07

Table A3: Optimizing Throughput Fairness

N	N1	Na	N2	J	S1	Sa	S2	A1	Aa	A2	S	A
1	1	0	10	0.657	33.8	0	43.11	0.61	0	0.78	76.91	1.38
2	1	1	10	0.9445	20.36	33.95	37.65	0.37	0.37	0.68	91.96	1.41
3	2	1	10	0.965	28.78	23.99	37.87	0.52	0.26	0.68	90.64	1.46
4	2	2	10	0.9589	22.06	36.98	33.71	0.4	0.4	0.61	92.75	1.4
5	3	2	10	0.9901	26.65	29.77	34.02	0.48	0.32	0.61	90.43	1.41
6	4	2	10	0.983	29.59	24.78	34.3	0.53	0.27	0.62	88.67	1.42
7	4	3	10	0.99	25.24	31.86	31.05	0.45	0.34	0.56	88.15	1.35
8	5	3	10	0.9961	27.42	27.67	31.37	0.49	0.3	0.56	86.45	1.35
9	6	3	10	0.9888	29	24.38	31.67	0.52	0.26	0.57	85.05	1.35
10	6	4	10	0.9971	25.86	29.11	29.01	0.47	0.31	0.52	83.98	1.3
11	7	4	10	0.9978	27.17	26.2	29.32	0.49	0.28	0.53	82.68	1.3
12	7	5	10	0.994	24.66	29.84	27.05	0.44	0.32	0.49	81.55	1.25
13	8	5	10	0.9993	25.76	27.26	27.36	0.46	0.29	0.49	80.38	1.24
14	9	5	10	0.9984	26.65	25.05	27.66	0.48	0.27	0.5	79.35	1.24
15	9	6	10	0.9973	24.63	27.88	25.71	0.44	0.3	0.46	78.21	1.2
16	10	6	10	0.9999	25.4	25.87	26	0.46	0.27	0.47	77.26	1.2
17	11	6	10	0.9985	26.05	24.1	26.27	0.47	0.26	0.47	76.42	1.2
18	11	7	10	0.9987	24.37	26.39	24.57	0.44	0.28	0.44	75.32	1.16
19	12	7	10	1	24.95	24.75	24.84	0.45	0.26	0.45	74.54	1.16
20	13	7	10	0.9985	25.44	23.29	25.1	0.46	0.25	0.45	73.83	1.16

Table A4: Optimizing Throughput-Airtime Fairness

N	N1	Na	N2	J	S1	Sa	S2	A1	Aa	A2	S	A
1	1	0	10	0.657	33.8	0	43.11	0.61	0	0.78	76.91	1.38
2	1	1	10	0.9276	20.36	33.95	37.65	0.37	0.37	0.68	91.96	1.41
3	2	1	10	0.9241	28.78	23.99	37.87	0.52	0.26	0.68	90.64	1.46
4	2	2	10	0.958	22.06	36.98	33.71	0.4	0.4	0.61	92.75	1.4
5	3	2	10	0.964	26.65	29.77	34.02	0.48	0.32	0.61	90.43	1.41
6	3	3	10	0.967	22.19	37.36	30.71	0.4	0.4	0.55	90.26	1.35
7	4	3	10	0.9761	25.24	31.86	31.05	0.45	0.34	0.56	88.15	1.35
8	4	4	10	0.9703	21.93	37.07	28.33	0.39	0.39	0.51	87.33	1.3
9	5	4	10	0.9804	24.17	32.66	28.68	0.43	0.35	0.52	85.5	1.3
10	6	4	10	0.9777	25.86	29.11	29.01	0.47	0.31	0.52	83.98	1.3
11	6	5	10	0.9817	23.29	32.89	26.72	0.42	0.35	0.48	82.9	1.25
12	7	5	10	0.9823	24.66	29.84	27.05	0.44	0.32	0.49	81.55	1.25
13	7	6	10	0.9814	22.54	32.85	25.08	0.41	0.35	0.45	80.47	1.2
14	8	6	10	0.9841	23.69	30.18	25.4	0.43	0.32	0.46	79.27	1.2
15	9	6	10	0.9816	24.63	27.88	25.71	0.44	0.3	0.46	78.21	1.2
16	9	7	10	0.9843	22.86	30.29	23.99	0.41	0.32	0.43	77.14	1.16
17	10	7	10	0.9839	23.68	28.22	24.28	0.43	0.3	0.44	76.18	1.16
18	10	8	10	0.9836	22.15	30.27	22.76	0.4	0.32	0.41	75.17	1.13
19	11	8	10	0.9847	22.87	28.39	23.04	0.41	0.3	0.41	74.3	1.12
20	12	8	10	0.9829	23.48	26.71	23.32	0.42	0.28	0.42	73.51	1.12

Table A5: Optimizing Throughput-Airtime Fairness with CW and load intensity

N	N1	Na	N2	W	q	J	S1	Sa	S2	A1	Aa	A2	S	A
1	1	0	10	16	0.4	0.6667	39.98	0	39.95	0.72	0	0.72	79.93	1.44
2	1	1	10	16	1	0.9667	22.61	34.58	33.3	0.41	0.41	0.6	90.49	1.41
3	2	1	10	16	1	0.9449	30.27	23.13	33.69	0.54	0.27	0.61	87.08	1.42
4	2	2	10	16	1	0.9768	22.39	34.6	29.26	0.4	0.4	0.53	86.25	1.33
5	3	2	10	16	1	0.9773	26.35	27.11	29.76	0.47	0.32	0.54	83.23	1.33
6	3	3	10	16	1	0.979	21.5	33.49	26.4	0.39	0.39	0.47	81.39	1.25
7	4	3	10	16	1	0.9852	24.05	28.05	26.92	0.43	0.32	0.48	79.02	1.24
8	4	4	10	16	1	0.9793	20.6	32.31	24.23	0.37	0.37	0.44	77.14	1.18
9	5	4	10	16	1	0.9874	22.43	28.09	24.74	0.4	0.32	0.44	75.25	1.17
10	6	4	10	16	1	0.9819	23.75	24.75	25.2	0.43	0.28	0.45	73.7	1.16
11	6	5	10	16	1	0.9876	21.18	27.79	22.99	0.38	0.32	0.41	71.96	1.11
12	7	5	10	16	1	0.986	22.24	24.97	23.44	0.4	0.29	0.42	70.65	1.11
13	7	6	10	16	1	0.987	20.17	27.36	21.56	0.36	0.31	0.39	69.09	1.06
14	8	6	10	16	1	0.9878	21.05	24.95	21.99	0.38	0.28	0.4	67.99	1.06
15	8	7	10	16	1	0.9859	19.34	26.9	20.36	0.35	0.3	0.37	66.61	1.02
16	9	7	10	16	1	0.9883	20.1	24.83	20.79	0.36	0.28	0.37	65.71	1.02
17	10	7	10	16	1	0.986	20.75	23.06	21.21	0.37	0.26	0.38	65.02	1.02
18	10	8	10	16	0.6	0.9879	19.38	24.77	19.84	0.35	0.28	0.36	63.98	0.98
19	11	8	10	16	0.5	0.9873	19.97	23.21	20.25	0.36	0.26	0.36	63.44	0.98
20	11	9	10	16	0.4	0.9871	18.78	24.7	19.02	0.34	0.28	0.34	62.49	0.96
21	12	9	10	16	0.3	0.9877	19.3	23.28	19.39	0.35	0.26	0.35	61.97	0.96
22	12	10	10	16	0.3	0.986	18.27	24.63	18.3	0.33	0.27	0.33	61.2	0.93
23	13	10	10	16	0.2	0.9875	18.72	23.3	18.59	0.34	0.26	0.33	60.61	0.93
24	14	10	10	16	0.2	0.9868	19.14	22.12	18.94	0.34	0.25	0.34	60.2	0.93
25	14	11	10	16	0.2	0.9869	18.26	23.33	17.97	0.33	0.26	0.32	59.56	0.91

VITA

Sudat Tuladhar was born on May 29, 1985 in Kathmandu, Nepal. He obtained a Bachelor of Engineering degree in Electronics and Communication Engineering from Pulchowk Campus, Institute of Engineering, Tribhuvan University, Nepal in April 2009. He worked as an embedded system designer for 4 years in Real Time Solutions Pvt. Ltd., Kathmandu, Nepal.

He received his Master's degree in Information Systems Engineering from Osaka Sangyo University, Osaka, Japan in March 2016. His Master's research involved digital image processing in tomographic reconstruction in the fields of particle image velocimetry.

He joined the University of Mississippi in August 2016 and received his Ph.D. in Electrical Engineering in May 2022. During his graduate studies, he worked as a teaching assistant, research assistant and a lab instructor at the department of electrical engineering. His research interest includes machine learning and wireless communications in WiFi, license assisted access and 5G. He is a student member of IEEE.